SMART NANOCOMPOSITES

Volume 7, Number 2, 2016

TABLE OF CONTENTS

Sensors, Materials with Luminiscent Properties, Porous Materials

nova
science publishers
New York

Smart Nanocomposites

This Journal presents new studies in the fast growing area of smart materials, in particular, composite nanostructured materials. It focuses on the physics and physical chemistry of surfaces, interfaces, thin films and coatings, nanoparticles and other nanostructures, as well as on their new and smart applications. Original approaches in fabrication and applications of nanostructured materials will get special attention. Nanostructured ceramics, alloys, various nanocarbon forms (nanotubes, fullerenes, graphene) and their composites used in sensors (including single molecule sensing) and actuators, artificial metabolism, drug delivery, selective membranes, fuel cells, energy storage, and photovoltaics are just a few examples of new classes of materials and applications that are within the scope of the Journal. It features the results of interdisciplinary research from universities, national labs, and privately owned companies.

The Journal is peer-reviewed with the highest standards and quality of publications. The purpose of this Journal is to bring the most up-to-date advances in nanotechnology together, and to give research groups the opportunity to compare their results with other groups' data. To achieve this, the Journal focuses mostly on practical applications of nanodevices, and on proof of the concept publications. Areas of interest include (but not are limited to): sensors, smart membranes, smart coatings for corrosion protection, aspects of significance to nanorobots: power supplies, nanorobot manipulating devices, and microchips for artificial intelligence. The Journal also deals with safety issues: safety of nanotechnology to the environment, controlling the nanodevices, and other aspects.

Smart Nanocomposites
is published in two issues per year by

Nova Science Publishers, Inc.
400 Oser Avenue, Suite 1600
Hauppauge, New York 11788-3619, U.S.A.
E-mail: nova.main@novapublishers.com
Web: www.novapublishers.com

ISSN: 1949-4823

Subscription Rate per Volume
Print: $245 Electronic: $245 Combined Print + Electronic: $367

Additional color graphics might be available in the e-version of this journal.

Smart Nanocomposites
Volume 7, Number 2
ISSN: 1949-4823

DATA INCONSISTENCY ON TRANSPORT PHENOMENA IN $A_2^V B_3^{VI}$ MATERIALS WITH THE HOLE CONDUCTIVITY

Sergey A. Nemov[1,2,*], Ali A. Allahkhah[1], and Arseny A. Rulimov[1]
[1]Peter the Great St. Petersburg Polytechnic University, St. Petersburg, Russia
[2]Zabaikal'skii State University, Chita, Russia

ABSTRACT

It is shown that accounting of interband scattering allows eliminating contradictions in the literature between interpretations of the electrical properties of $A_2^V B_3^{VI}$ materials with the hole conductivity and describing observed temperature dependences of the kinetic coefficients as well as the parameters of the band spectrum.

Keywords: $A_2^V B_3^{VI}$ materials, interband scattering, scattering parameter, kinetic coefficients, acoustic mechanism of hole scattering, $Sb_2Te_{2,9}Se_{0,1}$

INTRODUCTION

Investigations of layered semiconductor $A_2^V B_3^{VI}$ materials have been being carried out since the middle of last century.

Constant interest in these materials is caused by their wide usage in thermoelectric energy converters (in the form of ternary and quaternary solid solutions based on bismuth and antimony chalcogenides).

DISCUSSION

The experimental data obtained in the middle of the 20th century were summarized and systematized in Gol'tsman monograph [1]. However, the features of the energy spectrum of $A_2^V B_3^{VI}$ materials and the mechanisms of charge-carrier scattering are still discussed. Also the differences in the interpretation of experimental data of transport phenomena at low

* Corresponding author: Prof. Sergey Aleksandrovich Nemov, Professor of the Department "Materials Science and Technology of Materials," Peter the Great St. Petersburg Polytechnic University, St. Petersburg, Russia, Tel.: +7 (921) 347-30-33. E-mail: nemov_s@mail.ru

(T = 4.2 K) and medium (77 - 300 K) temperatures are stored. Results of the quantum oscillations research at liquid-helium temperatures have confirmed the Drabble-Wolfe one-band six-ellipsoidal model [2] for crystals with low hole concentration. There are some features, which are associated with the existence of the secondary extremes in the valence band in the samples with a higher Fermi energy [2, 3].

The secondary extremum parameters are discussed so far. In addition, the unique view of the Fermi surface of a crystal with high hole concentration is not defined [2, 3]. Specifically, in [2] an ellipsoidal shape is assumed, and in [3] the authors suggest a hyperbolic tubes connecting ellipsoids of light holes.

Anyway, holes of different varieties involved in the quantum oscillations. Therefore, in the analysis of experimental data the two-band model is used at low temperatures.

Most of experimental investigations of transport phenomena in $A_2^{V}B_3^{VI}$ compounds are related to the temperature range 77 - 300 K.

Unlike the low-temperature data, the kinetic coefficients (the conductivity σ, the thermopower α, the transverse Nernst-Ettingshausen effect Q) do not have any differences from the nature of the temperature dependences predicted by the theory within one-band model (at the temperature range 77 – 450 K). Therefore, the one-band model is widely used for analysis of the electrical properties of materials, estimates of energy spectrum parameters and for the calculations of the thermoelectric efficiency.

EXPERIMENTAL

It should be noted that the temperature dependences of the Hall coefficient (R) are characterized by a significant increase of R, the ratio between the Hall coefficients achieves a value $R_{300}/R_{77} \approx 2$. At the same time, in the experiment in the two-band model in the case of ordinary scattering mechanisms of light and heavy holes (scattering at acoustic phonons and the Coulomb potential of impurities and point defects) the thermopower coefficient has no expected significant increase (see Figure 1). In the physics of semiconductors this effect is commonly explained by the complex structure of the valence band.

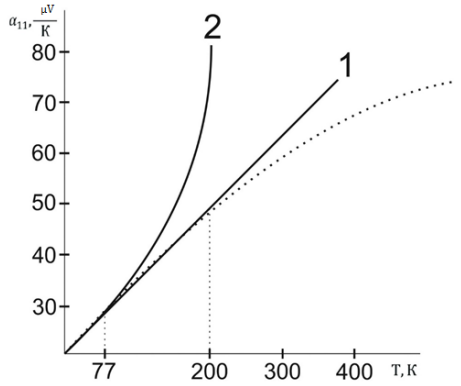

Figure 1. Temperature dependence of the thermopower (α_{11}) in the cleavage plane in the $Sb_2Te_{2,9}Se_{0,1}$ crystal. Dots – experiment; 1, 2 curves – the calculations in the one-band model for degenerate statistics and in the two-band model, respectively.

To explain the observed increase of the Hall coefficient with the temperature growth the two-band model is used, in which the valence band contains two non-equivalent extremes with the different density-of-state effective masses, separated by an energy gap with a width ΔE_v [4, 5].

RESULTS AND DISCUSSION

From our point of view, the above-mentioned contradictions in interpretation of the experimental data can be eliminated by correction of the mechanisms of hole scattering. $A_2^V B_3^{VI}$ crystals are characterized by rhombohedral symmetry, so the Nernst-Ettingshausen coefficient (Q) is a tensor quantity having three independent components Q_{123}, Q_{132} and Q_{321}.

According to available literature data all three components of the Nernst-Ettingshausen tensor are negative numbers at temperatures T ≥ 77 K in all investigated $A_2^V B_3^{VI}$ materials.

The $Sb_2Te_{2,9}Se_{0,1}$ solid solution crystal has the hole concentration $p \simeq 8{,}2 \cdot 10^{19}$ cm^{-3} according to the Hall effect at T = 77 K. Such a high charge-carrier concentration allows analyzing the experimental data using degenerate quantum statistics. In this case the components of the Nernst-Ettingshausen tensor are described by the following formula:

$$Q_{ikl} = \frac{k_0}{e} . \frac{\pi^2}{3} . \frac{k_0 T}{\mu} R_{ikl} . \sigma_{kk} . r_{kk}, \quad (1)$$

where:

k_0 – the Boltzmann constant;

e – the elementary charge;

R_{ikl} – the component of the Hall tensor;

σ_{kk} – the component of the conductivity tensor;

T – the absolute temperature;

μ – the chemical potential;

r_{kk} – the effective scattering parameter which characterizes the scattering mechanisms.

The Nernst-Ettingshausen coefficient is determined by the following expression [6, 7]:

$$Q = \frac{k_0}{e} (R\sigma) \frac{\pi^2}{3} \frac{k_0 T}{\mu} (r - \frac{1}{2}), \quad (2)$$

where r is the scattering parameter.

In the one-band model such behavior of the Nernst-Ettingshausen coefficient clearly indicates the dominance of the acoustic mechanism of hole scattering. According to the two-band model of the band structure the Nernst-Ettingshausen coefficient is determined by the contributions of the both extremes of the valence band in accordance with the expression [4]:

$$Q = Q_1 \frac{\sigma_1}{\sigma} + Q_2 \frac{\sigma_2}{\sigma} + Q_{12} \frac{\sigma_1 \sigma_2}{\sigma^2}. \quad (3)$$

Here, the subscripts 1 and 2 denote the corresponding partial kinetic coefficients for two bands and Q_{12} is a mixed term defined as:

$$Q_{12} = (\alpha_1 - \alpha_2)(u_1 - u_2), \tag{4}$$

where u_1 and u_2 are the hole Hall mobilities in the primary and the secondary extremes of the valence band, respectively.

In the two-band model in the samples with the Fermi level located closely to the top of the secondary extremum of the valence band ($\varepsilon \approx \varepsilon_F \approx \Delta E_v$) the channel of additional scattering of kinetic moment of charge carriers appears. Without energy change electrons can move from the primary extremum to the secondary extremum with momentum change.

This mechanism is called interband scattering. The concepts of interband scattering were originally introduced by N.V. Kolomoets [8] to explain anomalies in the concentration dependences of the thermopower in iron group alloys. In [8] from a combination of four kinetic coefficients according to the formula [6]:

$$\frac{Q}{R\sigma\alpha} = \frac{r - 0.5}{r + 1} \tag{5}$$

for three components of the Nernst-Ettingshausen tensor Q_{123}, Q_{132} and Q_{321} from the experimental data the scattering parameter (r) was calculated at the temperature range 77 – 450 K. It should be noted that the dependence of the relaxation time τ on charge-carrier energy ε describes as the power function $\tau \sim \varepsilon^{r-0.5}$ for the most important and used scattering mechanisms. It turned out that the values of scattering parameter found in this way are close to zero up to 200 K in the cleavage plane of crystals and in the direction of trigonal axis C_3. These results confirm the dominant character of hole scattering at acoustic phonons in different crystallographic directions. At higher temperatures the scattering parameters become negative and are growing rapidly in absolute value. This fact indicates the appearance of additional mechanism of hole scattering with a strong energy dependence of the relaxation time. This scattering mechanism is the above-mentioned interband scattering.

CONCLUSION

Produced estimates show that accounting of interband scattering allow describing observed temperature dependences of the kinetic coefficients and determining the parameters of the band spectrum more correctly.

REFERENCES

[1] B. M. Gol'tsman, V. A. Kudinov, I. A. Smirnov. Semiconductor thermoelectric Bi_2Te_3 based materials. *Nauka*, Moscow (1972). 320 p.

[2] von Middendorff, G. Landwehr. *Sol. State Com*., 11, 203, 1972.

[3] V. V. Sologub, R. V. Parfen'ev, A. D. Goletskaya. *JETP Letters*, 21, (12), 711 (1975).

[4] I. A. Chernik. The research of the transverse Nernst-Ettingshausen effect and transport phenomena in lead chalcogenides: Th. Candidate of Physical and Mathematical Sciences: I.A. Chernik. – L., 1968. – 242 p.

[5] D. A. Pshenai-Severin. The influence of the band structure features on thermoelectric properties of semiconductor/D. A. Pshenai-Severin, M. I. Fedorov//SSP. - 2007, - T.49, vol. 9. - 1559 - 1562 p.

[6] B. M. Askerov. Electronic transport phenomena in semiconductors. - M.: *Nauka*. -1985. 320 p.

[7] B. M. Gol'tsman. Film thermoelements: Physics and Application/B.M. Gol'tsman, Z. M. Dashevskii, V.I. Kaidanov, N.V. Kolomoets. *Film Thermoelements: Physics and Application* (Nauka, Moscow, 1985).

[8] N. V. Kolomoets, SSP, 1966, t.8, N 4, 997 p.

Smart Nanocomposites
Volume 7, Number 2
ISSN: 1949-4823

NONLOCAL KINETIC THEORY OF PLASMA NANOTECHNOLOGY

Igor D. Kaganovich[1], Dmytro Sydorenko[2], Yevgeny Raitses[1], Vladimir I. Demidov[3], Huihui Wang[4], and Alexander S. Mustafaev[*]

[1]Princeton Plasma Physics Laboratory, Princeton, New Jersey, USA
[2]University of Alberta, Edmonton, Alberta, Canada
[3]West Virginia University, Morgantown, West Virginia, USA
[4]School of Physical Electronics,
University of Electronic Science and Technology of China, Chengdu, China
[5]Saint Petersburg Mining University, Saint Petersburg, Russia

ABSTRACT

The purpose of the talk is to describe recent advances in nonlocal electron kinetics in low-pressure plasmas and plasma nanotechnology. Low-pressure discharges are widely used in industry as the main plasma sources for many applications including plasma processing, discharge lighting, plasma propulsion, particle beam sources and nanotechnology. Being partially-ionized, bounded, and weakly-collisional, the plasmas in these discharges demonstrate nonlocal electron kinetic effects, nonlinear processes in the sheaths, beam-plasma interaction, collisionless electron heating, etc. Such plasmas often have a non-Maxwellian electron velocity distribution function. The plethora of kinetic processes supporting the non-equilibrium plasma state is an invaluable tool, which can be used to adjust plasma parameters to the specific needs of a particular plasma application. We report on recent advances in nonlocal electron kinetics in low-pressure plasmas where a non-Maxwellian electron velocity distribution function was "designed" for a specific purpose: in dc discharges with auxiliary biased electrodes for plasma control, hybrid DC/RF magnetized and unmagnetized plasma sources, and Hall thruster discharges. We show using specific examples that this progress was made possible by synergy between full-scale particle-in-cell simulations, analytical models, and experiments.

Keywords: nonlocal electron kinetic effects, nonlinear processes in the sheaths, beam-plasma interaction, collisionless electron heating

[*]alexmustafaev@yandex.ru

1. INTRODUCTION

Low temperature plasmas (LTPs) are widely used in applications and are strongly affected by the presence of neutral species - chemistry adds enormous complexity to the plasma environment. Electron energies in such plasmas are of order a few electron volts with sufficient population of electrons with energies above the threshold energies of the excited states of neutral atoms and molecules. The power transfer from electrons to these atoms and molecules produces activated species (e.g., radicals, excited states, and photons). Due to the low degree of ionization, the mean energy of electrons and ions in such plasma considerably exceeds the temperature of the neutral species. This provides a unique set of conditions wherein plasma species can efficiently react with adjacent surfaces resulting in their beneficial modification. With such properties, low temperature plasmas are widely used in technological processes, ranging from manufacturing of semiconductor chips, solar and plasma-display panels, to the treatment of organic and bio-objects [1]. Examples of recent progress are described in Special Section of Physics of Plasmas "Electron kinetic effects in low temperature plasmas" [2].

The next logical step in the development of electron kinetics was not only explaining the observed kinetic phenomena but using this accumulated knowledge to explore ways of actively crafting electron energy distribution functions (EEDFs) to achieve required effects. This research is the focus of DOE funded Center for Predictive Control of Plasma Kinetics: Multi-phase and Bounded Systems [3]. The complex dependence of different chemical reactions on electron energy places an extraordinary premium on optimally shaping EEDFs to influence the rate of interaction of a particular process. The ability to control the efficiency of the interaction of charged particles with their environment (gas atoms and molecules, or surfaces) depends on the ability to craft and control charged particles and photons distribution functions. Advancing LTP science requires the ability to control and to shape charged particles and photons distribution functions for beneficial treatment of surfaces, which is a challenging task considering the diversity and complexity of the variety of discharge conditions. However, improving the performance of these new plasma tools is still a significant challenge for plasma engineering. Exploitation of nonlocal plasma properties allows additional dimensions and flexibility in adjusting plasma parameters. A remarkable property of such plasmas is that changing conditions in one place may lead to unexpected changes far away in another part of the plasma. Additionally, plasmas with nonlocal EEDF allow independent and effective managing of electrons belonging to different energy ranges [4]. This, in turn, allows modification of the plasma properties in desirable ways, because different energetic groups of electrons are responsible for different processes, and their density modifications yield control over corresponding plasma processes. We report on recent advances in nonlocal electron kinetics in low-pressure plasmas where a non-Maxwellian EEDF was "designed" for a specific purpose.

2. THEORETICAL AND EXPERIMENTAL STUDY OF HALL THRUSTERS

In series of publications we studied plasma properties of Hall thrusters, see Ref. [5] and Refs. within. It was experimentally shown that plasma properties are affected by choice of wall material. For example, changing material from boron nitride to carbon-based materials

yielded significant increase in electron temperature. Analytical and particle-in-cell simulation studies revealed that electron velocity distribution function (EVDF) in Hall thruster is non-Maxwellian, anisotropic and enriched by electron beams emitted from the wall due to secondary electron emission, as evident from Figure 1.

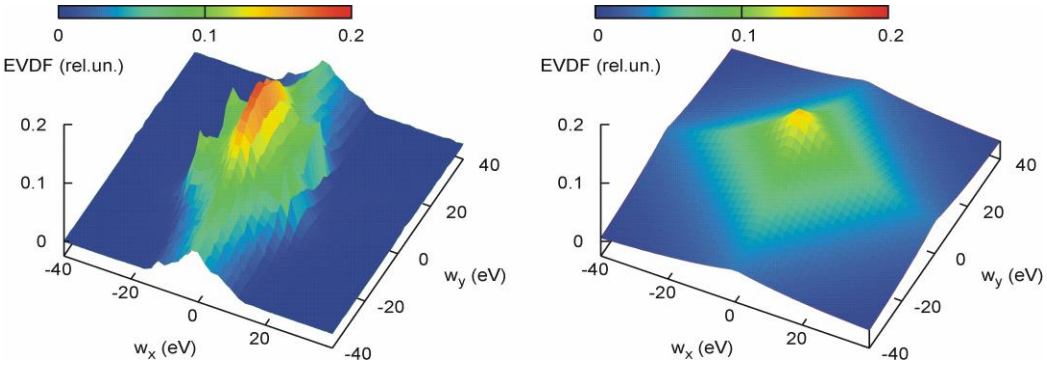

Figure 1.Complex structure of strongly anisotropic (T_x = 12eV, T_z = 37eV) electron velocity distribution function in the channel of a Hall thruster discharge (left) versus an isotropic Maxwellian EVDF (right) [5].

3. Theoretical and Experimental Study of DC Discharges with Auxiliary Electrodes

Second example of a device with nonlocal plasma properties is a short dc discharge (several millimeters in length at the pressure of a few Torr, 10–100 μm for atmospheric pressure). The discharge consists of the cathode and anode sheathes and a negative glow plasma without a positive column. The plasma is created by the energetic electrons emitted by the cathode and accelerated by the near-cathode sheath to the energies above the ionization potential for the gas atoms. In contrast to semiconductor devices, plasma discharges can be used under harsh conditions related, for example, to high temperatures and radiation levels of damaged nuclear plants [6].

A dc discharge with a hot cathode is subject to current and voltage oscillations self-generated by plasma, which have deleterious effects on device operation. The oscillations can be inhibited by installing an auxiliary electrode, placed outside of anode. By collecting a modest current through a small opening in anode, we show that the discharge becomes stable, in a certain pressure range. This method of avoiding current oscillations can be used, for example, for high current stabilizers.

4. Theoretical and Experimental Study of Hybrid DC/RF Plasma Sources

Third example is a plasma etching device used for plasma processing applications. It is a radio frequency (rf) discharge with applied additional dc bias on one of the electrodes [7]. Experimental measurements of electron energy distribution function in a rf/dc discharge with

800 V dc voltage reveal the presence of a peak of super-thermal electrons with energy in the range of 40-400 eV [7].The cathode in the experimental device could emit electrons thus producing an electron beam. We used a particle-in-cell code [8] to investigate acceleration of plasma electrons by an electron beam in a dc discharge with parameters close to those of Ref. [7]. The beam excites electron plasma waves via the two-stream instability. Simulations show that the two-stream instability is intermittent, with quiet and active periods. During the quiet periods, the beam propagates through the plasma with minimal perturbations. During the periods of activity of two-stream instability, the beam interacts with the plasma most intensively at locations where the global frequency of instability matches the local electron plasma frequency. There may be two resonance areas with intense oscillations usually near the edges of the plasma. These intense localized plasma oscillations produce peaks in the velocity distribution function similar to the ones measured in the experiment.

CONCLUSION

We show using specific examples that a lot of progress was made possible by synergy between full-scale particle-in-cell simulations, analytical models, and experiments in understanding and optimization of operation of several very important practical devices: Hall thruster for electric propulsion, dc discharge with thermionic emission for thermionic converters and high power current stabilizers, and rf/dc hybrid discharges for plasma processing applications (etching).

ACKNOWLEDGMENTS

This research was supported by U.S. Department of Energy and Air Force Office of Scientific Research.

REFERENCES

[1] At http://science.energy.gov/fes/news-and-resources/workshop-reports for 2008 Report on Scientific Directions for Low Temperature Plasma sponsored by Department of Energy.

[2] I. D. Kaganovich, V. Godyak, and V. I. Kolobov, *Physics of Plasmas*, Vol. 20, Article ID 101501 (3 pp.), 2013.

[3] See http://doeplasma.eecs.umich.edu/index.htm for the new Center for Predictive Control of Plasma Kinetics: Multi-phase and Bounded Systems, which is funded by a five-year grant from the U.S. Department of Energy.

[4] L. D. Tsendin, "Analytical approaches to glow discharge problems," *Plasma Sources Sci. Technol.*, Vol. 20, Article ID 055011 (18 pp.), 2011.

[5] Y. Raitses, I. D. Kaganovich, A. Khrabrov, D. Sydorenko, N.J. Fisch, A. Smolyakov, *IEEE Transactions on Plasma Science*, Vol. 39, 995-1006 (2011).

[6] S. Mustafaev, V. I. Demidov, I. D. Kaganovich, S. F. Adams, M. E. Koepke, and A. Grabovskiy, "Control of current and voltage oscillations in a short dc discharge making

use of external auxiliary electrode," *Rev. Sci. Instrum.*, Vol. 83, Article ID 103502 (4 pp.), 2012.

[7] L. Xu, L. Chen, M. Funk, A. Ranjan, M. Hummel, R. Bravenec, R. Sundararajan, D. J. Economou,and V. M. Donnelly, "Diagnostics ofballistic electrons in a dc/rf hybrid capacity velycoupled discharge" *Appl. Phys. Lett.*, Vol. 93, Article ID 261502 (3pp.), 2008.

[8] D. Sydorenko, I. Kaganovich, Y. Raitses, A. Smolyakov, "Breakdown of a space charge limited regime of a sheath in a weakly collisional plasma bounded by walls with secondary electron emission," *Phys. Rev. Lett.*, Vol. 103, Article ID 145004 (4pp.), 2009.

Smart Nanocomposites
Volume 7, Number 2
ISSN: 1949-4823

THE USE OF SHUNGITE PROCESSING PRODUCTS IN NANOTECHNOLOGY: GEOLOGICAL AND MINERALOGICAL JUSTIFICATION

Roman V. Sadovnichii, Sergey S. Rozhkov, and Natalia N. Rozhkova*

Institute of Geology, Karelian Research Centre, RAS,
Petrozavodsk, Russia

ABSTRACT

Carbon–rich shungite rocks are promising raw materials for production of adsorbents, catalysts and fillers for polymers of different polarity and inorganic blends. Recently shungite rocks attract attention as a natural source of nanosized carbon. It is considered as the natural carbon allotrope of a multi-level fractal structure produced by the consecutive aggregation of ~1 nm graphene fragments, stacks and the globular composition of the stacks. Aggregates of globules form 3D-net and complete the structure of shungite carbon. Each level is important for obtaining special properties in new materials with shungite carbon nanoparticles. However, heterogeneity of shungite rocks and poor reproducibility of its composition and properties lead to inability to use this valuable raw material in high-tech processes. The ways of homogenization of the raw material obtained of shungite rocks and improvement the efficiency of its application are discussed.

Keywords: shungite rocks, nanocarbon, nanosized quartz, natural composite, nanotechnology

INTRODUCTION

The term *shungite* is used to describe a large group of Precambrian (~2 Ga) carbonaceous rocks [1, 2] occurring in the North Onega synclinorium, Karelia, Russia (Palaeoproterozoic Onega structure, Karelian craton), where they are confined to the rocks of the Ludicovian and Kalevian superhorizons (Palaeoproterozoic) [3]. Shungite rocks vary in mode of occurrence, the timing of formation, genesis, mineralogical composition and other features [4, 5, 6]. The mineral constituent of shungite rocks consists of quartz, carbonates, micas, feldspars and sulphides [5, 7].

* rozhkova@krc.karelia.ru

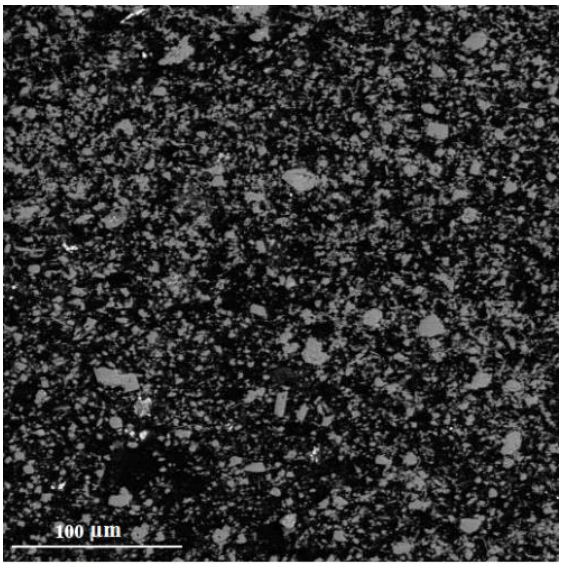

Figure 1. SEM image (BSE-detector) of carbon-quartz microstructure of shungite rocks: white – sulphides; grey – quartz and alumosilicates; black – carbon.

The demineralized organic matter of shungite rocks (*shungite matter*) is composed of carbon (96 – 98%), hydrogen (0.31 – 0.64%), nitrogen (0.51 – 0.81%), sulphur (0.18 – 1.22%) and oxygen (0.11 – 1.74%). Shungite matter also contains V, Ni, Mo, Cl, Si, Na and Fe distributed in a uniform manner dominantly as micromineral roscoelite, paragonite, pyrite, millerite, violarite, sphalerite and chalcopyrite inclusions measuring 2 – 10 μm [6].

The mineral constituent of shungite rocks from the Zazhogino deposit, consisting dominantly of quartz and lesser alumosilicates and sulphides, is distributed regularly in an amorphous carbon matrix (Figure 1) [8]. Mineral grains vary in size from 0.1 to 10 μm, but the most probable size is less than 1 μm. Shungite rocks display a two-frame structure: a silicate-quartz mineral framework pierces through the carbon matrix; a carbon framework is much more durable than a mineral one at the same volumetric concentration of the matter [1]. This hybrid carbon-quartz microstructure is responsible for the main physicochemical characteristics of shungite rocks [9].

Shungite rocks with such structure were formed in a colloid water environment under relatively mild thermodynamic conditions. The size and finely dispersed distribution pattern of mineral constituents in the carbon matrix are such that shungite rocks can be used for production of nanosized hybrid (carbon-quartz) fillers and pigments with high indices for some physicochemical properties [10, 11]. The goal of the study was to obtain high-quality products for nanotechnology from shungite rocks.

2. EXPERIMENTAL

In the frame of the study of structural and textural characteristics of shungite rocks and their constituents series of experiments were performed [8]. SEM analysis was conducted on a VEGA II LSH scanning electron microscope manufactured by TESCAN, coupled with an EDX - INCA Energy 350.

Thermal analysis (TG) was conducted on a Netzsch STA 449 F1 Jupiter in a dynamic mode at an airflow of 20 ml/sec. The sample was heated from room temperature to 1200°C at a rate of 10°/min. TG and DSC spectra were processed using Proteus software.

Raman analysis were carried out using a dispersive Nicolet Almega XR Raman spectrometer with the laser 532 nm, Nd-YAG. The spectra were collected at 2 cm^{-1} spectral resolution. Raman spectral data were determined using OMNIC software.

Powder X-ray Diffraction patterns were collected at room temperature, using ARL X'TRA diffractometer with CuKα radiation (λ = 1.54184Å). Data were collected at 2θ from ~2° to 156.5°, profiles of reflection peaks were measured with a step size of 0.01° and a step-counting of 3 sec. Apparent coherent length was determined using the Scherrer equation.

3. COMPOSITION AND STRUCTURE OF SHUNGITE ROCKS

The Zazhogino deposit, located in the Medvezhyegorsk district, Republic of Karelia, Russia, is now the only mined high-carbon shungite deposit. It consists dominantly of massive-, vein- and breccial-textured shungite rocks. Zazhogino shungite rocks are composed mainly of carbon and silica. Their carbon content varies from 15 to 50 wt. %, silica content from 40 to 75 wt. % and the total content of these components in the rock from 87 to 90 wt.% [6]. Massive-textured shungite rocks and the clastic portion of vein- and breccial-textured rocks consist of microgranular carbon-quartz aggregates with a small alumosilicate-sulphide impurity (Figure 1). Vein- and breccial-textured shungite rocks contain considerable quantities of morphologically varied quartz aggregates such as inclusions, veins, streaks and matrix zones in breccial-textured rocks. The veins and streaks often exhibit a complex, discontinuous distribution pattern and are about several millimeters thick. They consist dominantly of milky quartz, but some are composed of rod-like sericite aggregates. The matrix of shungite breccia consists mainly of quartz and lesser sericite, pyrite and shungite carbon. The colour of the matrix varies with the carbon concentration and morphology. Black-matrix and white-matrix breccias are thus distinguished [8].

4. CARBON OF SHUNGITE ROCKS

Structural hierarchy of shungite carbon (ShC) at a nanoscale of 1-100 nm has been thoroughly studied by complex experimental methods [12]. ShC formed under different conditions was characterized by a similar multi-level structural pattern and physico-chemical properties, attributed to distinctive interaction between the nanostructural elements of carbon and water. Water plays a key role in conservation of all the structural levels of carbon in shungite rocks [13]. The size distribution of pores for ShC from different deposits is characterized by the dominance of micro- and submesopores, less than 0.7 –5.0 nm in size, and correlates with the sizes of basic structural elements (graphene fragments ~ 1 nm) and with the sizes of primary shungite carbon aggregates [14]. Recently the microscopic concept of the structural arrangement of shungite carbon has been strongly supported by the analysis of the empirical data obtained by quantum-chemical modeling [15].

Substitution of water by non-polar molecular solvents drastically changes the size and structure of nanocarbon aggregates. Globules were transformed into stacks and flakes as

shown in condensate of carbon tetrachloride dispersion on a glass substrate (Figure 2a, b) [16]. It helps to clarify the differences in morphology of ShC in nature. Flaxes, stacks and films were reported in natural carbon of shungite rocks [17] as well as sp^2–bonded structures in contact with quartz – or chlorite-dominated rocks [7].

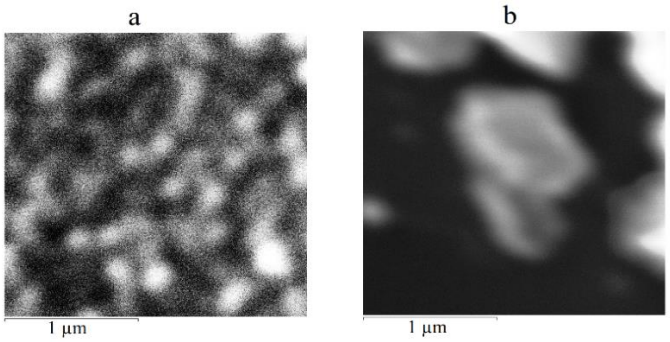

Figure 2. SEM images of shungite carbon nanoparticles dispersions condensate on glass substrate from water (a) and carbon tetrachloride (b).

5. QUARTZ OF SHUNGITE ROCKS

Quartz is the main mineral of shungite rocks from Zazhogino deposit. At least three morphological varieties of quartz are distinguished: I – quartz is a part of the carbon-quartz aggregate of massive-textured shungite rocks and the clastic portion of vein- and breccial-textured rocks (Figure 1); II – quartz from morphologically different veins and streaks that cross-cut shungite rocks; III – quartz of shungite breccia matrix [8].

The study of three morphological quartz varieties using X-ray diffraction analysis [18] has shown that they are all represented by well-crystallized α-quartz which is a part of the carbon-quartz aggregate, veins, streaks and matrix component of shungite breccia. The lattice parameters (a, b, c) of I and III quartz varieties are similar (a, b = 4.9138(2) Å, c = 5.4057(3) Å) and are comparable with those of rock crystal (a, b = 4.9140(1) Å, c = 5.4056(1) Å) and silicite (a, b = 4.9137(1) Å, c = 5.4054(2) Å), and the lattice parameters of II quartz variety (a, b = 4.9135(1) Å, c = 5.4050(2) Å) are similar to those of pegmatite quartz (a, b = 4.9132(4) Å, c = 5.4052(8) Å).

Apparent coherent length (ACL) shows the size of crystallites. The ACL of I and III quartz varieties is ~ 80 nm and that of II quartz crystallite variety is ~ 65 nm. Thus, quartz of shungite rocks from the Zazhogino deposit is nanosized.

The study of quartz of shungite rocks using thermal analysis and Raman spectroscopy [18] has shown that carbon is presented in various concentrations in all quartz samples analyzed. The variable structural ordering of ShC is reflected in the DSC curves of the samples [19]. The higher the maximum exo-effect temperature of the oxidation reaction of ShC corresponds to the higher structural ordering of shungite carbon (Figure 3).

Differences in the burning-out temperature of carbon have led the authors to conclude that shungite carbon of carbon-quartz aggregates or massive shungite rocks is associated with quartz variety I, more active carbon with quartz variety II and more ordered carbon with quartz variety III.

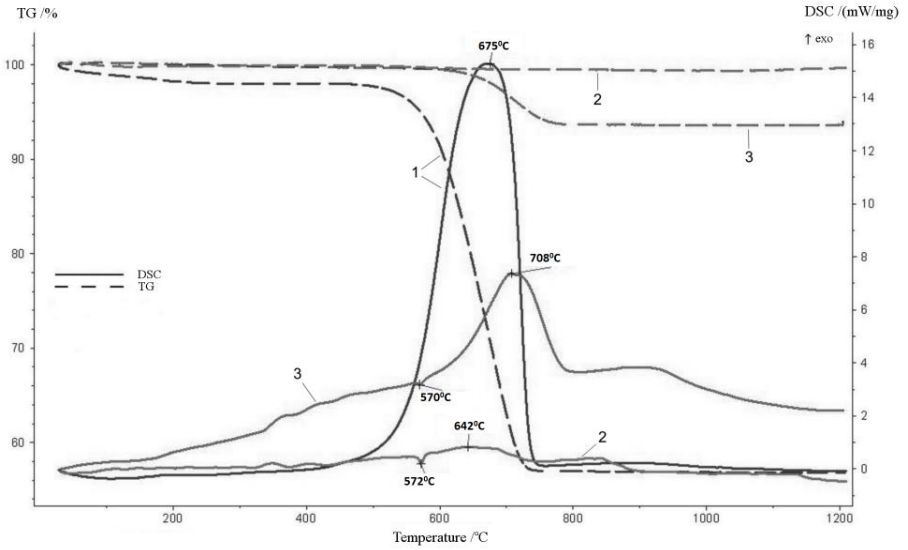

Figure 3. Thermal analysis curves (thermogravimetry (TG), differential scanning calorimetry, (DSC)) of massive-textured shungite rock samples (I quartz variety) – 1, vein quartz (II quartz variety) – 2 and quartz of matrix component of shungite breccias (III quartz variety) – 3.

The structural properties of carbon and quartz are interdependent. As carbon concentration changes (peaks D,G and S_2), the degree of covering of quartz grains changes as well, affecting the intensity and width of the Raman spectra of quartz (peaks at frequencies below 500 cm^{-1}) (Figure 4).

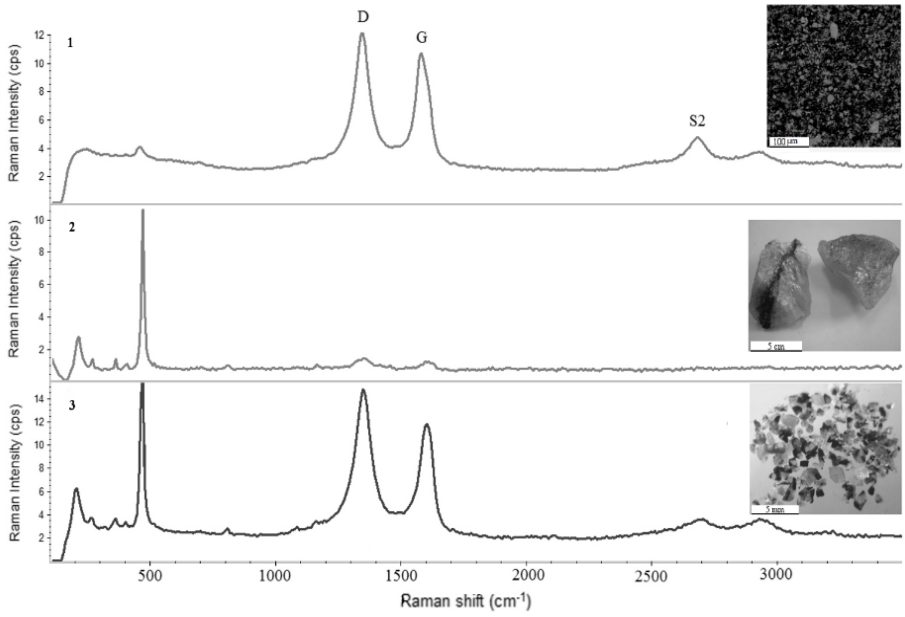

Figure 4. Raman spectra of the samples: 1 – massive-textured shungite rock, 2 – vein quartz, 3 – quartz of matrix component of shungite breccias

Thus, quartz is the distinctive constituent of shungite rocks responsible for their major physicochemical and technological properties. All textural types of shungite rocks seem to retain well-crystallized nanosized quartz which can be considered as an individual type of the mineral raw material of shungite rocks. A major role in maintaining and shaping of the nanosized quartz should be given to nanostructured shungite carbon.

6. PROCESSED SHUNGITE RAW MATERIALS FOR NANOTECHNOLOGY

Quartz of shungite rocks regardless of the formation revealed structural identity. Quartz, like shungite nanocarbon, is an important constituent of shungite rocks and could be regarded as a non-conventional raw material for shungite deposits (Figure 5, 1a) [18].

Shungite nanocarbon is a promising material for the development of nanotechnologies. Biomedical application is the most challenging as long as carbon nanoparticles are available in the form of stable dispersions in water (Figure 5, 2b) [20]. Water plays a role of a disperse medium and a regulator of intermolecular interactions among structural levels of nanoparticles. The advantage of shungite nanocarbon over known synthetic nanocarbons is in the way of its green synthesis, namely through stable aqueous dispersion without any additives.

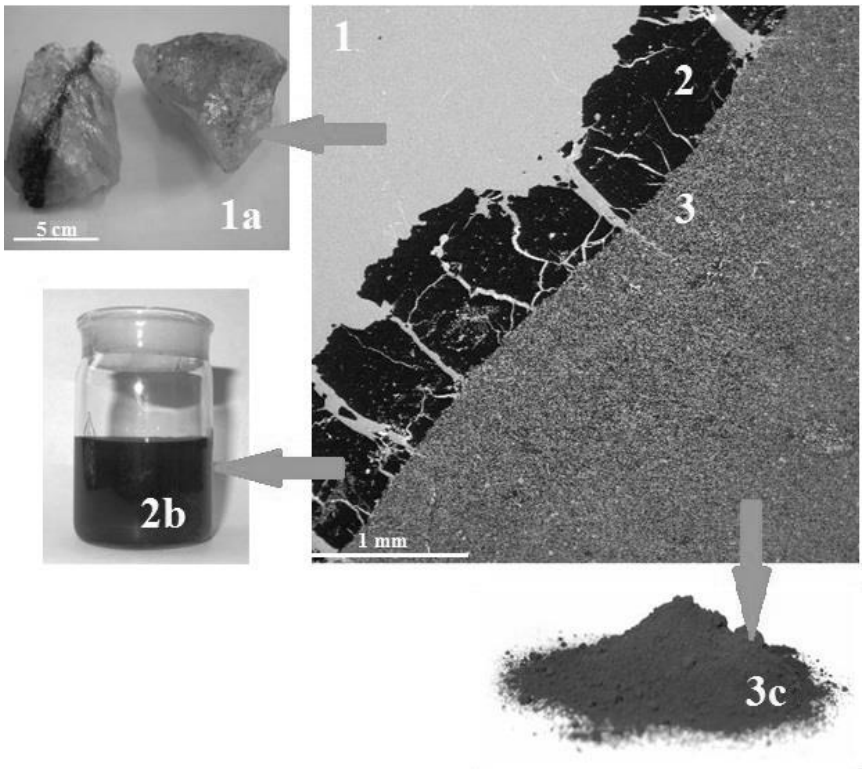

Figure 5. Scheme presenting results of mineralogical differences in shungite rocks and processing products: SEM image of vein shungite rock: 1 – quartz; 2 – shungite carbon; 3 – microgranular carbon-quartz aggregate, 1a – α-quartz with ACL ~ 65 nm, 2b – aqueous dispersion of ShC nanoparticles, 3c – powder of a nanosized hybrid ShC-silica.

Shungite rock material in a powdered form was used as a filler (ShF) for different polymeric matrixes. The size of ShF particles was in the range of 0.5-10 μm, surface area 22-45 m^2/g. Its distinctive feature was complex composition of every particle 1-3 μm in size, which contained both carbon and mineral phases [9].

It was reported on interconnection of physical and mechanical (elastic modulus, yield point), and electrical (conductivity on the AC and DC) properties of compositions of polypropylene (PP)–ShF and PP-polyethylene-ShF with the changes of the structural organization of the polymer matrix (the size of spherulites, the degree of crystallinity) in dependence of the volume fraction of the filler [21].

However, brittle fracture patterns happened with the introduction of small amounts of ShF. Furthermore, it was difficult to achieve a uniform distribution of filler particles in the polymer matrixes due to particle aggregation [21]. Obviously, the use of conventional processing technology resulted in poor reproducibility of the compositions and properties of ShF depending on the production method and the conditions of storage of raw materials.

Some effects produced by the filler introduction in polymer composites could be explained only due to the mobility of shungite carbon nanoparticles and their graphene structural unit [22].

The deciphering of the main structural element and structural hierarchy of shungite nanocarbon has made it possible to develop a method for stabilizing the composition and properties of shungite filler so that its amphiphilicity (ability to combine with matrices of different polarity) is retained. The shungite powder produced with particles less than 100 nm in size and surface area ~ 100 m^2/g, retains the interpenetrating nets of nanocarbon and nanosized silica (Figure 5, 3c) [11].

Studies have been conducted to determine the structure and properties of composite materials with the nanosized shungite filler (NShF) in comparison with the convenient ShF incorporating into PP.

A homogeneity of the emerging crystalline phase of PP in the presence of nanoscale NShF has been determined. Atomic-force microscopy images of the surface topography observed spherulite size reduction to 100-200 nm in PP with ~30 vol.% of NShF. When using ShF observed a decrease in the size of the spherulites from 80 μm (pure PP) to 2-10 μm (when filled with 30 vol.%).

The main result of the introduction of NShF is the increase of the elasticity of filled PP. Thus, when PP contains 5 and 10 vol.% of NShF, the elasticity of the samples (elongation at break) was 450 and 50%, respectively. Whereas, when the introduction of 5 vol.% of ShF occurs brittle fracture (elongation at break is 15%). This fact confirms that the introduction of NShF resulted in its uniform distribution in the thermoplastic matrix.

The new filler is well distributed in the polar polymers as well, namely carbamide-formaldehyde resin for wood chipboards [10]. The composition with NShF shows a significant decrease in indicators of swelling and water absorption. There has been a significant increase of the strength of composition also. If compared with the control composition flexural strength increased by 41% and the tensile strength perpendicular to the plate increased by 104%. Such high rates of physical and mechanical properties can be due to the previously established ability of shungite carbon nanoparticles to form a 3-dimensional nanocarbon net that could structure and reinforce polymeric matrix.

CONCLUSION

Geological and mineralogical study of shungite rocks helped to identify the main structural and mineral features to control for applying shungite rocks in the field of nanotechnology. The hybrid carbon-quartz microstructure of shungite rocks and finely dispersed distribution pattern of mineral constituents in the carbon matrix made it possible to produce nanosized fillers and pigments with high indices of the main physicochemical properties. Shungite carbon, forming concentrated mineral inclusions in shungite rocks, could be used in the manufacture of nanoparticles dispersions for the biotechnological applications. Quartz of shungite rocks was formed of nanosized crystallites with similar parameters of the unit cell and was considered as a new non-traditional raw material of shungite rocks.

Heterogeneity of shungite rocks and poor reproducibility of its composition and properties could be solved in several steps, starting from mineralogical control and separation at the stage of extraction of raw materials. One of the new approaches for such control has been suggested recently [23]. The next step concerns separate processing of each type of the raw materials: carbon-quartz hybrid, shungite nanocarbon and quartz.

ACKNOWLEDGMENTS

The work was partly supported by the RFBI grant 13-03-00422.

REFERENCES

[1] Buseck, P. R.; Galdobina, L. P.; Kovalevski, V. V.; Rozhkova, N. N.; Valley, J. W.; Zaidenberg, A. Z. *Canadian Mineralogist* 1997, vol. 35, Part 6, 1363–1378.

[2] Melezhik, V. A.; Filippov, M. M.; Romashkin, A. E. *Ore Geol Rev* 2004, vol. 24, 135–154.

[3] Medvedev, P. V.; Melezhik; V. A.; Filippov, M. M. *Paleontological Journal* 2009, vol. 43, N 8, 972–979.

[4] Chazhengina, S. Y.; Kovalevski, V. V. *Eur. J. Mineral* 2013, vol. 25, 835–843.

[5] Melezhik, V. A.; Medvedev, P. V.; Svetov, S. A. In *Reading the Archive of Earth's Oxygenation.* Vol.1 Global Events and the Fennoscandian Arctic Russia – Drilling Early Earth Project; Melezhik, V. A. Frontiers in Earth Sciences; Springer: Heidelberg, 2013; pp. 387 – 493.

[6] Filippov, M. M. *Shungite-bearing rocks of the Onega structure*; Karelian Research Centre, RAS: Petrozavodsk, 2002; 282 p. (in Russian).

[7] van Zuilen, M. A.; Fliegel, D.; Wirth, R.; Lepland, A.; Qu, Y.; Schreiber, A.; Romashkin, A. E.; Philippot, P. *Geochimica et Cosmochimica Acta* 2012, vol. 83, 252–262.

[8] Sadovnichii, R. V.; Rozhkova, N. N. *Transactions of the Karelian Research Centre of RAS Precembrian Geology Series* 2014, Vol. 1, 148–158 (in Russian).

[9] Rozhkova, N. N. *Composite Interfaces* 2001, vol. 8. N 3, 4, 307-312.

[10] Panov, N. G.; Pituhin, A. V.; Rozhkov, S. S.; Tzvetkov, V. E.; Sanaev, V. G.; Firyulina, O. V. *Forest gazette. Moscow State Forest University* 2012, vol. 2, 135-139 (in Russian).
[11] Rozhkov, S. S.; Rozhkova, N. N. Patent RF 2448899 (2012).
[12] Rozhkova, N. N.; Emel`yanova, G. I.; Gorlenko, L. E.; Jankowska, A.; Korobov, M. V.; Lunin, V. V. *Smart Nanomaterials* 2010, vol. 1, 71-90.
[13] Rozhkova, N. N.; Gribanov, A. V.; Khodorkovskii, M. A. *Diam Rel Mat* 2007, vol. 16, 2104-08.
[14] Rozhkova, N. N. *Nanocarbon of shungites*; KarRC, RAS: Petrozavodsk, 2011; 100 p. (in Russian).
[15] Sheka, E. F., Rozhkova, N. N. *Int. J. Smart Nano Mater* 2014, vol. 5, 1–16.
[16] Razbirin, B. S.; Rozhkova, N. N.; Sheka, E. F.; Nelson, D. K.; Starukhin, A. N. *JETP* 2014, vol. 145, N 5, 838-850.
[17] Rozhkova, N. N.; Mikhaylina, A. A.; Rozhkov S. S. *Geology and Mineral Resources of Karelia 2014*, vol. 17, 86-93 (in Russian).
[18] Sadovnichii, R. V.; Mikhaylina, A. A.; Rozhkova, N. N.; Inina, I. S. *Transactions of the Karelian Research Centre of RAS Precambrian Geology Series* 2015, vol. 2, 73-87 (in Russian)
[19] Zaidenberg, A. Z.; Rozhkova, N. N.; Kovalevski, V. V.; Tupolev, A. G. Fullerene *Science and Technology* 1998, vol. 6, N 3, 511–517.
[20] Rozhkova, N. N.; Rozhkov, S. P.; Goryunov, A. S. In *Carbon Nanomaterials Sourcebook*. Vol. I: *Graphene, Fullerenes, Nanotubes, and Nanodiamonds*. Sattler, K. D.; Ed.; CRC Press. 2016; pp. 151-174.
[21] Rozhkov, S. S.; Kedrina, N. F.; Timofeeva, V. A.; Chmutin, I. A.; Ryvkina, N. G.; Solov'eva, A. B. *Russian Journal of Physical Chemistry* A 2007, vol. 81, N 11, 1863–1869.
[22] Rozhkova, N. N. In *Perspectives of Fullerene Nanotechnology*; Osawa, E.; Ed.; Kluwer Academic Pub: Dordrecht, 2002; pp. 237-251.
[23] Sadovnichii, R. V.; Rozhkova, N. N.; Gorbunova, E.V.; Chertov, A.N. *Obogashchenie Rud* (Mineral processing) 2016, N1,10-15 (in Russian).

Smart Nanocomposites
Volume 7, Number 2
ISSN: 1949-4823

DEVELOPMENT OF SOLID STATE HYDRIDE SYNTHESIS OF SURFACE-NANOSTRUCTURED DISPERSE METALS

Andrey G. Syrkov[1,*], Vadim R. Kabirov[1], and Vitalii S. Kavun[2]
[1]Mining University, St. Petersburg, Russia
[2]Lappeenranta University of Technology, Finland

ABSTRACT

It is established that conducting the solid-state hydride synthesis (SHS) of metals using methane as a carrier-gas at stages of drying and reduction initial oxide by silicon-hydride reagent leads to the increase of specific surface area and hydrophobicity of metal product by no less than 1.5 times, maintaining the high oxidation stability (0.1 - 0.4 mcg/cm^2 at 900˚C in 100h). The cause of this effect is that formation of hydrophilic centers of the surface is being blocked at all stages of SHS.

Keywords: solid-phase reduction of metals in vapor of organohydridesiloxanes, methane chemisorption, hydrophobicity, specific surface area, metals with carbosiloxane groups on surface

INTRODUCTION

Solid-state hydride synthesis (SHS) of metals is known as a method of obtaining surface-modified metals and thermochemical stabilizing their surface [1-3]. SHS is based on the reduction of solid metal substances, in the open flow system, according to the special program, using volatile and thermally stable hydrogen compounds (N, C, Si and others). One of the modes of SHS, in which solid oxides or chlorides of Ni (II), Fe (II), and Cu (II) are reduced to the metal as a result of consistent interaction of the solid phase with vapors of methyldichlorosilane (MDCS) and methane (purified natural gas) under heating, is described in paper [1]. As the result of the synthesis, carbosiloxane and silicon carbide protection films are formed on the surface of dispersed metals [1, 2]. The obtained Si-C-containing metallic materials have proved to be extremely stable during the high-temperature oxidation in air.

* Corresponding author: syrkovandrey@spmi.ru

It was presented in the paper [3] that in order to remove the chlorine-containing reagent (methyldichlorosilane) and to avoid evolution of HCl(g) during SHS, the vapors of hydrophobic silicone-organic liquid (HSL) based on ethylhydridesiloxane were tested as silicon hydride reducing agent. HSL is used as a water-repellent modifier and is usually applied from liquid phase [4].

Application of the HSL vapors at one of the stages of SHS and the higher-temperature treatment in the CH_4 environment in order to destruct the Si-H-bonds and to seal the protective carbosiloxane film, has not led to noticeable heat stability enhancement of the material in air [3]. MDCS or HSL vapors were delivered to the reaction in stream of Ar [1, 3].

The aim of this work was to estimate the impact of carrying out all stages of SHS in the CH_4 environment on the hydrophobicity and specific surface area of metallic products of SHS and to compare them with the corresponding characteristics of the solid products of synthesis, which were obtained using modes, which were previously described [1, 3].

EXPERIMENTAL METHODS

Pretreatment of reagents, temperature conditions and methods of the synthesis were discussed in works [1, 3, 5]. The synthesis consists of three stages: 1 – drying of the initial solid oxide (chloride) in a noble gas environment, 2 – reduction of dehydrated metal compound by silicon hydride reagent (MDCS or HSL) in the stream of carrier gas, 3 - high-temperature treatment in methane. The structural and chemical characteristics of the solid products of SHS, obtained using three different modes were compared with each other. Mode I: drying of the oxide or chloride by heating in the stream of methane; reduction by HSL-94 vapors (GOST 10834-76) in the methane environment; high temperature treatment in methane environment (TU 58841-87). Mode II: drying initials in the stream of Ar; reduction by MDCS vapors in the stream of Ar; high temperature treatment in methane. Mode III: drying in the stream of Ar; reduction by HSL vapors in the stream of Ar; high temperature treatment in CH_4. In order to compare accurately properties of metallic products of SHS, obtained in different modes, analogical stages of the synthesis were carried out at the same temperature. The temperature of the experiment did not exceed: at the stage of drying – 350˚C, at the stage of reduction – 340˚C, at the stage of high temperature treatment – 600˚C [1-3, 5]. The water vapor adsorption on the samples was determined gravimetrically using desiccator method at relative pressure of P/Ps = 0.96–0.98 (20˚C). The value of specific surface area of the samples was measured by using BET multipoint method (low-temperature adsorption of nitrogen). The heat stability (HS) of SI-C-containing metallic products of SHS was determined by placing samples at the same time in laboratory muffle furnace “Snol” with free access of air to the samples. The HS of the samples (confirmed by XRF and EDX-spectroscopy) was defined gravimetrically after treatment of the solid products of SHS in furnace at 900˚C for 100 hours [3]. The furnace temperature was maintained with accuracy ±5˚C. Atmospheric pressure was from 101.0 to 101.3 kPa; relative humidity was 70 ± 10 %.

The initial powders of oxides of Cu (II), Ni (II), Fe (II) and chloride of Fe (II) had qualification not lower than “chemically pure” and specific surface area was about 1 m^2/g.

RESULTS AND DISCUSSION

From the Table, it follows that the metallic products of SHS, obtained in mode I, have the largest specific surface area and are the most hydrophobic (decrease in adsorption of water vapors by almost 2 times). As it can be seen from the Figure, the dependence between specific surface area (S_{sa}) of the samples and hydrophobicity ($1/aH_2O$) for different metals is almost linear. Another fact which follows from the results, shown in Table and Figure, is very interesting. The fact is that depending on the used mode of the SHS, the hydrophobicity and S_{sa} of solid products increase. It is important to note that high heat stability of the samples stays the same using different modes. The growth of S_{sa} and decrease in the value of adsorption amount of water on the sample corresponds to the sequence of modes: mode II – mode III – mode I. The novelty of the last two statements is that they are formally in contradiction with existing understanding that the increase of dispersion of solids, generally, leads to the increase of chemical activity. It is especially relevant for the oxidation of disperse metals [6, 7] (remind of the combustion of iron powder in the air, which is obtained by decomposition of its oxalate). The improvement of the hydrophobicity of the solid product of SHS, obtained using mode I can be explained by the following fact. Apparently, carrying out all stages of synthesis in the environment of thoroughly dried (by using low-temperature zeolite trap [3, 5]) methane leads to blocking the hydrophilic centers of solid surface due to dissociative chemisorption of methane. According to Trapnel [8], the dissociative chemisorption of CH_4 takes place even at low temperatures. Due to the thermostability of the C-H bonds, methyl groups are detected on the oxide and metal surface above 600˚C [5, 9, 10]. The data of the IR-spectroscopy directly shows the presence of alkyl groups in the solid products of SHS after the reduction and high temperature treatment stages [3, 5].

The increase of water-repellent properties of the surface at the stage of drying of NiO is evidenced by the following experimental facts. For the same gas flow - 0,5 L/min (of CH_4 in mode I or Ar in mode III) the constant mass of the samples was reached faster in the mode I (1.3 and 2.0 h, respectively). In addition, the NiO powder, dried in Ar, almost immediately settles to the bottom, when it was placed in a glass of water. In case of NiO, dried in CH_4 (mode I), the powder particles spent hours floating on the water surface, the smaller particles – up to several days.

Table 1. The structural and chemical characteristics of the solid products obtained using different modes of SHS (I, II, III)

The sample on the metal basis	I The conduct of all stages in CH_4 environment (reduction by HSL)			II Reduction by MDCS in Ar environment			III Reduction by HSL in Ar environment		
	S_{sa}, m^2/g	$\Delta m_{H2O}/m$, %	HS, μg /cm^2	S_{sa}, m^2/g	$\Delta m_{H2O}/m$, %	HS, μg /cm^2	S_{sa}, m^2/g	$\Delta m_{H2O}/m$, %	HS, μg /cm^2
Nickel	15	0.42	0.399	11	0.89	0.401	10	0.85	0.398
Iron	3	0.11	0.100	1	0.19	0.101	2	0.20	0.102
Copper	18	0.51	0.300	12	1.00	0.303	13	0.98	0.301

*where S_{sa} – specific surface area; $\Delta m_{H2O}/m$ – mass of sorbed water (Δm_{H2O}), relative to mass (m) of initial sample, at p/p_s=0.98 (20˚C); HS –heat stability of the sample (900˚C, 100 h); HSL – hydrophobic silicon-organic liquid ; MDCS – methyldichlorosilane.

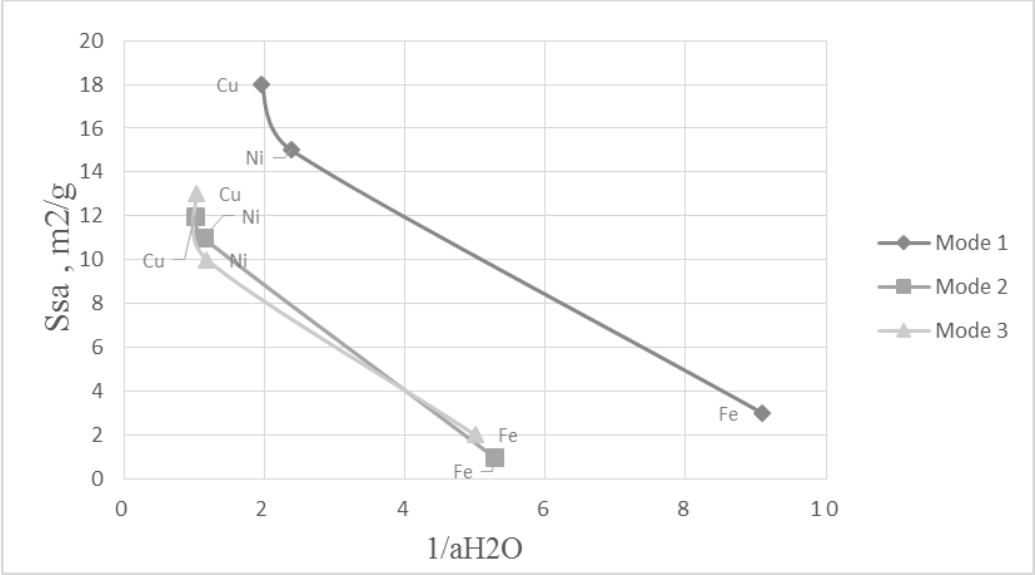

Figure 1. The dependence of S_{sa} from value $1/aH_2O$ for different modes of SHS.

SHS is the complex physics and chemical process, which is associated with breaking M-O, M-Cl (M-metal) bonds in the solid reagent at the stage of reduction and breaking Si-H bonds in chemisorbed HSL at the stage of high temperature treatment in CH_4 [2, 5]. The mentioned processes of destruction of chemical bonds lead to the appearance of corresponding radicals on the solid surface of metals – the centers of chemisorption of CH_4. During the synthesis in mode I initially adsorbed (at drying stage) methyl hydrophobic groups prevent particles from sticking due to the regular mechanism of the formation of hydrogen bonds [7]. Apparently, the same process, predetermines the formation of high specific surface area of solid phase at the reduction stage and in the final product. The obtained powder with increased specific surface area does not show enhanced chemical activity during the high-temperature oxidation. The reason for that, in our opinion, lies in the peculiarities of the synthesis of metals, using SHS method. Even in case of formation of more developed surface in mode I, the surface is saturated by molecules that passivate the metal [2]. Not only molecules of CH_4, but also the molecules of silicon-organic reducing agent [3, 5] with more reactive Si-H bond, than C-H [4] take part in modification of the surface of metals. The mechanism of thermochemical stabilization of metal surface due to strong heteroatomic interaction $M \rightarrow Si$ (according to XPS), which takes place in the reduction of Ni, Fe, Cu by vapors of HSL in terms of SHS, is discussed in detail in paper [3].

CONCLUSION

Using methane as a carrier-gas at stages of drying and reduction initial oxide by silicon-hydride reagent leads to the increase of specific surface area and hydrophobicity of metal product by no less than 1.5 times, maintaining the high oxidation stability (0.1 - 0.4 mcg/cm^2 at 900˚C in 100 h). The cause of this effect is that formation of hydrophilic centers of the surface is being blocked at all stages of SHS.

Rows of increase of specific surface area (S_{sa}) and hydrophobicity of the metal product at the different modes of SHS were established. The dependence between S_{sa} and hydrophobicity of metal product (~ $1/aH_2O$) for each of three studied modes of SHS, which are characterized by increase of S_{sa} in the next sequence: Fe-, Ni-, Cu- sample, is found.

ACKNOWLEDGMENTS

The work was carried out with the financial support of the Ministry of education and science of the Russian Federation (State contract № 14.577.21.0127 from 20 October 2014. Unique identifier of applied research RFMEFI57714X0127).

REFERENCES

[1] Syrkov A. G. *J. Inorg. Chem.* 1993, Vol. 38, no 5, pp. 753-759.
[2] Meretukov M. A., Tsepin M. A., Syrkov A. G., Vorob'ev S. A. *Clusters, structures and materials of the nano-scale: an innovative and technical prospects*; Moscow: Ore & Metalls Publ.House, 2005; 128 p.
[3] Tufrikova V. F., Syrkov A. G., Remzova E. V., Zhurenkova L. A. *Condensed matter and interphase boundaries*. 2011, Vol. 13, no 3, pp. 345-347.
[4] Khananashvili L. M., Andrianov K.A. *Technology of organoelemental monomers and polymers*; Moscow: Chemistry Publ., 1983; 416 p.
[5] Syrkov A. G. From Laboratory to Industry, *Smart Nanoobjects;* Ed. by Levine K. New York: Nova Science Publishers, Inc., 2013; 214 p.
[6] Roberts M., Makki Ch. *Surface chemistry of the gas-metal interface;* Moscow: Mir Publ., 1981; 539 p.
[7] Anderson Dzh. *Structure of metallic catalysts*; Moscow: Mir Publ., 1978; 482 p.
[8] Trepnel B. *Chemisorption*; Moscow: Mir Publ., 1958; 320 p.
[9] Ehrlich G., Stewart CN. *Chem. Phys. Letters*. 1972, Vol. 16, no. 1, pp. 203-210.
[10] Davydova L. P., Popovskii V. V., Bulgakov N. N. et al. *Kinetics and Catalysis*. 1988, Vol. 29, no 5, pp. 1162-1168.

Smart Nanocomposites
Volume 7, Number 2
ISSN: 1949-4823

THE USE OF SURFACE PASSIVATION ON THE NANOSCALE LEVEL AND NANOTRIBOLOGY ON MODERN MINING-CHEMICAL INDUSTRIES FOR CONTROL PROPERTIES OF LUBRICANT AND PROTECTION OF METALLIC EQUIPMENT

A. G. Syrkov[1,*], I. V. Pleskunov[2], and A. A. Vinogradova[1]
[1]Mining University, St. Petersburg, Russia
[2]IMC Montan, London, Great Britain

ABSTRACT

The experience of the implementation into enterprises mineral complex of the nanostructured methods of protection of steel constructions in salt mines and extend the life of the transmission equipment using surface-modified metal additives has analyzed. It's shown the efficiency of evaluation and control of anti-friction properties of the lubricant by level hydrophobicity of additive and stability to high temperature oxidation.

Keywords: protection of metal constructions, nanotribology, control of lubricant, mining-chemical enterprises

INTRODUCTION

Modernization of mineral resources complex is one of the most important directions of the science and technology policy of Russia. Need of introduction of high technologies, including nanotechnology, is closely connected with the solution of import problems which escalated in 2014-2016 caused by the sanctions of the Western countries regarding domestic producers. In this study the experience of implementing and testing nanotechnology for protection from corrosion of steel constructions and increasing operating life of the transmission nodes in the mining and chemical plant equipment on the example of the factory "Belaruskaliy" was analyzed. Among components of air atmosphere of this factory are aggressive impurities (KCl, HCl, SO_2) at the level of 0.04 - 0.20 mg/m3 at a relative humidity of at least 70%.

* Corresponding author: syrkovandrey@spmi.ru

MATERIALS AND METHODS

Two methods were used to create protective coatings on metal in the Scientific and Educational Center of Nanotechnology at the Mining University (St. Petersburg):

1. Layering on steel traditional painting materials (bitumen lacquer, varnish natural, primer - enamel HV and aluminium-containing paint -BT) containing a small amount of nano-structured filler with submicron particle size, obtained by using solid-state hydride synthesis [1, 2].
2. Layering in different sequence on the surface of the steel 3 (St) nanofilms made from domestic cationic tensides and of the hydrophobic silicone-organic liquid (HSL) [1-4].

The procedure used in the presentation of the experimental data of this study [2] is shown in relative units. The hydrophobicity (HP) of the sample with the lowest level of water vapor adsorption ($p_o/p \rightarrow 1$) was taken as a unit. Also, the unit was defined by the protective properties (PP) of the sample with a minimum specific weight gain ($\Delta m/m$) under corrosion in atmosphere, which was similar to atmosphere of salt mines. HP and PP of other samples were normalized according to the specified pattern (St/T/A) and were expressed as the relevant parts of the unit. T is underlayer of triamon, A is an external layer of alkamon. A and T are cationic tensides, based on quaternary ammonium compounds.

RESULTS AND DISCUSSION

At the beginning of the study there was no information in the literature about the relation between the protective properties and hydrophobicity of the surface of steel containing nanofilms applied according to the second approach. We handled the experimental data [2] and the obtained results which are shown in the coordinates PP – HP in relative units (Figure 1). The detected dependence is linear, as the observed by us earlier dependence for micron thickness coatings in case of traditional coatings $PP_1 = 0{,}8\ HP_1$, for the same coatings with filler $PP_2 = 0{,}9\ HP_2$ [2].

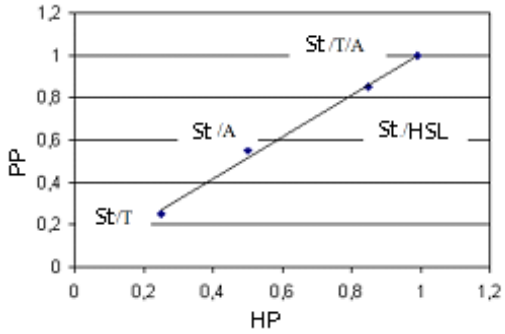

Figure 1. The dependence of the protective properties from hydrophobicity for the surface of steel 3 with applied nanofilms of triamon (T) alkamon (A), T and A (T/A) and from HSL.

As can be seen from Figure 1, the sample St/T/A is the most corrosion-resistant, which was treated sequentially with triamon and alkamon. The dependence from Figure 1 of applied nanofilms is characterized by quite big angle of inclination of a straight line and can be represented by the formula PP = 1,01 HP, where the proportionality coefficient on the right-hand side has the mistake of ±0,01. After corrosion testing of nanostructured samples on the steel basis in industrial air atmosphere of salt mines of Soligorsk enriching factory (SEF), with the method of X-ray photoelectron spectroscopy the binding energy of the electrons Fe2p in the surface layers containing protective coatings was measured. The results are shown in Table. 1

It was discovered that the binding energy (oxidation state) of iron in the surface layer of the sample St/T/A (710,0 eV), containing "triamon" underlayer and prepared in water solution, after the testing, and the initial steel to corrosion (710.2 eV) are almost identical.

This demonstrates that the combination of layers T/A has stronger passivating metal effect than one A-layer or even the "thickest" and effective, according to other studies, coatings of two layers of bituminous lacquer (2 Bl) or two layers of boiled linseed oil natural varnish, reinforced by nano-structured filler - 2OH (H), or a combined coating on steel HSL/P, where P is the phosphate underlayer. In the full-scale testing: relative humidity of 70-90%, the content of corrosive impurities 0,07-0,50 mg/m3. The tested steel plates with applied layers were simultaneously secured to SEF equipment. Thus, the corrosion of the samples shown in Table 1, was carried out in the same real-world production environment. Long-term (more than 6 months) tests made it possible to measure the binding energy Fe2p of the samples St/2OH(H) и St/2BL. In fact that in early corrosion stages boiled linseed oil film and bitumen lacquer had micrometer thickness (20 - 30 microns), which did not allow to measure Xray - spectra of iron on the steel surface. During the film tests, OH and Bl were subjected to destruction, including due to the influence of solar radiation. They became thinner, less uniform in thickness, what made the surface of the steel under the cover acceptable for study by X-ray Photoelectron Spectroscopy.

Comparison of physical and chemical characteristics of the steel 3 (St) and the surface-modified steel samples treated with quaternary ammonium compounds (QAC) Table. 2 shows that consistent treatment by triamon and alkamon (St/T/A-sample) is favorable to maximize the effectiveness of inhibitory action (Z = 53%), and the inhibitory effect (γ = 2.1) among the studied modifiers. At the start of our studies alkyl trimethylammoniumchloride (ATMAC) (a radical C10-C16 near nitrogen atom) has been known and used as a corrosion inhibitor of ferrous metals in an acid environment. From the fact of energy conservation of iron in the surface layer of electrons at the sample 710 eV for sample StT/A, the observed surface passivation of steel, based on the data Table. 2, can be seen as the result of some sort of synergistic effect on the level of binding energies N1s and $Fe2p_{3/2.}$

This effect is based on the comparison of the relevant characteristics of the samples St/T, St/A, St/T/A, characteristic not only of the electron binding energy and anti-corrosion properties, but also expressed in strengthening of water repellency St/T/A (Table 2). The advantages of the developed techniques are to avoid the chlorine-containing corrosion inhibitors (ATMAC) and that the using of alkamon and triamon capable of applying modifiers metal surface not only from the gas phase, but also from aqueous solutions, which is favorable for the treatment of extended steel constructions (pipes, towers, conveyors, etc.).

Table 1. The binding energy of Fe2p levels in samples based on steel (VG ESCALAB 220iXL device)

Sample	Before corrosion	After corrosion testing of samples on the steel basis in industrial air atmosphere (195 days)					
	St	St	St/2OH(H)	St/P/HSL	St/T/A	St/A	St/2Bl
The binding energy of the electrons Fe2p, eV	710,2	711,2	710,7	711,4	710,0	712,0	712,3

Table 2. Comparative physical and chemical characteristics of the initial samples St and steel surface-modified by tensides based on quaternary ammonium compounds (QAC)

Sample	St	St/T/A	St/A	St/T	St/ATMAC
The binding energy of the electrons. N1s, eV	-	404,2	402,4	402,1	402,3
Corrosion (Δm/m) in salt mines (196 days.), %	1,85	0,87	1,16	1,15	1,22
The binding energy of the electrons $Fe2p_{3/2}$, eV after corrosion (196 days)	711,2	710,0	712,0	712,3	710,7
Z- effectiveness of inhibitory action, %	0	53	37	38	34
Inhibitory action γ	1,0	2,1	1,6	1,6	1,5

Table 3. Characteristics of the sample surface on the basis of the steel 3 according to atomic - force microscopy (Solver P47 Pro microscope)

Sample	"peak to peak," nm	Roughness, nm
Steel (St)	1485	170
St/P/HSL	780	65
St/T/A	1460	150
St/T	1475	160
St/A	1470	155

Table 4. Ration of linear and nonlinear components of D=P (x)* for Cu-containing tribosystems (Spec. surf. area of additive is 0.34±0.02 m^2/g)

Type of additives	*D* (exp)	*D* (calc)	*a*	1/*a*	Linear component *L* = *A* + *Bx*	Nonlinear component |*N*p|	*N*/*L*,%
Cu/A	580	574	0.0205	48.78	574	$2\cdot10^{-90}$	≈0
Cu/A	1300	1360	0.0299	33.44	1360	$1\cdot10^{-19}$	≈0
Cu/T	1100	1102	0.0268	37.31	1162	59	5.0
Cu/T/A	270	269	0.0260	38.46	1103	833	75.5
Cu	-	1923	0.0445	22.47	1923	$6\cdot10^{-220}$	≈0
Cu/ (A+T)	1480	1421	0.0310	32.25	1421	$3\cdot10^{-31}$	≈0

* D_{calc} is defined: $D_x = A + Bx + N(x) = 3075.51 - 51.255x - 833.84e^{-2(x-38.462)^2}$.

Saving the oxidation degree of iron (Fe2p level binding energy) in the sample St/T/A almost constant, as follows from the data in Table 1, can be seen apparently as a result of some kind of competition between iron reduction processes by electrons of the nitrogen and iron oxidation by components from the air atmosphere [5]. This effect passivation of steel can be used for protection of steel with success in a hostile reentry environment of salt mines containing trace HCl, SO_2, KCl.

In [6], the authors obtained the equations that allow to calculate the activity coefficients of the SAS (surface active substances) in the surface layer, the Gibbs energy change due to the hydrophobic effect, as well as factors related to the binding energy of the metal - SAS. The analyzing of the SAS adsorption on lead showed that the SAS is an effective corrosion inhibitor when there is a sufficiently strong bond SAS- metal SAS activity coefficients in the surface layer are high enough that promotes the formation of two-dimensional "islands" of the adsorbed molecules. It will be easily understood, that these results correspond to whatever ideas about the mechanism of SAS adsorption and passivation of the surface, which are presented in this and our other studies [1-5].

Currently, one of the weak links in the development of nanotechnology in our country and in the CIS Inadequate numbers of real-world implementations of these technologies and nanomaterials in specific areas of engineering and typical for the CIS industrial fields. One of our scientific and practical results was the introduction of layered mixtures and surface treatment of metal and triamon and alkamon for corrosion protection of metal for mining and chemical enterprise, is developed salt (potassium) mines, as an example of "Belaruskali." This implementation included not only the use of SAS nanofilms, but also other types of nanostructured coatings of filled natural varnish that developed by I. V. Pleskunov and A.G. Syrkov. It was possible to reduce the rate of corrosion of metal on SEF by 2-5 times, which corresponds to the production of high-resistant of metallic materials [7].

In addition to micro coating of varnish with nano-structured filler and nanofilms SAS in the tests performed well nanocoating on steel type P/HSL, where P - phosphate matching underlayer; HSL - external layer deposited from 0.5% HSL -94 solution. Characteristics of the sample surface on the basis of the steel according to atomic - force microscopy (Solver P47 Pro microscope).

The Table 3 presents a comparison of parameters of the surface measured by AFM, to the original steel and different types of nanocoating. Clearly traced reduction of the values «peak to peak» parameters and roughness after layering of HSL and cation-active substance. Strengthening the difference these parameters from the corresponding original parameters of steel takes place in a series of samples: St /T, St /A, St /T/A, St /P/ HSL. It is known that the AFM method can't accurately determine the thickness of the applied nanolayer even on the surface of compact materials. Is estimated to, the thickness of the most "thick" film on the steel - HSL/P (with underlayer) - according to view of experts from center "Chemical assembly of nanomaterials" (Sosnov E. et al.) less than 200 nm. Consequently, the thickness of the other film derived from cationic SAS roughly an order of magnitude or more below as parameters of the respective surfaces of the samples are reduced by 10-25 nm and 105-705 nm than (nearly 2-fold compared to the original steel) as in sample Ст/P/HSL (Table 3). It is important that the AFM measurements confirm nanometer scale of thickness for protective films applied from alkamon and triamon.

Application of specific techniques of surface treatment of steel constructions (pipes, towers, roof-hopper mineral wagons) depends on the time of year (HSL better to put in the

winter) and on the financial capabilities of the enterprise. In any case, the protection of steel surfaces from corrosion by two methods discussed above are often cheaper and better for the environment than the application of plasma-chemical coating or use of oil paints and protective formulations containing epoxy resin [5, 8].

In addition to the corrosion protection of steel structures, functioning in the open air in the atmosphere of man-made salt mines, remains a topical problem of increasing the service life of pipelines and transmission components other equipment in a chemically active environment.

For significant progress in solving this problem depends on the correct choice of lubricants and special additives to it [9]. Theorists and practitioners in the field of tribology and tribotechnology note that the preliminary results of the monitoring of the friction coefficient (k) and other friction characteristics of the lubricant in the friction pair on special stands are often poorly reproduced, depend on many poorly controlled factors, and most importantly - do not give the ability to predict reliability of lubrication for a long period in real conditions [9-12].

We suggest to use more accurate and simple measurement of the water adsorption and chemical properties of the additive and an approximation of the dependence from them for tribosystem friction integral index in the form of a superposition of a linear function and nonlinear components in the form of a "Gaussian" to control the tribological characteristics of anti-friction materials and select effective additives for lubricant in the form of surface - modified metals. This proposal was based on the successful experience of use as an additives to the oil I -20 surface-modified metal powders (M = Al, Cu) [13, 14], which is widely used in the domestic industry.

Our research shows that an addition of the modified powder (according to the second approach which you can see above) to the oil in a quantity less than 1 wt. % of metal with different size molecules of SAS (QAC) reduce friction integral index D in a pair of steel-steel friction in 3-7 times in comparison with the original oil I-20. There is a 15 MPa right-side shift on the pressure axis (P), on the area of dependence D = f (P), which is respond for the "dry friction" mode [5, 13].

When oil is squeezed out of the tribological contact area at high load pressures (40-60 MPa), the value of D is mainly determined by the anti-friction properties of the particles of the solid additive [14]. These protective properties are and are thought to be [11, 15], determined by the hydrophobicity of nanofilms surfactants, the adhesion to the metal, and the modified additives stability to the oxidation [13, 14, 16]. Therefore, it is necessary to determine the hydrophobicity and stability to oxidation of the additive during the heating while controlling tribological properties of used materials. These characteristics will determine the reliability of the lubrication in case of high load pressure and long-term operation. In addition, the evaluation of the hydrophobicity by the value of the water vapor adsorption (a) by additive desiccator method and gravimetric determination of the high temperature oxidation rate made much easier and more accurate than the measurement of k or D on the tribological stands and does not require expensive equipment [5].

This approach lead to the determination of the mass (±0,0005 g) on an analytical balance and it's efficiency illustrated in the article [17].

An increase of additive hydrophobicity value, decrease the value of D for lubricants with a Cu-modified. The most refractory Cu-, Fe-powders obtained by solid state hydride synthesis of, provide the greatest resources lubrication work hours. From the results of [17] it follows

that the correlation D with a linear function of the value of hydrophobicity value and imagining of components adjusted for non-linear effects from the "Gaussian" form, allows to achieve a satisfactory agreement between the calculated D and D values measured in the experiment (Table 4).

Similarly, the good agreement between the calculation result D with the measurement data D acoustic emission method [5, 12] has been achieved in the approximation equation of the form D = L(x)+ N(x), where x is the oxidation rate of the additive, N(x) - nonlinear component according to D = f (x) [18].

CONCLUSION

In the present study, we analyzed the experience of implementing and testing nanotechnology for protection from corrosion of steel surfaces and increasing operating life of the transmission nodes in the mining and chemical plant equipment on the example of the factory "Belaruskaliy."

Described in the research and development implemented with an economic effect in "Belaruskaliy," "Soligorsk Institute of Resource Saving Problems with pilot production," in "Belgorkhimprom" and "Lukoil" oil company, which is confirmed by the relevant acts [5, 19].

REFERENCES

[1] Syrkov A. G., Pleskunov I. V., Remzova E. V.//*Notes of the Mining Institute*. 2007. V. 173. P. 237-239.
[2] Pleskunov I., Syrkov A., Bystrov D.//*CIS Iron and Steel Rev*/ 2008. No 1-2. P. 23-28.
[3] Pat. RF. №242591. Syrkov A. G., Pleskunov I.V., Bystrov D.S. et al. Publ. 10.08.2011.
[4] Syrkov A. G. Russ. *J. Gen. Chem.* 2013. V. 83. No.8. P. 1621-1622.
[5] Syrkov A. G. Nanotechnology and nanomaterials for the mineral resource complex. St. Petersburg: Publishing House of the Polytechnic. University Press, 2014. 130 p.
[6] Afanas'yeva B. N., Akulova Yu.P., Polozhentseva Yu.A.//*Protection of Metals*. 2008. V. 44. No2. P. 146-152.
[7] Database of steels and alloys/ed. V. G. Sorokin. M.: *Engineering*, 1989. 320 p.
[8] Safronchik V. N. Corrosion protection of building structures and technological equipment. L. *Stroyizdat*, 1988. 255 p.
[9] Fuels and lubricants, technical liquids. *Handbook*/Ed. VM Shkol'nikova. M: *Chemistry*, 1989. 360 p.
[10] Garkunov D. N. Tribotechnology. M: *Mashinostroeniye*, 2000. 424 p.
[11] Dedkov G. V.//*Successes of physical sciences*. 2000. V. 170, No 6. P. 585-618.
[12] Myshkin N. K., Petrokovets M. I. Friction, lubrication, wear. M.: Fizmatlit, 2008. 368 p.
[13] Bystrov D. S., Syrkov A. G., Pantyushin I. V.//*Chemical Physics and mezoskopy*. 2009. V. 11. No 4. P. 424-466.
[14] Bystrov D. S., Syrkov A. G., Pantyushin I. V.//*Notes of the Mining Institute*. 2009. V. 182. P. 227-230.

[15] Abramzon A. A., Zaychenko L. P., Fayngol'd S.I. Surface-active substances. Synthesis, analysis, properties and application. L.: *Chemistry*, 1984. 393 p.
[16] Pshchelko N. S., Syrkov A. G., Vakhreneva T.G. et al.//*Russian Nanotechnologies*. 2009. V. 4. No 11-12. P. 42-47.
[17] Syrkov A. G., Fadeev D. V., Taraban V.V., Silivanov M.O.//*Condensed matter and interphase boundaries*. 2014. V. 16. No 2. P. 215-219.
[18] Syrkov A. G., Simakov A. S., Vinogradova A.A.//*Condensed matter and interphase boundaries.* 2013. V. 15. No 2. P. 179-183.
[19] Scientific and educational centers of the National Nanotechnology Network. Infrastructure. Products. Services: collection catalog/Ed. by V.V. Luchinin, SPb: SPbGETU «LETI», 2013. P. 103-110.

Smart Nanocomposites
Volume 7, Number 2
ISSN: 1949-4823

THE 3D ELECTRODE MATERIAL BASED ON POLYACRYLATE HYDROGELS AND CONDUCTING POLYANILINE

P. V. Vlasov, I. Yu. Dmitriev, and G. K. Elyashevich*
Institute of Macromolecular Compounds, Russian Academy of Sciences,
St. Petersburg, Russia

ABSTRACT

Electroactive composite systems based on polyacrylic acid and polyacrylamide hydrogel and a conducting polymer, polyaniline, were prepared. The structural, electrical and mechanical properties of the samples have been investigated. The contributions of the electronic and ionic constituents of conductivity have been determined and swelling degrees were measured. The specific capacity of the composites has been calculated using the data on galvanostatic charge–discharge cycling, and the stability of the capacity at cycling has been evaluated.

Keywords: conducting polymers, hydrogels, polyaniline, polyacrylamide, mechanical properties, conductivity

INTRODUCTION

Conducting polymers are promising materials for the application in various fields [1]. However, known conducting polymers are characterized by drastically low solubility and melting ability, and consequently poor processability. The elaboration of composite systems based on conducting polymer which provides through conductivity to the material and polymer matrix which supports mechanical integrity, strength and elasticity of the material is a perspective way in this field development [2]. This study was aimed to obtain novel electoactive systems containing polyaniline (PANI) as conducting component and hydrogel matrices characterized by swelling ability to form 3D electrode material for energy storage applications.

* Corresponding Author: Prof. G.K. Elyashevich, Dr.Sci. (Polymer Physics), Institute of Macromolecular Compounds, Russ.Acad.Sci, 199004 Saint-Petersburg. Tel./Fax: +7 812 3286876. E-mail: elya@hq.macro.ru

MATERIALS & METHODS

Hydrogels based on poly(acrylic acid) (PAA) were prepared by the standard free-radical copolymerization of acrylic acid (99%, Sigma Aldrich) and *N*,*N*'_methylenebis-acrylamide (a crosslinking agent 98%, Sigma Aldrich). A system based on ammonium peroxydisulfate (PSA) (98%, Sigma Aldrich) and *N*,*N*,*N*',*N*'_tetramethylethylenediamine (99%, Sigma Aldrich) was used as an initiator. The AA: crosslinking agent ratio was 300: 1, mol/mol. PANI/PAA composite hydrogels were synthesized according to the technique given in [3].

Acrylamide (99%) used for the synthesis of linear polyacrylamide (PAAm) was purchased from Sigma Aldrich. PANI was prepared by oxidative polymerization from aniline hydrochloride (>99.0%, Fluka) in 1 M HCl; PSA was used as oxidant. To obtain PANI in the form of nanofibers, *p*-phenylenediamine was added while performing the synthesis. *p*-Phenylenediamine is characterized by lower oxidation potential than aniline hydrochloride and forms reaction sites for the subsequent propagation of PANI fibers, increasing the reaction rate in its initial step. At the first stage, PANI was synthesized in the solution of linear PAAm; at the second stage the obtained PANI/PAAm dispersion was precipitated in acetone. The loss of solubility and the formation of a 3D hydrogel network were registered for PANI/PAAm systems. Electroconductivity of all hydrogels under study was measured using standard four-point probes method. The contributions of the electronic and ionic conductivities into the overall conductivity of PANI/PAAm composites were determined by chronoamperometry [4]. The sample was placed in a two-electrode cell onto which a constant potential was applied (300 mV), and the dependence of the current on time was recorded.

The redox transitions of the conducting polymer in the composite were studied by cyclic voltammetry (CVA). CVA curves were recorded under potentiostatic regime at the potential sweep rate of 1 mV s^{-1}. The measurements were performed in a three-electrode cell; electrolyte containing 1 M HCl and 1 M KCl was used. PANI/PAAm sample acted as the working electrode, a platinum wire was used as the current electrode, and a silver chloride electrode was the reference electrode.

The specific electrical capacity of PANI/PAAm composites was determined in a three-electrode cell with a platinum electrode and a silver chloride electrode in the galvanostatic regime from the results of charge–discharge cycles.

The structure of the samples was studied by SEM, DMA and mechanical testing at compression and extension.

RESULTS AND DISCUSSION

PANI/PAAm hydrogels obtained by the proposed procedure demonstrated better electric properties than PANI/PAA hydrogels obtained using standard approach (Table) due to uniform distribution of PANI within PAAm volume. SEM images (Figure 1) show that PANI is assembled into anisotropic (500x100 nm) nanoparticles which form the structure characterized by a high degree of continuity of its elements. PANI/PAAm samples exhibited redox transitions between different oxidation states of PANI.

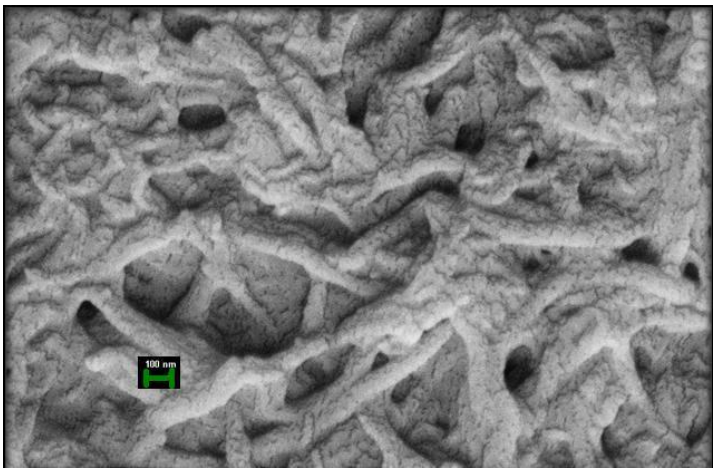

Figure 1. SEM image of PANI/PAAm composite hydrogel. Magnification equals x 100 000.

The formation of a spatially continuous conducting phase and the appearance of the electronic conductivity in PANI/PAAm composite systems are observed at lower concentrations of the conducting polymer than for spherical PANI particles [5] due to the anisometric shape of PANI particles. As it is seen in Figure 2, PANI/PAAm dispersions exhibit electronic conductivity already at PANI content equal to 1-2 wt %.

The data given in Table demonstrates that PANI/PAAm precipitation in acetone increases the contribution of the electronic conductivity to the overall conductivity of the system, which reaches 53%, whereas in case of PANI/PAA composites prepared according to the standard technique [3] this contribution is as low as 0.2%.

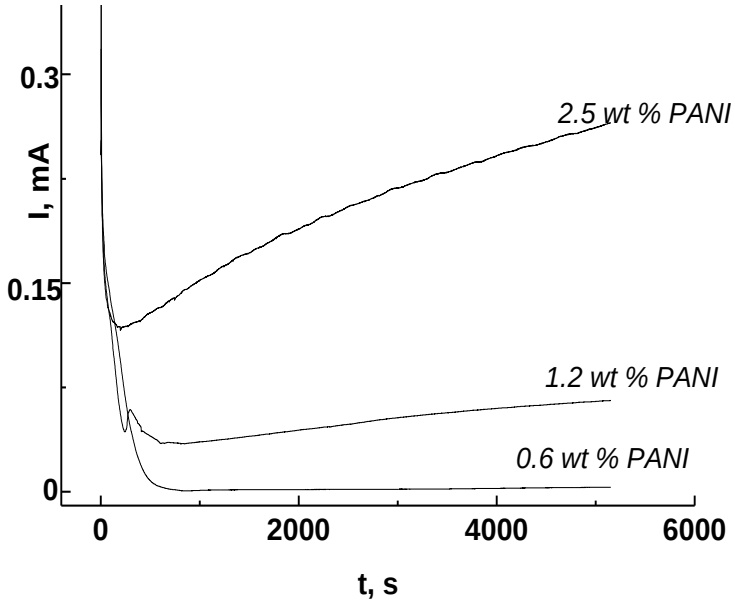

Figure 2. Chronoamperometric curves of PANI/PAAm dispersions with different PANI content.

Table. The characteristics of PANI/polyacrylate electroactive hydrogels

Sample	Total conductivity σ, S/cm	Contribution of electron conductivity to the total value of σ, %	Swelling degree in water Q, g/g	Content of PANI in matrix, wt %
PANI/PAAm	$5x10^{-3}$	53	3.7	6
PANI/PAA	$5x10^{-7}$	0.2	10	80

CVA curves of PANI/PAAm demonstrate oxidation peaks at 450 and 700 mV and a broad reduction peak in the region of 250 mV (Figure 3). The first oxidation peak corresponds to the leucoemeraldine → emeraldine transformation of PANI, and the second one is related to further oxidation of emeraldine to pernigraniline.

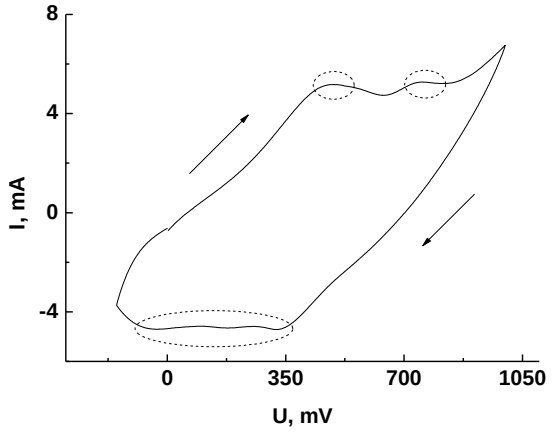

Figure 3. CVA curve of PANI/PAAm hydrogel. Areas marked with dotted circles correspond to characteristic redox peaks of PANI.

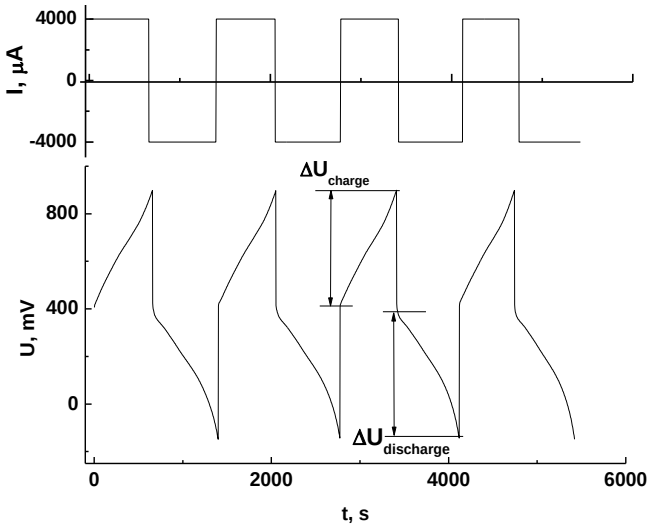

Figure 4. Galvanostatic charge-discharge curves of PANI/PAAm hydrogel sample. Current density equals 0.2 A/g.

Similar peak positions were reported in research [6]. The absence of the second reduction peak is probably caused by the confluence of two reduction peaks into a broad single one.

The galvanostatic charge–discharge cycles of PANI/PAAm composites at the current density of 0.2 A g^{-1} are shown in Figure 4. Cycling was performed within –150-900 mV. Such potential gap was chosen according to CVA data on the redox transitions between PANI forms with different states of oxidation.

The specific capacity was calculated from the cycling results using the formula:

$$C = \frac{I \cdot t}{\Delta U \cdot m}$$

where C is the specific capacity; I is the current; t is the time of attainment of the final potential; ΔU is the difference between the final and initial potentials; and m is the weight of PANI in composite system. The specific capacity of PANI/PAAm composites reaches 300 F g^{-1}, which is a relatively high value compared to the average value for the known supercapacitors based on conducting polymers [7, 8]. Figure 4 shows that the cycling does not lead to significant changes in the specific capacity; it means that the electroactive properties of composites are stable enough.

It was shown by the investigations of PANI/PAAm mechanical properties and behavior in different solvents that the samples under study are hybrid systems, i.e., they are bound by physical and chemical crosslinks both, and demonstrate the equilibrium swelling ability. The obtained PANI/PAAm hydrogels are the electroactive ones, and they preserve the values of specific capacity about 300 F/g at charge-discharge cycling.

ACKNOWLEDGMENTS

This work was supported by The Programme of the Division of Chemistry and Material Science, Russian Academy of Sciences № 7 “The Elaboration of Scientific Fundamentals of Ecologically Safe and Resource Saving Technological Processes” (2015-2017), the Russian Foundation for Basic Research (Project № 16-03-00265a) and Project of Collaborative Research of the Russian Academy of Sciences and the University of Ljubljana (Slovenia) (ARRS-BI-RU/16-18-017).

REFERENCES

[1] Han, G. and Shi, G., *Thin Solid Films*, 2007, vol. 515, no. 17, pp. 6986–6991.

[2] Wu, Y., Alici, G., Sprinks, G.M., and Wallace, G.G., *Synth. Met.*, 2006, vol. 156, nos. 16–17, pp. 1017–1022.

[3] Tang Q., Wu J., Lin J., *Carbohydrate Polymers*, 2008, vol. 73, pp. 315 – 321.

[4] Devendrappa, H., Subba Rao, U. V., and Ambika Prasad, M. V. N., *J. Power Sources*, 2006, vol. 155, no. 2, pp. 368–374.

[5] Olinga, Th., Foulc, M. P., Lacomme, S., et al., *Composites Sci. Technol*., 2013, vol. 74, pp. 107–112.

[6] Gharibi, H., Kakaei, K., Zhiani, M., and Taghiabadi, M. M., *Int. J. Hydrogen Energy*, 2011, vol. 36, no. 20, pp. 13301–13309.

[7] Pan, L., Yu, G., and Zhai, D., *Proc. Nat. Acad. Sci*., 2012, vol. 109, no. 24, pp. 9287–9292.

[8] Koysuren, O., Chunsheng, D., Ning, P., and Bayram, G., *J. Appl. Polym. Sci*., 2009, vol. 113, pp. 1070–1081.

Smart Nanocomposites
Volume 7, Number 2
ISSN: 1949-4823

INTRODUCTION TO THE PROCEEDINGS OF THE INTERNATIONAL CONFERENCE - SYMPOSIUM "NANOPHYSICS AND NANOMATERIALS" – 2016 (ST. PETERSBURG MINING UNIVERSITY, NOVEMBER 16 – 17 2016)

The international seminar-symposium "Nanophysics and Nanomaterials" has been a regular annual event since 2013 at the venue of St. Petersburg Mining University. It is organized with the assistance of the Ministry of Education and Science of the Russian Federation and the regional UNESCO branch. At this time it was commemorative to Professor Petr Weimarn, graduate of Mining Institute, where he served as a Professor at the department of Physical chemistry until 1916, where he wrote his most viable monographs. P. Weimarn is acknowledged as a founder of nanotechnologies in Russia.

Symposium was internationally contributed by such well known schools as Princeton University (USA), University of Duluth (USA), University of Campinos (Brasil), and others.

Scientific goal of the Symposium was in increasing the efficiency of scientific and research projects in nanotchnologycl area.

Traditionally, proceedings of the Symposium are divided in few sections.

Results in the area of alloys and composite materials were reported by groups of Bogdanov, Christyuk and Khalimonenko. Their work was emphasized on ion transport and porosity phenomena's.

Analytical methods section was contributed by Nikonorova (dielectric spectroscopy of fullerene containing compounds), Fedortsov (thin films, transparent films), Yurova (computer simulation methods). Quantum dots responsible for colors of crystalline samples were analyzed by Beloglazov.

Corrosion and electrochemistry section was represented by Saltykov dealing with corrosion of low carbonized steel and Bazhin (graphite based cathodes).

As usually, high interest was paid to energy storage methods and devices. This section was contributed by Arsentev, Belorus and Ivanova with results related to lithium batteries, substrates for supercapacitors, and electrochemical research in the area of pseudo-capacitors.

Interest paying to carbon structures, including ones with reduced dimensions, such as fullerenes, has been arising from the end of the last century is being kept until now. This have resulted in a number of reports in the area of fullerenes and carbon-based materials contributed by Barbin and Krasny (fullerenes, thermodynamic modeling), Kovalchuk (processing of carbon nanoparticles), Rozhkova (shungite expert).

Traditional to Mining University were publicationns with the emphasis on oil and gas exploration technologies and their safety issues (Bochkov, Zaharova).

Plasma related technological methods capable of production nano-sized materials were reported by Mustafaev and Grabovsky. Plasma filtering from biological contaminations was described by Levine. Low frequency absorption was studied by Ponomarev.

Polymer section of the journal was represented by Khoroshavina (hydrophobic rubbers), Elyashevich and Kurindin continuing trend in studying hydrogels, large scale project of the institute of Macromolecular compounds.

Semiconductor-related technologies were, as usually, booming topic of studying of many research groups. Study in A_3B_5 in phosphorous semiconductors was reported by Belorus. Thin layer technologies were assessed by Ezhovskii (atomic layer deposition of alumina nanolayers), and Zakharova (deposition of silicon oxide layers onto Boron nitride). Ilinsky presented paper in vanadium dioxide study, while transport phenoma's in semiconductor crystals were reported by Nemov.

Section with the emphasis on practical application was contributed by Kononova (maltisensor systems), Malygin (luminescent phosphors), Maraeva (sensors), Pak (multiple application porous materials), and Pshchelko (band stop optical filters).

SHORT THESES ABSTRACTS

OPTICS AND LUMINESCENCE

Smart Nanocomposites
Volume 7, Number 2
ISSN: 1949-4823

SYNTHESIS OF $NaBaPO_4:Eu^{2+}$ LUMINESCENT PHOSPHORS WITH ENHANCED DISPERSION

Vadim V. Bakhmetyev*, Vitalii V. Malygin, Mariia V. Keskinova, Maxim M. Sychov, and Sergey V. Mjakin
Department of Material Science, Saint Petersburg State Institute of Technology (Technical University), Saint Petersburg, Russia

ABSTRACT

$NaBaPO_4:Eu^{2+}$ luminescent phospors with enhanced dispesity are obtained by sol-gel precipitation followed by high temperature annealing in molten NaCl. The suggested approach involving annealing in molten NaCl provides $NaBaPO_4:Eu^{2+}$ phosphors with nanocrystalline structure, 3.8-fold reduced average particle size and 11-fold increased content of finely dispersed (less than 1 μm) fraction compared with a similar material synthesized without NaCl addition.

* Corresponding Author: vadim_bakhmetyev@mail.ru

Smart Nanocomposites
Volume 7, Number 2
ISSN: 1949-4823

X-RAY FLUORESCENCE ANALYSIS OF PEAT FOR THE PRESENCE OF LIGHT AND HEAVY ELEMENTS IN BIOFUEL

K. V. Epifancev*[†] *and A. N. Nikulin
St. Petersburg State Mining University, Russia

ABSTRACT

In Russia peat fuel production has great difficulties because of out-of-date equipment, and also a high level of quality and ecological risks. X-ray fluorescence analysis helps definition dangerous elements.

Keywords: analysis of raw materials extracted, forming peat fuel, quality of fuel

[†] Corresponding Author: Assistant Epifancev K.V. Department management of quality, St. Petersburg State Mining University, Saint-Petersburg, Russia, Tel.: + 7963 3437759, E-mail:epifancew@gmail.com

PLASMA TECHNOLOGIES

Smart Nanocomposites
Volume 7, Number 2
ISSN: 1949-4823

PROBE PLASMA DIAGNOSTICS WITH NO VELOCITY SPACE SYMMETRY

A. Mustafaev[1], A. Grabovskiy[1], A. Strakhova[1], and V. Soukhomlinov[2]

[1]St. Petersburg Mining University, Russia
[2]St. Petersburg State University, Russia

ABSTRACT

This paper is devoted to the development of the probe method used for analysis of non-equilibrium anisotropic plasmas. The probe method for determination of full electron and ion velocity distribution functions (EVDF) in axially symmetric plasmas was theoretically and experimentally approved [1, 2]. To recover the full EVDF to the Legendre polynomials of order N it is necessary to measure the second derivative of probe current I" U in probe's N different orientations. In [3] there are the theoretical principles of the EVDF recovering method for plasmas with no velocity space symmetry. To determine the full EVFD with the same degree of accuracy it is necessary to measure I" U in flat probe's N^2 orientations. This paper gives further development of probe method. While restoring the full EVDF in plasma objects with bilateral symmetry it became possible to reduce the number of the probe's angular orientations by two. It opens up new possibilities to obtain new information about Langmuir paradox in plasma [4].

Keywords: plasma chemistry, anisotropic plasmas, asymmetrical velocity space, distribution function of charged particles

Smart Nanocomposites
Volume 7, Number 2
ISSN: 1949-4823

SECONDARY ELECTRON EMISSION IN THE LIMIT OF LOW ELECTRON ENERGIES IN TRANSVERSE MAGNETIC FIELD

A. Mustafaev[1], A. Grabovskiy[1], A. Strakhova[1], and V. Soukhomlinov[2]

[1]St. Petersburg Mining University, Russia
[2]St. Petersburg State University, Russia

ABSTRACT

A detailed review of experimental and theoretical studies of secondary electron emission (SEE) at low incident electron energies has been recently given in paper [1]. In particularly, discussion of some authors' statement [2, 3] on increase of the SEE yield up to unity if the primary electron energy tends to zero was reviewed. Present paper considers a technique for measurements of SEE yield near a sample surface [4] making use of a magnetic field parallel to the surface. Using this technique it was shown that the SEE yield can approach unity for a polycrystalline, but not for a monocrystalline sample. This result was explained by additional reflection of primary electrons from a potential barrier near the sample surface. Therefore for suppression of the deleterious effects of SEE, e.g, for better performance of accelerators, it is important to monitor and control micro electric-fields arising near a polycrystalline surface.

Keywords: surface effects, magnetic diagnostic, secondary emission, potential barrier.

Smart Nanocomposites ISSN: 1949-4823
Volume 7, Number 2

THE DEVIATION OF THE LAMBERT-BEER LOW FOR THE ELECTROMAGNETIC WAVES ABSORPTION AT THE NEAR THZ FREQUENCY RANGE FOR THE ASTRALENES AND CARBON NANOPOROUS MICROFIBERS

A. N. Ponomarev[1,†], L. A. Melnikov[2], and V. V. Rybalko[3]
[1]SPbGPU, St. Petersburg, Russia
[2]STU, Saratov, Russia
[3]The Open Institute of The High Professional School, Moscow, Russia

ABSTRACT

Authors have researched of the peculiarities the electromagnetic waves absorption by the different kinds of nanocarbon particles at near THz frequency range. The fullerenes (C-60 and C-70), two types of multiwall carbon nanotubes (MWCNT arc and gas phase technology made), colloidal graphite, astralenes [1], sulfo-adducts of the two or three-layer graphenes and carbon nanoporous microfiber (CNPMF) [2] have been studied. As it was founded, for the wide range of the wave lengths (75μ-6000μ) and for the numeral part of the most famous type nanocarbon particles the relations between the absorption coefficients and the concentrations of these particles in the transparent medias are rather goodly conformed with the Lambert-Beer low in the concentration range 1%-25% mass. However, it is not so for the astralenes and CNPMF. This case the relations between the absorption coefficients and concentrations of these types of the nanocarbon particles became highly non-linear from a rather small concentrations (2,5%-4,5% mass.). Authors explain this phenomena as consequence of the intensive agglomerating processes have taken place for these particles by external electromagnetic waves influence.

Keywords: Terahertz waves, absorption, spectra, absorption spectra, nanoparticles, nanocarbon clusters, carbon, carbon nanotubes, astralenes, nanoporous carbons, carbon microfibers, nonlinear properties, strong non-linearity of concentration's dependence of absorption, optical-electronic medias, electro-optical media

† 9293522@gmail.com

Smart Nanocomposites
Volume 7, Number 2
ISSN: 1949-4823

WATER PURIFICATION FROM BIOLOGICAL CONTAMINATIONS BY ELECTRICAL PLASMA FILTER

Kirill L. Levine[1], Fatima Arslanova[1], Natalia Boikova[1], Rimma A. Kreneva[2], Mikhail Sh. Barkan[1]. Maria A. Pashkevich[1], and Alexandr S. Mustafaev[1]

[1]St. Petersburg Mining University, St. Petersburg, Russia
[2]Institute of Macromolecular compounds RAS, St. Petersburg, Russia

ABSTRACT

Contamination of water resources is a serious ecological problem of the present world. Drinking water as a matter of fact contains risk of carrying biologically hazardous species: bacteria, and microorganisms. Filtration does not solve the problem, because the size of pores of filtering material is usually larger than the size of species. In this study water treatment by electrical plasma filter is applied to purify from microorganisms. E-coly was chosen as contamination. Exponential decrease of e-coly contents with treatment time was registered. Therefore method was fond to be effective to for water cleavage from biological hazards.

Keywords: water purification, electrical discharge, biological contaminations, e-coli

SEMICONDUCTORS

Smart Nanocomposites
Volume 7, Number 2
ISSN: 1949-4823

CORRELATION DISAPPEARANCE OF GAP IN VANADIUM DIOXIDE

Aleksandr V. Ilinskiy[1], Rene A. Kastro[2] Vladimir A. Klimov[1], Evgeniy I. Nikulin[1], and Evgeniy B. Shadrin[1,*]

[1]Ioffe Physical Technical Institute of the Russian Academy of Sciences, Russia
[2]Herzen State Pedagogical University, Russia

ABSTRACT

By method of investigation of temperature dependence of electroconductance (in an interval $77 < T < 273$ K) is determined a width of the gap ($E_g = 0.8$ eV) in nanocrystallic VO_2-film and energy depth of donor centers ($E_d = 0.04$ eV). It is shown, that at growth of temperature in an interval $273 < T < 300$ K the energy E_g decreases from 0,8 eV up to 0 eV, that is caused by narrowing of a energy gap due to the correlation effects inherent of vanadium dioxide.

Keywords: vanadium dioxide, correlation effects, dielectric spectroscopy

* E-mail: shard.solid@mail.ioffe.ru

Smart Nanocomposites
Volume 7, Number 2
ISSN: 1949-4823

CHARGE CARRIERS AND CONDUCTIVITY MECHANISM IN VO_2 FILMS

Evgeny A. Tutov[1,†], Husam I. Al-Khafaji[2], and Vladimir P. Zlomanov[3]

[1]Voronezh State Technical University, Voronezh, Russia
[2]Department of Chemistry, College of Engineering, Al-Nahrain University, Baghdad, Iraq
[3]Moscow State University, Moscow, Russia

Fundamental and applied investigations of the semiconductor–metal phase transition in vanadium dioxide (VO_2) proceed more than half of century with not decreasing interest. During transition along with conductivity of vanadium dioxide its optical characteristics also considerably change, that is attractive for elaboration the termochromic "smart" glasses [1]. One of effective ways of impact on surface states of vanadium dioxide and, consequently, on transition parameters is use of field effect arising at chemisorptions of various gases on its surface [2, 3]. The present work is devoted to analysis of the conductivity mechanism of polycrystalline (powder) and film vanadium dioxide in temperature region near phase transition. Influence of chemisorptions of ethanol and water vapors on parameters of the semiconductor – metal phase transition in vanadium dioxide films is also studied.

Powder of polycrystalline vanadium dioxide (n-type on measurements of Seebeck effect), was synthesized by reduction of vanadium pentoxide with oxalic acid when heating on air up to the temperature of 600 - 700 °C according to reaction: $V_2O_5 + H_2C_2O_4 = 2VO_2 + H_2O + 2CO_2$. On a direct current and alternating current (12 Hz – 100 kHz) are measured resistance of the tablet pressed from the synthesized VO_2 powder and serially released thermoresistor (TP-68) on the basis of VO_2 film, both in the closed case, and with the open case was used. The measurements were carried out in a tubular heater in the microcompressor-produced air flow with saturated ethyl alcohol vapor and water vapor.

On a film surface of n-type VO_2 as a result of atmospheric oxygen sorption, in principle, the inversion layer (with hole conductivity) can be formed. Its resistance in the reduction atmosphere has to increase, as is observed in experiment. The measured resistance of vanadium dioxide consists of resistance of a bulk layer and a surface layer. The last can significantly increase or decrease at chemisorptions of gases – donors or acceptors of electrons.

† E-mail: tutov_ea@mail.ru

It is established that in conductivity of a semiconductor phase of vanadium dioxide give a contribution both zone (activation), and the hopping mechanism. Chemisorptions (including change of quantity of atmospheric oxygen adsorbed on a film) affect, apparently, both concentration of zone charge carriers, and parameters of the defect centers involving in conductivity on the hopping mechanism.

The energy zone model is offered for explaining "anomalous" response to the adsorption of donor gases due to inversion of conductivity type in surface layers of vanadium dioxide.

REFERENCES

[1] Tutov E. A., Al-Khafaji H. I., Manannikov A. V., Kvasova V. Yu. Prospects of chromogenic composite coatings for smart windows. - Smart Nanocomposites 7 (2016) 95-98.

[2] Tutov E. A., Zlomanov V. P. Effect of chemisorption of donor and acceptor gases on the semiconductor–metal phase transition in vanadium dioxide films. - Physics of the Solid State 55 (2013) 2351–2354.

[3] Tutov E. A., Kryukov P. I., Zlomanov V. P. Chemisorptions field effect in nano-crystalline films of vanadium oxide. - *Smart Nanocomposites* 4 (2013) 75-77.

Smart Nanocomposites
Volume 7, Number 2
ISSN: 1949-4823

STUDY OF PRODUCING SENSORS BASED ON POROUS GAP SEMICONDUCTORS WITH THE USE OF ELECTROADHESION CONTACTS

Veniamin L. Koshevoi[1] and Anton O. Belorus[2]
[1]Saint Petersburg Mining University, Saint Petersburg
[2]Saint Petersburg Electrotechnical University "LETI"
Saint Petersburg, Russian Federation

ABSTRACT

This paper describes the study of porous layers of semiconductors A_3B_5 group. Using SEM were determined pore size and thickness of the porous layer of obtained films. These films are used as the working fluid in sensors using electrodiffusion contacts.

Keywords: semiconductors, sensors, transducers, etching, porous semiconductors, transport, electrodiffusion contact

THIN FILMS

Smart Nanocomposites
Volume 7, Number 2
ISSN: 1949-4823

NEW EMPIRICAL APPROACH FOR THE COVALENT BONDING CLASS OF (SYSTEM OF) ATOMS IN SIMULATION OBTAINING THIN FILMS PROCESS TECHNOLOGY

V. A. Tupik, V. I. Margolin, and Chu Trong Su*

Department of Radio Microelectronics and Radio Engineering of Saint Petersburg Electrotechnical University "LETI," Saint Petersburg, Russia

ABSTRACT

Obtaining thin films process technology to get high quality of a thin film or some specific coating is one of the actual challenges today. One promising way was shown in this paper. It's using a computer simulation with an appropriate calculation method. In more detail, using the numerical calculation "top-down" approach is more suitable to all classes of researchers including young ones, i.e., by using empirical and classic physics was shown. Based on the specific of atomic orbital for anisotropic bonding a new model of an atom and interatomic interaction of bonding were created in order to an adequate description of thin films growth process. In this work the results of computer simulation were shown, as well as limitations of the new given algorithm and a discussion of it.

Keywords: Empirical interatomic potential, computer modeling, thin film process technology

* Email: chusu171@mail.ru

POLYMERS

Smart Nanocomposites
Volume 7, Number 2
ISSN: 1949-4823

SAXS AND WAXS INVESTIGATIONS AND THERMAL ANALYSIS OF STRUCTURAL TRANSFORMATION OF POLYORGANOSILOXANE AND OF THE SYSTEMS OF POLYORGANOSILOXANE – SILICATE AND POLYORGANOSILOXANE – OXIDE WITHIN THE TEMPERATURE RANGE FROM 20° TO 600°C

Irina B. Glebova*, MD, and Valery L. Ugolkov, PhD
Institute of Silicate Chemistry of the Russian Academy of Sciences,
St. Petersburg, Russia

ABSTRACT

The structural transformations of polyorganosiloxane (PDMPhS) and of the systems of PDMPhS – silicate and PDMPhS – oxide were investigated by the SAXS and WAXS methods. For PDMPhS, within the temperature range from 20 to 300ºC, dependences of the scattering intensity on the scattering angle are fully reversible. At 150-160ºC, a clearly expressed kink connected with the structural unfreezing is observed. In the case of PDMPhS filled by silicates, this process shifts to higher temperatures and, in the case of oxide, this effect becomes less pronounced and depends on the concentration. According to data of the SAXS and WAXS investigations and of the thermal analysis, the intense destruction processes begin at the temperature higher than 350° - 450°C. Silicates decrease the loss in weight of composites by 15 – 20%, whereas Cr_2O_3 does not change it. Therefore, it is advisable to use about 50% of silicates and less than 12% of Cr_2O_3 for OCM synthesis.

Keywords: SAXS, WAXS polymers, polyorganosiloxanes, silicate, oxide

* Corresponding Author: iraglebova@mail.ru

Smart Nanocomposites
Volume 7, Number 2
ISSN: 1949-4823

HYDROPHOBIC AND SUPERHYDROPHOBIC COATINGS BASED ON FLUOROSILOXANE BLOCK COPOLYMERS

Yu. V. Khoroshavina[1,*], Yu. V. Frantsuzova[1], I. N. Tsvetkova[2], O. A. Shilova[2], and G. A. Nikolaev[1]

[1]Institute of Synthetic Rubber, St. Petersburg, Russia
[2]Institute of Silicate Chemistry of the Russian Academy of Sciences, St. Petersburg, Russia

ABSTRACT

The kinetically and sedimentation stable sols were synthesized on the basis of methyltriethoxysilane and additives of polyphenylsilsesquioxane-polymethyl-(3,3,3-trifluoropropyl)siloxane block copolymers and hydrogenated Aerosil. The method of obtaining hydrophobic and superhydrophobic coatings based on the sol-gel compositions was developed. The resulting coatings are transparent; they have got an improved adhesion to glass.

Keywords: Hydrophobic and Superhydrophobic Coatings, Sol-Gel Synthesis, Polyphenylsilsesquioxane – Polymethyl (3,3,3- Trifluoropropyl)Siloxane

[*] Corresponding author: Yulia Khoroshavina, Senior scientific researcher, Institute of Synthetic Rubber, Saint-Petersburg, Russia. Tel.: + 79112913931. E-mail: julhor@yandex.ru

Smart Nanocomposites
Volume 7, Number 2
ISSN: 1949-4823

MECHANICAL PROPERTIES OF POLYACRYLIC ACID - POLYVINYL ALCOHOL HYDROGELS AT COMPRESSION AND EXTENSION

I. S. Kuryndin, I. Yu. Dmitriev, N. V. Bobrova, Z. F. Zoolshoev, and G. K. Elyashevich †
Institute of Macromolecular Compounds, Russian Academy of Sciences,
St. Petersburg, Russia

ABSTRACT

Cylinder and ring shaped samples of hydrogels were prepared by polymerization of acrylic acid in the solution of polyvinyl alcohol. The swelling degree and mechanical properties of the hydrogels were determined. The two-components hydrogels are characterized by a higher breaking strength and elasticity than the polyacrylic acid gels. It was found that the hydrogels demostrate the electromechanical response.

Keywords: hydrogels, polyacrylic acid, polyvinyl alcohol, swelling degree, mechanical properties

† Corresponding Author: Prof. G.K. Elyashevich, Dr.Sci. (Polymer Physics), Institute of Macromolecular Compounds, Russ.Acad.Sci, 199004 Saint-Petersburg. Tel./Fax: +7 812 3286876; E-mail: elya@hq.macro.ru

EXTENDED THESES ABSTRACTS

ALLOYS AND COMPOSITE MATERIALS

Smart Nanocomposites
Volume 7, Number 2
ISSN: 1949-4823

APPLICATION OF POWDERS OF REFRACTORY MATERIALS WITH NANOFILMS RECEIVED BY IODIDE TRANSPORT

Sergei P. Bogdanov*
St. Petersburg State Institute of Technology (Technical University),
St. Petersburg, Russia

ABSTRACT

The results of the coating (of the precipitation of metal nanofilms) on the powders of refractory materials: diamonds, boron nitride, silicon carbide, tungsten carbide, metallic tungsten by the iodide-transport method were presented. The developed method allows to obtain coatings on the powders with a particle size of between ten nanometers to several micrometers, and surface-marker products. Powders of solid materials modified with nanofilms of metals and their compounds, the obtained composite materials.

Keywords: coatings on powders, diamond, cubic boron nitride, silicon carbide, tungsten carbide, tungsten, composite materials, iodide transport

INTRODUCTION

Consolidation of the powders of refractory materials has a number of difficulties such as: the need of high temperatures during compaction, possible recrystallization of the grains in the sintering process, the difficulty of homogenization of the composition [1]. One of the ways to intensify the process and improve the result of compaction - create on the surface of the functional coating. The main purpose of the coating – activation of the sintering process. When obtaining functional coatings on micron and nano-dimensional powders, the most suitable method is the deposition from the gas phase, including gas transport.

The aim of this work consists of applying the method of iodide transport [2-4] thin films on powders of refractory materials and in exploring the possibility of generating composites. The objects of the study were powders of diamond, cubic boron nitride (cBN), carbides of silicon and tungsten (SiC and WC), tungsten (W) in different grain sizes. As a metal deposited on the surface of these powders of refractory materials, used Ti, Cr, Co, Ni, Fe, Mo.

* E-mail: BogdanovSP@mail.ru

THE RESULTS OF THE STUDY AND DISCUSSION

The developed method allows to obtain coatings as powders with a particle size of between ten nanometers to several millimeters, and the surface marker products [5]. The thickness of the coatings varies in the range from 1 nm up to several micrometers.

Single crystal diamond grains with a size of 200-250 μm, the obtained film of titanium and titanium carbide with a thickness of about 50 nm. This composite can be used in the abrasive tool, and for heat dissipating substrates. The application of iodide transport technique afforded plating of detonation nanodiamonds (DND). This material is a grain size less than 50 nm, consisting of a blocks size of 1.6 nm. The thickness of the coating of titanium compounds for different samples ranged from 0.5 to 3 nm. The material used for the sintering of cutting inserts by hot pressing at a pressure of 4-5 GPA. The strength of the sintered composite clad plates from the DND up to 14 GPA, which is 3 times the strength of known as the ceramic, and tungsten carbide (WC) alloys. The microhardness of the plates reaches 60 GPa, and commensurate with the hardness of polycrystalline diamond [1].

By the method of iodide transport were obtained coatings on powders of boron nitride, silicon carbide, tungsten carbide, boron carbide, used for cutting tools, refractory, armored and wear-resistant ceramics.

Tests made of inserts of clad powders, cBN, showed that the structure of the composite is homogeneous between the cBN grains is observed a uniform layer of the products of chemical interaction between the activating substances with the surface of the grains. Since the method allows to obtain coatings of different composition from the metal titanium, products of its interaction with the boron nitride – TiN, TiB, and TiB_2, or TiN one. Thus, we can adjust the contents of different phases (Ti, TiN, TiB and TiB_2) in the coating composition. In combination with infiltration of aluminum, it allows you to adjust the phase composition of the composition within wide limits, which opens the way to the soft regulation of the properties of the cutting element under specific operating regimes and types of the processed materials [6]. The use of cBN powders clad with molybdenum, possible to create a composite material, successfully operating in the mode of cutting with the beat.

Nano-WC powders plated with titanium and titanium carbide used for the application of protective coatings by micro-plasma spraying on titanium alloy [7]. Received a protective coating superior in corrosion resistance of the coating, deposited from tungsten carbide powders, and wear resistance they are superior to coatings deposited from powders of titanium.

REFERENCES

[1] Novikov, N. V., Ed., Polikristallicheskie materialy na osnove almaza (Diamond_Based Polycrystalline Materials), Kiev: Naukova Dumka, 1989 [in Russian].

[2] Bogdanov S. P. Preparation of Coatings on Powders by the Iodine Transport Method, *Glass Phys. Chem*., 37, (2), (2011), 172–178.

[3] Bogdanov S. P. Iodide transport method for obtaining coatings onto powders, Bulletin of the Saint Petersburg State Institute of Technology (Technical University), 16(42), (2012), 24-28. [in Russian].

[4] Bogdanov S. P. Chemical activity of coatings prepared by iodide transport method, *Glass Phys. Chem*.,.38, (6), (2012), 750-754. [in Russian].

[5] Hristyuk N. A., Bogdanov S. P., Sychov M. M., Actual methods of preparing of the chromium–containing coatings on steel by means of gas transportation method, Bulletin of the Saint Petersburg State Institute of Technology (Technical University), 29(55), (2015), 10-14. [in Russian].

[6] Bogdanov S. P., Garshin A.P., Ponomarenko V. A., Composite material based on boron nitride micropowder with a coating, *Refractories and Industrial Ceramics*, 56, (6), (2016), 615-620.

[7] Bobkovaa T. I., Farmakovskii B. V., Bogdanov S. P., Creation of Composite Nanostructured Surface-Reinforced Powder Materials Based on Ti/WC and Ti/TiCN Used for Coatings with Enhanced Hardness, Inorganic Materials: *Applied Research*, 7, (6), (2016), 855–862.

Smart Nanocomposites
Volume 7, Number 2
ISSN: 1949-4823

THE USE OF IODINE TRANSPORT FOR CHROMIZING STEEL WITH DIFFERENT CARBON CONTENT

N. A. Hristyuk* and S. P. Bogdanov, PhD
State Institute of Technology, Saint Petersburg, Russia
Department of Theoretical Foundations of Material Science

ABSTRACT

Chromium diffusion coatings combine high corrosion resistance and wear resistance and are used for cladding steels in aggressive environments at high temperatures. The work presents opportunities of iodine transport for production these coatings.

Keywords: chromizing, steel, iodine transport

Iodine transport is applied successfully for refining metals [1] and the cladding powder [2], but in the literature [3] there are no data about its application for pack chromizing of steel. We have carried out experiments on the diffusion chromium plating three materials other than carbon, this is steel AISI 1020, AISI 1045 and armco iron at temperature 500°C, 600°C, 700°C, 800°C, 900°C. The time of thermochemical treatment was of 1.5 hours, 3 hours and 6 hours. The resulting coatings were determined in the thickness of the etched cross sections on metallographic microscope. The chemical composition was investigated by X-ray fluorescence analysis (XRF) of the surface and by scanning electron microscopy (SEM) with energy dispersive microprobe analysis (EDMA). Phase composition was determined by X-ray diffraction (XRD) analysis. Also we defined roughness and surface microhardness.

It is found that the chromium-containing coating is formed even at 500°C. At constant temperature, the coating thickness increases proportionally to the square root of the treatment time and reaches 10 microns on AISI 1045, treated at 900° C for 6 hours. At armco - iron under the same conditions the coating thickness is 30 microns.

According EDMA for samples of steel was produced at a temperature 900°C the surface mass content of chromium is about 90%, at the armco - iron has a diffusion zone with a chromium content of 15 - 20%. According to the obtained XRD coatings on steel is containing in its composition as a metallic phase and carbides.

By reducing the temperature along with the general decrease in the thickness of the coating it decreases the average chromium content, while increasing the proportion of iron.

* Corresponding Author Email: nikolai.hristyuk@mail.ru

Just at the same time reduced sintering initial pack mixture and the surface roughness of up to Ra = 1,0 - 1,5 mm. The microhardness of the surface increases with increasing temperature and carbon content of the steel and only slightly dependent on the treatment time, reaching 17 GPa to AISI 1045.

REFERENCES

[1] Rolsten R. F. Iodide Metals and Metal Iodides, New York: Wiley, 1961.
[2] Bogdanov S. P. *Glass Phys. Chem*., 37, (2), (2011) 172–178.
[3] Czerwinski F. Heat Treatment – Conventional and Novel Applications. Edited by Frank Czerwinski, Published by InTech, Janeza, Croatia 2012. – 408p.

Smart Nanocomposites
Volume 7, Number 2
ISSN: 1949-4823

THE DEPENDENCE OF THE PROPERTIES OF CERAMIC CUTTING TOOLS ON ITS POROSITY

Aleksei D. Khalimonenko [*] ***and Dmitrii A. Osminko***
Saint Petersburg Mining University,
Saint Petersburg, Russia

ABSTRACT

The article examines the forecasting operability of the cutting tool equipped with a removable ceramic inserts by measuring the porosity of the ceramic that have an impact on its cutting properties. It is proposed to measure the porosity of the ceramic based on its correlation with electrical resistivity of the removable ceramic insert.

Keywords: cutting ceramics, porosity of the material, operability of the ceramic tool

GOALS

The aim of this work is to determine the operability and cutting properties of the ceramic tool, affecting the quality of machining on lathes.

The operability and cutting properties of ceramic tool depends on microstructural parameters and porosity of this material. Thus the operability of ceramic tool can be defined as the porosity of the material, determined through correlation of porosity from electrical resistivity ceramics.

INTRODUCTION

One of the most important factors in modern mechanical engineering is the improvement of production technology. Feature of modern production is the use of tool materials that have high cutting properties. These materials include cutting ceramics.

Now more and more ceramic cutting tool is widely used, which is used for processing the precision machine parts. Share a cutting of ceramics in the total mass of the applied tool materials currently does not exceed 5...8%. According to forecasts, the share of ceramics in the near future is expected to grow to 15% [2].

[*] khalim76@rambler.ru

During operation of the cutting ceramics is observed that the accuracy of the details under the same processing conditions is different. This fact is based on the differences of the microstructure and porosity of ceramic plates. The definition and justification of these parameters will give an objective picture of the most rational use of ceramics for specific processing conditions [1, 3].

This will allow you to control the quality of processing and performance of ceramic tool in turning process.

Besides the other factors, the operability of ceramics is greatly influenced by the porosity of the material. The lower the porosity, the better the cutting properties and operability of a ceramic tool.

Thus, the solution of the problem of forecasting operability of a ceramic tool can be achieved by determining the dependence of the cutting properties on the ceramic material's porosity.

MATERIALS AND METHODS

The pores of a ceramic tool can be attributed to the mesopores and micropores.

Under normal conditions, to determine the number of pores, the size of which is 0.1...10 nm, such methods are used, the application of which in industrial environments is very difficult. There are many types of porous systems; the pores vary greatly in shape and size. In addition, all pores can be classified into closed, open and through [1, 3].

Closed pores can be estimated only by methods that destroy the structure of the material.

Open pores, depending on their size, can be measured by either gas adsorption methods or by the method of mercury porosity measurements. There is also the method of gas permeability of the material.

The porosity of the ceramic can be assessed with a microscope, and the ceramic insert itself for the study should be carefully prepared in a special way, that takes a very long time.

Equipment for the evaluation of porosity is very expensive, therefore, to assess the performance of ceramic tool is not suitable.

To solve this problem, it is proposed to use a correlation dependence of the porosity of cutting ceramics on the specific electrical resistance of the ceramic insert [1, 4].

RESULTS AND DISCUSSION

Researches have shown the existence of the dependence of the ceramic's porosity P on the value of its electrical resistivity, and allowed to determine its quantitative component.

Processing results of the study prove that the inserts from cutting ceramics with the value of electrical resistivity $R \approx 100$ Ω porosity of the material is about 8%. In cutting inserts of ceramic with the size of the electrical resistance $R \approx 10$ Ω porosity of the material is about 14% [3].

Thus, it can be concluded that the cutting ceramics with electrical resistivity value of $R \approx 100$ Ω quantity and pore size will be minimal compared with the ceramics with the value of the electrical resistance $R \approx 10$ Ω [3].

Ceramics with a parameter of the electrical resistance R ≈ 100 Ω will have a higher tool life period. Ceramic tool with such electrical resistance can be used for machining precise parts [1, 5].

CONCLUSION

In the end, it can be concluded that the greater would be the value of the specific electric resistance of the cutting ceramics, the greater would be the operability of the instrument.

Cutting tool with high values of electrical resistivity and therefore lower porosity should be used to process the most accurate elements of machine parts, as its operability will be greater than that of the tool with ceramic plates with small electrical resistivity.

Selection of ceramic tools for machining different precision parts of machinery can be done either at the factory that makes ceramic tool, either at the place of operation of the cutting ceramics.

REFERENCES

[1] Maksarov V. Machining quality when lathing blanks with ceramic cutting tools / *Agronomy Research* V. Maksarov, A. Khalimonenko, D. Timofeev. *Tartu: Estonian University of Life Sciences,* 2014, Vol. 12, №1, P. 269-278.

[2] Margules A. U. Cutting metals cermets. M.: Machine building, 1980, 160 p.

[3] Maksarov V. V. The quality management of the process of turning the instrument of the cutting ceramics. Monograph/V.V. Maksarov, J. Olt, A. D. Khalimonenko. SPb: NWTU, 2010, 172 p.

[4] Maksarov V. V. A study of tools, equipped with removable inserts of the cutting ceramics/V. V. Maksarov, J. Olt, T. Laatsit, A.D. Khalimonenko. *SPb: Tools and technologies,* 2008, N 30-31, P. 132-136.

[5] Maksarov V. Effect of porosity on the performance of cutting ceramics/Agronomy Research/V. Maksarov, A. Khalimonenko, *J. Olt. Tartu: Estonian University of Life Sciences,* 2016, Vol. 14, Special issue №1, P. 1043-1052.

ANALYTICAL METHODS AND THEORETICAL INVESTIGATIONS

Smart Nanocomposites
Volume 7, Number 2
ISSN: 1949-4823

DETERMINATION OF DIMENSIONAL PARAMETERS OF MATERIALS BY DISPERSING METAL PARTICLES AND MINERALS

I. I. Beloglazov [*] ***and A. A. Byzova***
Automation of Technological Processes and Production Department,
Faculty of Mineral Processing, Saint Petersburg Mining University, Russia

ABSTRACT

Dispersing agents to nanometer size particles leads to emergence of qualitatively new physical properties. The most striking example of a fundamental change of matter properties are the optical properties of metal nanoparticles (MNP) of the limited size of the object, which can be very different from the same characteristics of the "bulk" material. Such particles are capable to absorb electromagnetic radiation in the spectral ranges, where the bulk material did not absorb. These features are the cause of manifestation of unique colors, for example, nanoparticles of copper, gold, silver, and various minerals.

Keywords: nanomaterials, metal nanoparticles, dimensional characteristics

INTRODUCTION

Similar effects involving the MNP and minerals are the object of research and find numerous applications in both the scientific and practical purposes. Among the wide range of devices, which are based on the optical properties of the MNP can be mentioned optical filters, nonlinear-optical switches and guides light, spectral and polarization-selective film materials for optical data storage, reversible photosensitive glass, label biomolecules; these properties also can be used to increase the sensitivity of Raman spectroscopy, etc.

The optical characteristics of the MNP and minerals are studied by using classical spectroscopy, therefore the majority of works (Kiefer et al., 2015; Bovand et al., 2016; López-Lorente and Mizaikoff, 2016; López-Lorente and Valcárcel, 2016; Majedi and Lee, 2016) devoted to different methods of producing nanoparticles and investigation of their

[*] Assist. Prof. Dr. Beloglazov I.I. Automation of Technological Processes and Production Department, Faculty of Mineral Processing, Saint-Petersburg Mining University, Russia. Tel.: + 79217785984.
E-mail: beloglazov@spmi.ru

physical properties are analyzed primarily the absorption spectra. Optical spectra contain information about the most important physical characteristics of the media with the MNP such as the particle and distribution size, degree of aggregation, the thickness of adsorbed layers, etc.

These spectra allow observing changes in the electronic structure of the minerals in the transition from the "volume" of a substance to small particles. Such small particles are widely distributed among the natural and technogenic objects. These include minerals, metals, alloys, microorganisms, ash, dust, fumes etc. An extensive literature study on the properties of nanoparticles has been accumulated, the special properties of nanomaterials that cannot always be explained in terms of classical physics (Smirnov, 2000a; Gusev, 2007; Roco et al., 2011; Yoda et al., 2012) identified. Many issues of the physics of nanoparticles remain unresolved. These include the issue of the upper size limit of the nanoparticles, the role of structural defects, and the methods of producing nanomaterials with stable properties.

The following abnormal properties are set to nanomaterials: changing the melting point of metals, the eutectic temperature for alloys, specific heat, thermal conductivity, a significant increase in hardness and reduced ductility and variation of the crystal structure type and other characteristics. It is essential that the dependence of "size - property" is nonmonotonic.

The lack of data about the upper limit of nanoparticles leads to non-reproducibility properties of nanomaterials, which complicates their practical use. The maximum size of nanoparticles are calculated on the basis of geometrical considerations (Palumbo, Erb and Aust, 1990; Yoda et al., 2012), and do not include any type of crystal structure or the size of the unit cells of various substances.

Abnormal properties of nanoparticles explain a significant share of interfaces that is the increase in the number of surface chemical bonds with decreasing particle size.

By reducing the size of small particles, the number of internal (volume) and external (surface) bonds reduced in proportion to the III and II degree linear parameter ($v = a^3$; $s = 6a^2$). At the nanoscale comes equal number$N_s \approx N_v$.

Dimension unit (N_s/N_v) equal to 1, meaning that the number of surface bonds equal to the number of volume. With such a ratio, as shown by the experimental data, the physical properties change abruptly nanoparticles. It was found that for different substances sized module of 1, implemented at different linear dimensions, but also a quantitative assessment in (Smirnov, 2000b; Beloglazov and Syrkov, 2005; Gusev, 2007; Roco et al., 2011) is not given.

DIMENSIONS OF THE UNIT CELLS

In this paper, we propose to carry out the calculation of dimensional characteristics of small particles by determining the number of unit cells of the crystal structure of the material relating to the volume (V_v) and the surface (V_s) "cubes" predetermined linear dimension. Consider the "cubes" with linear dimensions of 10, 100, 1000 and 10000 nm. Then the number of surface connections is equal 6S nm^2/s nm^2, and the number of surround connections ($Vnm^3/v\,nm^3$) - (6S nm^2 / s nm^2) where S - the surface of a given «Cube», s - surface of the unit cell, V - volume given cube, and v - volume of the unit cell. Then the dimension of the module R is equal to:

$$R = \frac{v_s}{v_v - v_s}$$

where v_v - number of unit cells in a volume of "cube" and v_s- the number of elementary cells on the surface of the "cube".Different in composition and crystal structure of metals and minerals considered in Tables 1 and 2.

These data show that the particle size of the linear dimensionl_0 ≈10 nm close to the unit 1 and is from 0.3 to 4.1 for different substances.When the line size $l_0$is 100 nm or more, dimension module significantly less than 1 and it is from 0.002 to 0.02 or lower.Thus, the upper limit of the nanoparticle size varies for different materials and depends on the size of the unit cells. For substances with low unit cell volume (diamond, platinum, periclase), the upper limit of the nano-particle size is below 10 nm. For minerals with large unit cells the upper limit of the size of the nanoparticles is greater than 10 nm (grossularite, leucite).

Table 1. Dimensions of the unit cells of minerals

№	Mineral	The parameter of the unit cell, a_o, nm	The volume of the unit cell, v_o, nm^3
1	Diamond (C)	0,36	0,074
2	Platinum (Pt)	0,39	0,059
3	Periclase (MgO)	0,42	0,074
4	Pyrite (FeS_2)	0,54	0,157
5	Halite (NaCl)	0,56	0,176
6	Galena (PbS)	0,59	0,205
7	Magnetite (Fe_3O_4)	0,84	0,593
8	Sozalit $Na_4(AlSiO_4)Cl$	0,89	0,704
9	Grossular ($Ca_3Al_2(SiO_4)_3$	1,19	1,685
10	Leucite ($KAlSi_2O_6$)	1,34	2,410

Table 2. Dimension modules R_v and R_d for the nano and small particles of different sizes l_0, nm

Mineral	Linear size cubes, l_0, nm							
	10		100		1000		10000	
	R_v	R_d	R_v	R_d	R_v	R_d	R_v	R_d
Diamond (C)	0,28	2,5	0,04	1,09	0,004	1,01	0,0004	1,00
Platinum (Pt)	0,31	2,8	0,03	1,10	0,003	1,01	0,0003	1,00
Periclase (MgO)	0,34	3,0	0,03	1,11	0,003	1,01	0,0003	1,00
Pyrite (FeS_2)	0,48	4,7	0,06	1,14	0,002	1,01	0,0002	1,00
Halite (NaCl)	0,51	5,1	0,02	1,14	0,002	1,01	0,0002	1,00
Galena (PbS)	0,55	5,8	0,03	1,22	0,003	1,01	0,0003	1,00
Magnetite (Fe_3O_4)	1,02	-251(?)	0,05	1,22	0,005	1,02	0,0005	1,00
Sozalit $Na_4(AlSiO_4)Cl$	1,15	-3,04	0,05	1,24	0,005	1,02	0,0005	1,00
Grossular ($Ca_3Al_2(SiO_4)_3$	2,50	-5,7	0,07	1,33	0,007	1,03	0,0007	1,00
Leucite ($KAlSi_2O_6$)	4,10	-4,3	0,08	1,38	0,008	1,03	0,0008	1,00

Small particles of micron size, obtained by dispersion of minerals, contain a significant number of structural defects (clastic small particles (Revnivtsev V.I., Dolivo-Dobrovolskaya G. I., 1992)). Defective connection, obviously, reduce the amount of volume (not dangling) bonds and increase the number of defective ties, similar surface. sized module R_d was calculated for the debris of small particles and is calculated as follows:

$$R_d = \frac{N_s + N_d}{N_v - N_s - N_d}$$

where N_d - number of defective bones. The number of defective bonesN_d can be considered equal to$N_v/2$ in the crystal structure of clastic particles deformed by mechanical action.

R_d calculation module size based on defective connections shown that $R_d \approx 1$ is realized in small particles of debris in their linear size from 0.1 to 10 microns and a very small change in composition of the different metals and minerals.

CONCLUSION

It follows that for small particles obtained by mechanical dispersion, the presence of structural defects becomes a major influence, and not the size of the unit cells.

Thus, the upper limit of the size of the nanoparticles is in the range 1-10 nm, depending on the unit cell size of the substance, and the upper limit of small debris particles of micron scale is more than 0.1 m and not dependent on the size of the unit cells. This limit is determined by the number of defective bonds in the molecule. A larger or smaller number of defective connections depends in turn on the type of crystal structure and is defined as previously shown, the size of the mineral defectiveness (Dementieva G.I., Beloglazov I.N., 2005).

REFERENCES

Beloglazov, I. N. and Syrkov, A. G. (2005) 'Nanostructured metals and materials: Actuality of problems and availability of investigations', (9), pp. 4–5.

Bovand, M., Rashidi, S., Ahmadi, G. and Esfahani, J. A. (2016) 'Effects of trap and reflect particle boundary conditions on particle transport and convective heat transfer for duct flow - A two-way coupling of Eulerian-Lagrangian model', *Applied Thermal Engineering*, 108, pp. 368–377. doi: 10.1016/j.applthermaleng.2016.07.124.

Dementieva G. I., Beloglazov I. N., S. S. N. (2005) 'Defektoemkost kristallicheskoi strukturi,' *Tsvetnye Metally*, 9, pp. 54–56. Available at: http://rudmet.ru/journal/1073/article/17501/.

Gusev, A. I. (2007) *Nanomaterialy, nanostruktury, nanotechnologii*. Fizmatlit.

Kiefer, J., Grabow, J., Kurland, H. D. and Müller, F. A. (2015) 'Characterization of Nanoparticles by Solvent Infrared Spectroscopy', *Analytical Chemistry*. American Chemical Society, 87(24), pp. 12313–12317. doi: 10.1021/acs.analchem.5b03625.

López-Lorente, Á. I. and Mizaikoff, B. (2016) 'Recent advances on the characterization of nanoparticles using infrared spectroscopy', *TrAC Trends in Analytical Chemistry*. doi: 10.1016/j.trac.2016.01.012.

López-Lorente, Á. I. and Valcárcel, M. (2016) 'The third way in analytical nanoscience and nanotechnology: Involvement of nanotools and nanoanalytes in the same analytical process', *TrAC Trends in Analytical Chemistry*, 75, pp. 1–9. doi: 10.1016/j.trac.2015.06.011.

Majedi, S. M. and Lee, H. K. (2016) 'Recent advances in the separation and quantification of metallic nanoparticles and ions in the environment', *TrAC Trends in Analytical Chemistry*, 75, pp. 183–196. doi: 10.1016/j.trac.2015.08.009.

Palumbo, G., Erb, U. and Aust, K. T. (1990) 'Triple line disclination effects on the mechanical behaviour of materials', *Scripta Metallurgica et Materialia*. Pergamon, 24(12), pp. 2347–2350. doi: 10.1016/0956-716X(90)90091-T.

Revnivtsev V. I., Dolivo-Dobrovolskaya G. I., V. P. S. (1992) *Технологическая минералогия обломочных малых частиц/*Nauka. Saint-Petersburg: Наука. С.-Петербург. отд-ние,.

Roco, M. C., Mirkin, C. A., Hersam, M. C. and Hersam, M. C. (2011) *Nanotechnology research directions for societal needs in 2020 : retrospective and outlook*. Springer.

Smirnov, B. M. (2000a) *Clusters and Small Particles*. New York, NY: Springer New York (Graduate Texts in Contemporary Physics). doi: 10.1007/978-1-4612-1294-2.

Smirnov, B. M. (2000b) *Clusters and Small Particles*. New York, NY: Springer New York (Graduate Texts in Contemporary Physics). doi: 10.1007/978-1-4612-1294-2.

Yoda, M., Garden, et al. (2012) 'Nanostructured Materials', in *Encyclopedia of Nanotechnology*. Dordrecht: Springer Netherlands, pp. 1766–1766. doi: 10.1007/978-90-481-9751-4_100564.

Smart Nanocomposites
Volume 7, Number 2
ISSN: 1949-4823

CONTACTLESS METHOD FOR THE MEASUREMENT OF THE CHARGE CARRIER DIFFUSION LENGTH IN SEMICONDUCTORS

Vasilii V. Manukhov[1], Aleksandr B. Fedortsov[2,*], and Aleksey S. Ivanov[2]
[1]Saint Petersburg State University, Russia
[2]Saint Petersburg Mining University, Russia

ABSTRACT

The described method is based on the two laser beams counteraction in semiconductors. The injecting radiation generates excess charge carriers in semiconductor. That leads to the changing of the optical characteristics of the material and to the modulation of the probing radiation directed through the semiconductor sample. Changing the distance between the point of carrier generation and the probed point the decrease of the charge carrier density is registered. The decrease depends on the diffusion length which is determined by comparing the theoretical and experimental dependences of the probing signal on the distance between injecting and probing beams.

Keywords: diffusion length, probing radiation, injecting radiation, charge carrier density, probing radiation modulation

INTRODUCTION

Presently many methods of the diffusion length direct measurement are offered. The most known of them are mobile probe method [1, 2, 3, 4, 5] and its variants and moving electron probe method [1, 5, 6]. The realization of these methods needs electric contact of the probe with the semiconductor surface which limits their use when the surface covered with insulator. New contactless laser-interference method, which earlier was successfully used for determining of the other electro-physical semiconductor parameters [7-10], is offered here.

* borisovitch-f@yandex.ru

DESCRIPTION OF THE METHOD

The offered method [11, 12] was realized by the experimental set up shown in Figure 1. The beam of the long-wave probing laser 1 is directed to the fixed point on the surface of the sample 3 and undergoes the multi beam interference in the sample. The photon energy of the probing radiation is less than the semiconductor forbidden gap and is chosen from the optical transparency range of the semiconductor. The probing radiation passed through the sample is registered by the photo detector 4 connected to the selective voltmeter 6.

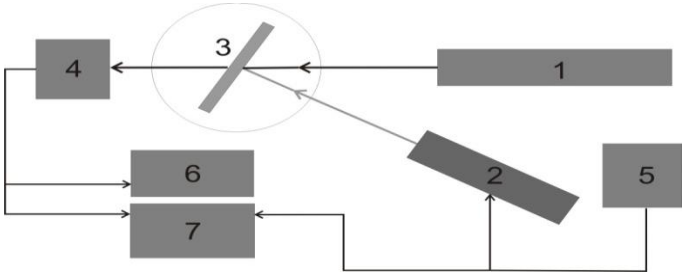

Figure 1. The experimental setup.

The injecting laser 2 beam is also directed to the surface of the sample 3. The photon energy of this radiation is larger than the semiconductor forbidden gap. The injecting radiation absorbed by the semiconductor generates excess electron-hole pairs changing thus the free carrier density as well as optical characteristics of the semiconductor. If the power of the injector laser radiation is modulated (by generator 5) the power of the probing radiation will be also modulated because of the modulation of the optical characteristics of the material. Some of the electro-physical semiconductor parameters can be determined by the probing beam modulation parameters.

The experimental setup permits to change the distance between the point of the carriers generation by the injector laser beam and the probed point as well as register the probing signal dependence on the distance between these points. As the probing signal is in direct ratio to the charge carrier density the dependence of this density on the distance to the carriers generation point become known. This dependence is determined by the charge carrier diffusion length which can be obtained by comparing the experimental and theoretical dependences of the probing signal on the distance between the injector and probing beams.

The amplitude of the probing signal is measured by the millivoltmeter 6. Dual-channel oscilloscope 7 is used for the visual monitoring of the signals from the generator 5 and photo detector 4.

CONCLUSION

The measurements showed the offered method to be simple in realization and to give reliable results. The significant advantage of the method is the possibility to investigate the semiconductor samples covered with the insulator layer if the latter is transparent for the injector and probing beams. It is very important for the measurements during the process of the semiconductor devices manufacturing.

REFERENCES

[1] V. V. Batavin, Yu. A. Kontsevoi, and Yu. V. Fedorovich, *Measurements of Parameters of Semiconductor Materials and Structures* (Radio iSvyaz', Moscow, 1985) [in Russian].

[2] T. Moss, G. Burrell, and B. Ellis, *Semiconductor Opto-Electronics* (Halsted Press Division, Wiley, 1973; Mir, Moscow, 1976).

[3] L. P. Pavlov, *Measurements on the Parameters of Semiconductor Materials* (Vyssh. Shkola, Moscow, 1987) [in Russian].

[4] N. F. Kovtonyuk and Yu. A. Kontsevoi, *Measurements of Parameters of Semiconductor Materials* (Metallurgiya, Moscow, 1970) [in Russian].

[5] P. Blood and J. W. Orton, Zarubezh, *Radioelektron.*, No. 1, 3 (1981).

[6] P. Blood and J. W. Orton, Zarubezh, *Radioelektron.*, No. 2, 3 (1981).

[7] A. B. Fedortsov and Yu.V. Churkin, *Sov. Tech. Phys. Lett*. 14, 142 (1988).

[8] V. B. Voronkov, A. S. Ivanov, K. F. Komarovskikh, D. G. Letenko, A. B. Fedortsov, and Yu. V. Churkin, *Sov. Tech. Phys*. 36, 184 (1991).

[9] A. G. Areshkin, L.E. Vorob'ev, A. S. Ivanov, K. F. Komarovskikn, D. G. Letenko, A. B. Fedortsov, and Yu. V. Churkin, *Izv. Akad. Nauk, Ser. Fiz*. 56 (12), 121 (1992).

[10] D. G. Letenko, A. B. Fedortsov, V. N. Savvateyev, and Yu. V. Churkin, *J. Mater. Sci.: Mater. Electron*. 3, 203 (1993).

[11] V. V. Manukhov, A. B. Fedortsov, and A. S. Ivanov, *Semiconductor*, 49 (9), 1119 (2015).

[12] V. V. Manukhov, A. B. Fedortsov, and A. S. Ivanov, *Russian patent № 2578731*.

Smart Nanocomposites
Volume 7, Number 2
ISSN: 1949-4823

THE INCREASE OF THE ACCURACY OF SOLID AND LIQUID TRANSPARENT FILMS THICKNESS MEASUREMENT

Igor V. Gonchar, Aleksandr B. Fedortsov*, and Aleksey S. Ivanov
Saint Petersburg Mining University, Russia

ABSTRACT

New method of data processing at the determination of the film thickness from the angle dependence of the measured film reflection coefficient of the laser beam is offered. The method and the setup realizing it permits to lower the film thickness measurement error to 150 nm within the measurement range from 10 to 1000 μm.

Keywords: film thickness, interference maximum, reflection coefficient

INTRODUCTION

Methods of the film thickness measurement based on the counting of the number M of interference maxima of the laser beam reflection coefficient $R(\Theta)$, changing the incidence angle from θ_1 to θ_2, are well known [1-6]. The film thickness d is calculated from the equation

$$d = \frac{M\lambda}{2\left(\sqrt{n^2 - sin^2\,\theta_2} - \sqrt{n^2 - sin^2\,\theta_1}\right)}, \quad (1)$$

where λ – is the laser wavelength, n –the refraction index of the film material. This method doesn't have enough accuracy for the number of applications. As the periodical interference dependence of $R(\theta)$, which is measured changing the incidence angle form θ_1 to θ_2,can have non-integer number of periods the error of counting the number of maxima M is equal to 1. The error of the film thickness determination in this case can be some micrometers.

There is a method [7, 8] where the film thickness d is determined from the calculated dependence $R(d)$ with an error less than 10 nm from the reflection coefficient R measured at

* borisovitch-f@yandex.ru

the fixed incidence angle θ. In this method, because of the periodical character of the dependence $R(d)$, it is needed to know the range of the expected value d with the accuracy of the half-period of the $R(d)$ function.

DESCRIPTION OF THE METHOD

Using the experimental dependence $R(\theta)$ within the range from θ_1 to θ_2 it is determined not only the number of the observed maxima but the value $R(\theta)$ as well at the known incidence angle θ^*, corresponding to one of the steep sections of the dependence $R(\theta)$.

The range of the possible values of d is determined by counting the number of the observed interference maxima M. The range is limited by the values d_1 and d_2, corresponding to M and M+1. The exact value of the film thickness d (which is between the beforehand chosen values d_1 and d_2) is determined by the value R, measured at the fixed incidence angle θ* from the dependence $R(d)$, calculated for the known film refraction index n.

EXPERIMENT

The optical-mechanical unit described in [4, 5] was used in the experimental setup.

The structure of the digital data processing is shown in Figure 1. During each rotation turn of the flat mirror the signal comes to ADC. The signal which is in direct ratio to $R(\theta)$ from optical-mechanical unit comes to ADC, which converts this dependence into single-dimension array.

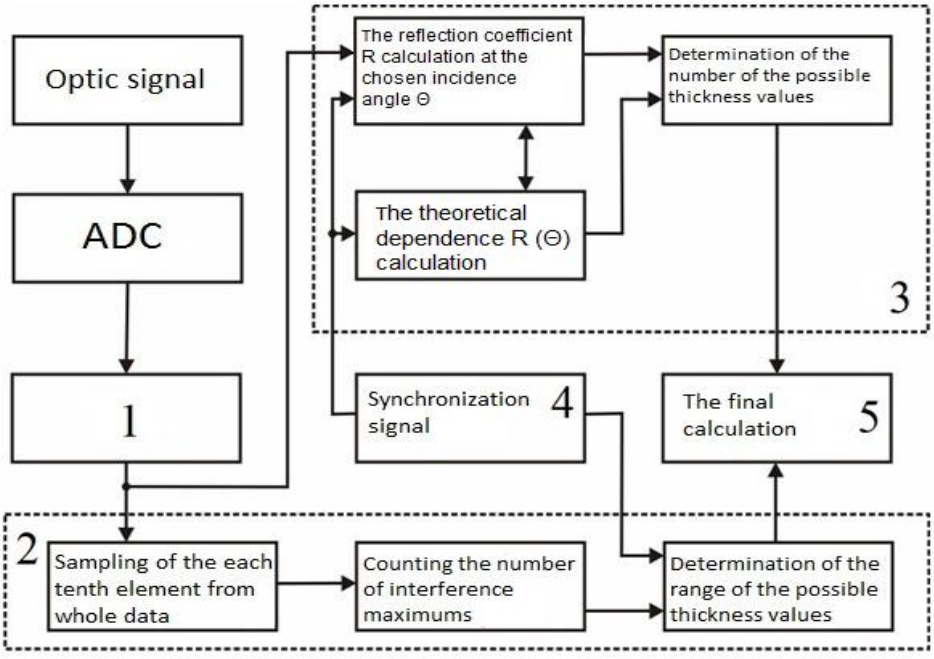

Figure 1. Data processing structure.

The unit 1 duplicates the signal from ADC and divides it into two flows going to the units 2 and 3.

To determine the range of possible thicknesses, which is based on counting the interference maximum number, the detailed reproduction of the signal is not needed. The selection of the each tenth element from the serial array is enough. This is fulfilled by the unit 2 which calculates maxima number and determines the range of the possible thickness with the accuracy of one period of the $R(\theta)$ function using the equation (1).

The full information from the ADC comes to the unit 3. For the calculations in this unit the data on the reflection coefficient R at the fixed incidence angle θ are used. For this purpose a reference signal from ADC comes to the unit 3. The unit 3 determines the half period of the $R(d)$ function corresponding the reference signal.

The unit 5 gets the data from units 3 and 4, makes the final calculations and sends the determined value of the film thickness to the monitor in symbol and graphic representation.

The test experiments showed that the offered method permits to measure the film thickness in the range from 10 to 1000 μm with accuracy of the order of 150 nm, i.e., with ten times better accuracy than in the prototype [1, 5].

REFERENCES

[1] T. Ohyama, Y.H. Mori. *Rev. Sci. Instrum*. 58, 1860 (1987).
[2] T. Ohyama, K. Endoh, A. Micami, Y. H. Mori. *Rev. Sci. Instrum*. 59, 2018 (1988).
[3] T. Nosoko, Y. H. Mori, T. Nagata. *Rev. Sci. Instrum*. 67, 2685 (1996).
[4] A.B. Fedortsov, D.G. Letenko, Yu. V. Churkin, I.A. Torchinsky, A.S. Ivanov. *Rev. Sci. Instrum*. 63, 3579 (1992).
[5] L. M. Tsentsiper, A. B. Fedortsov, D. G. Letenko. Instrum.*and Experimental Techn*. 39, 139 (1996).
[6] R. Ohmura, S. Kashiwazaki, Y. H. Mori. *J. of Crystal Growth*. 218, 372 (2000).
[7] Franz, W. Langheinrich. *Solid-State Electronics*, 11, 59 (1968).
[8] A. B. Fedortsov, K. E. Ugarova. «*Electron Technique*» (materials), 1974, № 4, p. 117.

Smart Nanocomposites
Volume 7, Number 2
ISSN: 1949-4823

THEORETICAL DEPENDENCE OF THE LOCAL CHARGE CARRIER DENSITY ON THE DISTANCE FROM THE POINT OF THEIR GENERATION BY THE POINT SOURCE (LIGHT SPOT)

Vasilii V. Manukhov[1], Aleksandr B. Fedortsov[2,†], and Aleksey S. Ivanov[2]
[1]Saint Petersburg State University
[2]Saint Petersburg Mining University

ABSTRACT

The diffusion length is determined comparing two dependences – theoretical and experimental – defining the carrier density decrease in the fixed point with the increase of the distance between this point and the carrier generation region. Presently unlike in the earlier used well-known methods the offered method uses the excess charge carrier generation by the injecting laser (light spot) and the carrier density is spherically symmetric. This demands the obtaining of the new theoretical dependences defining the carrier density decrease.

Keywords: diffusion length, charge carrier generation, excess carrier density, injecting and probing radiation

INTRODUCTION

To determine the charge carrier diffusion length it is needed to compare the experimental dependence of the local density of the excess carriers in the probed point on the distance between this point and the point of their generation with the similar theoretical dependences calculated for different values of the diffusion length as it was made in contact methods [1, 2, 3, 4].

In above mentioned works the generation region had the shape of the narrow strip of light, so the spatial distribution of the excess carriers is cylindrically symmetric. The offered method [5, 6] means the formation of the light spot on the semiconductor surface and the

† borisovitch-f@yandex.ru

excess carriers distribution becomes spherically symmetric. That demands the calculation of the proper theoretical dependences.

DERIVIATION OF THE OUTPUT FORMULAS

The excess carrier density can be determined from the continuity equation for the minority carriers. In our case it is better to present it in spherical coordinates

$$\frac{d^2\delta p}{dr^2}+\frac{2}{r}\frac{d\delta p}{dr}-\frac{\delta p}{L^2}=0 \tag{1}$$

where δp–is the excess holes density, $L=\sqrt{D\tau}$ - the charge carrier diffusion length, τ–the charge carrier lifetime, D –the diffusion coefficient, *r*–the distance between the point o the carriers generation and the point where their density is calculated.

After the variable substitution = r/Lи $\delta p = x^{-\frac{1}{2}}z$,we'll get the next equation

$$\frac{d^2z}{dx^2}x^2+\frac{dz}{dx}x-\left(x^2+\frac{1}{4}\right)z=0 \tag{2}$$

This equation is the modified Bessel equation. Taking into account the boundary conditions this equation solution will be

$$\delta p(r)=\delta p_0\frac{1}{\sqrt{r/L}}K_{\frac{1}{2}}(r/L), \tag{3}$$

where $K_{\frac{1}{2}}(r/L)$ – is the McDonald function.

If the distance from the point of the charge carriers generation to the point where the carrier density is determined exceeds significantly the sample thickness as well as the diffusion length *L* the solution (3) can be simplified:

$$\delta p(r)=\delta p_0\sqrt{\frac{\pi}{2}}\frac{\exp(-r/L)}{r/L}. \tag{4}$$

The relative error in this case will be

$$\frac{\Delta\delta p}{\delta p}<\frac{L}{r}. \tag{5}$$

CONCLUSION

The data got with the accordance to (3) and (4) was compared with the experimental results. Theoretical and experimental dependences coincide satisfyingly in the range of the big r (r > 1000 μm). Their mismatch in the range of the small r is apparently connected with the transverse dimension of the laser-injector beam (when the formulas were derived the radiuses of the injector and probe beams were supposed negligible). The difference of the results calculated using formulas (3) and (4) was less than 1 percent which permits to use the simpler formula (4). The use of these formulas in [5] showed that the use of the simpler formula gives the error much less than the error of the experimental results.

REFERENCES

[1] V. V. Batavin, Yu. A. Kontsevoi and Yu. V. Fedorovich, *Measurements of Parameters of Semiconductor Materials and Structures (*Radio iSvyaz', Moscow, 1985) [in Russian].

[2] L. P. Pavlov, *Measurements on the Parameters of Semiconductor Materials* (Vyssh. Shkola, Moscow, 1987) [in Russian].

[3] N. F. Kovtonyuk and Yu. A. Kontsevoi, *Measurements of Parameters of Semiconductor Materials* (Metallurgiya, Moscow, 1970) [in Russian].

[4] P. Blood and J. W. Orton, Zarubezh, *Radioelektron.*, No. 1, 3 (1981).

[5] V. V. Manukhov, A. B. Fedortsov, and A. S. Ivanov, *Semiconductor,* 49 (9), 1119 (2015).

[6] V. V. Manukhov, A. B. Fedortsov, and A. S. Ivanov, *Russian patent № 2578731.*

Smart Nanocomposites
Volume 7, Number 2
ISSN: 1949-4823

FULLERENE-CONTAINING NANOCOMPOSITES BASED ON POLY(PHENYLENE OXIDE): DIELECTRIC SPECTROSCOPY

Natalia A. Nikonorova[1,*], Alexey A. Kononov[2], Kirill L. Levine[3], and Rene A. Castro[2]

[1]Institute of Macromolecular Compounds of Russian Academy of Sciences, Saint Petersburg, Russia
[2]Herzen State Pedagogical University of Russia, Saint Petersburg, Russia
[3]Saint Petersburg Mining University, Saint Petersburg, Russia

ABSTRACT

Nanocomposites based on poly(phenylene oxide) (PPO) and fullerene C_{60} (1, 2, 4 and 8 wt. %) were studied by dielectric spectroscopy. In all samples, two relaxation processes, local β and segmental α process, were observed. Molecular mobility in the region of the β process varies slightly with C_{60} concentration. In the case of the α process, molecular mobility changes non-monotonically with increasing fullerene concentration.

Keywords: molecular mobility, dielectric relaxation, nanocomposites, poly(phenylene oxide), fullerene C_{60}, glass transition temperature

1. INTRODUCTION

Polymer membranes are widely used for concentration and fractionation of gases and liquid mixtures, purification of products from the concomitant impurities [1-3]. Poly(2,6-dimethyl-1,4-phenylene oxide) (PPO) and nanocomposites based on it are commercially available product used as a structural and membrane material [4]. Dielectric spectroscopy (DS) is a modern research technique that allows us to identify the observed relaxation processes and attribute them to the mobility of certain kinetic units that include polar groups [5, 6]. In this paper, DS is used to investigate molecular mobility of poly(phenylene oxide) (PPO) and fullerene containing nanocomposites based on it with 1, 2, 4, and 8 wt.% of C_{60}

* Corresponding author: E-mail: n-nikonorova2004@mail.ru. Tel: (812) 3288535. Fax: (812) 328 68-69.

2. EXPERIMENTAL

Dielectric spectra, in the 10^{-1} to $5 \cdot 10^{6}$ Hz frequency range at temperatures varying from -100 to 330°C, were obtained using a broadband dielectric spectrometers "Concept 81 and 21." (Novocontrol Technologies).

3. RESULTS AND DISCUSSION

Dielectric spectra (qualitatively similar for all studied samples) show two regions of ε''_{max}: β and α processes. The analysis of dielectric spectra was performed by describing complex permittivity ε^* with the empirical Havriliak-Negami (HN) equation [6].The relaxation time values for the β and α processes calculated according to the HN formula are presented (as an example, for PPO-4) in the figure below. Dependences of $-log\,\tau_{max}=\varphi(1/T)$ for the β are linear and for α process are curvilinear and may be reliably described by the empirical Vogel–Tamman-Fulcher equation [6].

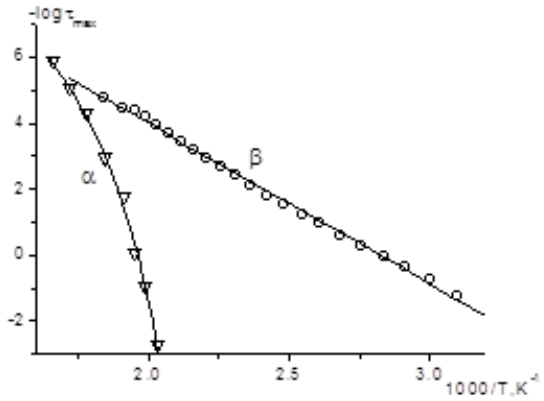

CONCLUSION

The studies of dielectric behavior of PPO nanocomposites contained 1, 2, 4, and 8 wt. % fullerene C_{60} show two relaxation processes: α and β. Molecular mobility responsible for the β process is defined mainly by intramolecular interactions and varies slightly with addition of fullerene. In the case of the α process, molecular mobility is determined predominantly by intermolecular interactions, and changes non-monotonically with C_{60} concentration.

REFERENCES

[1] Polotskaya G., Biryulin Yu., Pientka Z., Brozova L., Bleha M.: Transport properties of fullerene - polyphenylene oxide homogeneous membranes. *Fullerenes, Nanotubes, and Carbon Nanostructures*, 12, 365-369 (2004). DOI: 10.1081/FST-120027194.

[2] Polotskaya G. A., Penkova A. V., Toikka A. M., Pientka Z., Brozova L., Bleha M.: Transport of small molecules through polyphenylene oxide membranes modified by fullerene. *Separation Science and Technology*, 42, 333–347 (2007). DOI: 10.1080/01496390600997963.

[3] Penkova A. V., Polotskaya G. A., Toikka A. M., Trchová M., .louf M., Urbanová M., Brus J., Brozová L., Pientka Z.: Structure and pervaporation properties of poly (phenylene-*iso*-phthalamide) membranes modified by fullerene C_{60}. *Macromolecular Materials and Engineering*, 294, 432–440 (2009).DOI: 10.1002/mame.200800362.

[4] Penkova A. V., Polotskaya G. A, Toikka A. M. Pervaporation separation of acetic acid – methanol – methyl acetate – water reactive mixture. *Chemical Engineering Science*, 101, 586–592 (2013). DOI: 10.1016/j.ces.2013.05.055.

[5] Kremer F., Schönhals A.: Broadband dielectric spectroscopy. Springer Berlin Heidelberg, Berlin (2003).

[6] McCrum N. G., Read B. E., Williams G.: Anelastic and Dielectric Effects in Polymeric Solids. John *Wiley* & Sons, London (1967).

Smart Nanocomposites
Volume 7, Number 2
ISSN: 1949-4823

POROUS SILICON (POR-SI) LAYERS IMPEDANCE SPECTROSCOPY IN THE RANGE OF LOW FREQUENCIES

M. P. Sevryugina[1,*], Yu. M. Spivak[2], V. A. Moshnikov[2], and N. S. Pshchelko[1]

[1]Saint Petersburg Mining University, Saint Petersburg, Russia
[2]Saint Petersburg State Electro Technical University "LETI", Russia

ABSTRACT

Dielectric properties of porous silicon structures is investigated. Two types of polarization in the investigated structure: dipole relaxation and m migratory polarization in the low-frequency region are detected. The existence of relaxation processes associated with the diffusion of ions in the material is found.

Keywords: electric field, porous silicon, impedance spectroscopy, polarization, dielectric coefficients, frequency dispersion

Obtaining of complex compounds in the form of single crystals is a technologically difficult task, so most functional materials have a disordered heterogeneous structure. The electric transport of charge carriers in structurally heterogeneous samples has a number of specific features. Usage the method of impedance spectroscopy allows to get information about the electrophysical properties of the disordered structure, qualitatively and quantitatively to describe the contributions to the conductivity arising from the volume inclusions, surface and interphase boundaries.

This paper is devoted to the experimental study of the dielectric properties of layers of porous silicon by the method of impedance spectroscopy in the range of low frequencies.

The production of porous silicon layers was carried out by electrochemical anodic etching of monocrystalline silicon KEF - 5 (111), KEF-1 (111) KDB-10 (100) for 10 min at a current density of anodizing of 20 mA/cm^2 in galvanostatic mode [1]. The electrolyte used was an aqueous solution of hydrofluoric acid with the addition of isopropanol.

Measurements of frequency dependencies of dielectric coefficients of the layers of por-Si were performed using the spectrometer Concept-41 of the company Novocontrol

* E-mail: marysevrugina@yandex.ru

Technologies in frequency interval of $10^{-3} < f < 10^{6}$ Hz at a temperature of 293 K. the Setup consisted of a frequency impedance analyzer, measurement cell, and a system of automatic data collection with a computer interface.

The frequency dependence of the real and imaginary component of the impedance find the variance, expressed in the decrease in the values of components of complex impedance with frequency of the electric field. In the low frequency region, the sharp decline of the function $Z'(f)$ is observed in the range of $5 \cdot 10^{-3} - 2 \cdot 10^{-2}$ Hz, and for a function $Z'(f)$ such decline is observed up to 1 Hz. Since the frequency values $f > 1$ Hz and $f > 20$ Hz, the spectra of the imaginary and the real component of the impedance, respectively, meet constant minimum level. Dispersion of the impedance is characterized by the electric relaxation time, which is determined graphically by plotting the dependence of the imaginary components of the impedance Z'' vs the real Z'.

The diagrams of the impedance of the porous silicon layer in the coordinates of the Z''-Z' for areas of low and high frequencies are arcs of circles with centers at the frequencies $f_{01} \sim 7 \cdot 10^{-3}$ Hz and $f_{02} \sim 6 \cdot 10^{2}$ Hz, respectively, which pass into rectilinear sections. Such character of dependence $Z''(Z')$ suggests the existence of relaxation processes associated with the diffusion of ions in the material, namely, migratory polarization which is characteristic to heterogeneous semiconductor structures. Migratory polarization is characterized by the movement of charges in the inclusions to their borders and the accumulation of charges at the interfaces.

To describe linear diffusion processes the Warburg impedance for semi-infinite diffusion length Ws [2] is used:

$$Z_W = \frac{(1-j)W}{\omega^{0,5}},$$

where W is the Warburg constant that depends on particle concentration and diffusion coefficient.

Parts of the diagrams corresponding to the arc of a circle, characterized by the Debye type relaxation with a single relaxation time τ. The center of the semicircle is offset below the axis Z', which indicates the deviation from ideal the Debye behavior in the field of the relaxation losses, and is also characteristic of complex structures. The value of τ can be estimated by the frequency f_0 corresponding to the maximum of Z'':

$$\tau = \frac{1}{2\pi f_0}.$$

For low frequencies $f_{01} = 7 \cdot 10^{-3}$ Hz and we find $\tau_1 = 22{,}7$ s, for high - $f_{02} = 600$ Hz we find $\tau_2 = 130 \cdot 10^{-6}$ s.

Study of impedance characteristics of porous silicon allows to make a conclusion about the existence of two types of polarization in the investigated structure: dipole relaxation and m migratory polarization in the low-frequency region [3]. The contribution of the migration component of polarization is due to the existence of ions in porous silicon absorbed in the electrically active state which move to the border section of the porous and form a spatial charge.

Thus, porous silicon is a material with complex structure, the polarization processes in which are highly dependent on external factors, in particular, on the frequency of the applied electric field.

REFERENCES

[1] Moshnikov V. A., Spivak Yu. M. "Electrochemical methods for production of on - ristich materials for fuel cells." Chapter 5//*Basics of hydrogen energy*. Under the editorship of V. A. Moshnikov, I. E. and Terukov. 2-nd ed. S-Pb.: Publishing house of "LETI". - 2011, 288 p.

[2] Warburg E. Uber das Verhalten sogenannter unpolarisierbarer Electroden gegen Wechselstrom//*Ann. Phys. Chem*. -1899. vol. 67, No. 3. p. 493-499

[3] Sevrugina M. P., Spivak Yu. M., Pshchelko N. S. Low-frequency dielectric spectroscopy of the por-Si layers//Intermatic – 2014/Materials of international scientific-technical conference "Fundamental problems of electronic instrument engineering." –M., MIREA, 2014, part 3, p. 59-61.

Smart Nanocomposites
Volume 7, Number 2
ISSN: 1949-4823

THE SIMULATION OF MIXERS SIGNALS IN THE COMPUTER PROGRAM FASTMEAN

Yu. A. Nikitin and Valentina A. Yurova*
The Bonch-Bruevich Saint Petersburg State University of Telecommunications,
Saint Petersburg, Russia

ABSTRACT

In the paper we obtained the basic spectral and temporal characteristics of the output signal of the frequency mixers on the basis of which the constructed schemes of the spectrum analyzers. We present results of a comparative analysis of the linearity of the signals multiplication by using a generic approach and the same parameters of the active elements.

Keywords: bipolar transistor, frequency multipliers, spectrum analyzer, spectral characteristics, temporal characteristics

INTRODUCTION

In modern electronics are widely used various materials, its combinations and the layered structures and the new are created. Currently, the typical dimensions of the electronic devices are several hundreds or thousands of nanometers. Therefore, the one of major task in the manufacture of electronic equipment is to measure the spectral characteristics with high accuracy. It means that such devices as spectrum analyzers are make the strict demands on the linearity of the multiplication of the measurement signals at the circuits of frequency mixers, i.e., the level of nonlinearity of the active device. Generally, the different approaches, evaluation indicators and the mathematics are used in the investigations, devoted to the analysis parameters and operation modes of amplifiers and frequency converters. It's making difficulty to compare the parameters of the considering electrical circuits. So the aims of our research are obtaining spectral and temporal characteristics of the circuits of frequency mixers based on transistors, and a comparative analysis of the linearity of the multiplication, using a common approach and the same active elements parameters.

* Corresponding author: Valentina A. Yurova, Docent, the Bonch-Bruevich Saint - Petersburg State University of Telecommunications, Saint – Petersburg, Russia, E-mail: va-yurova@mail.ru

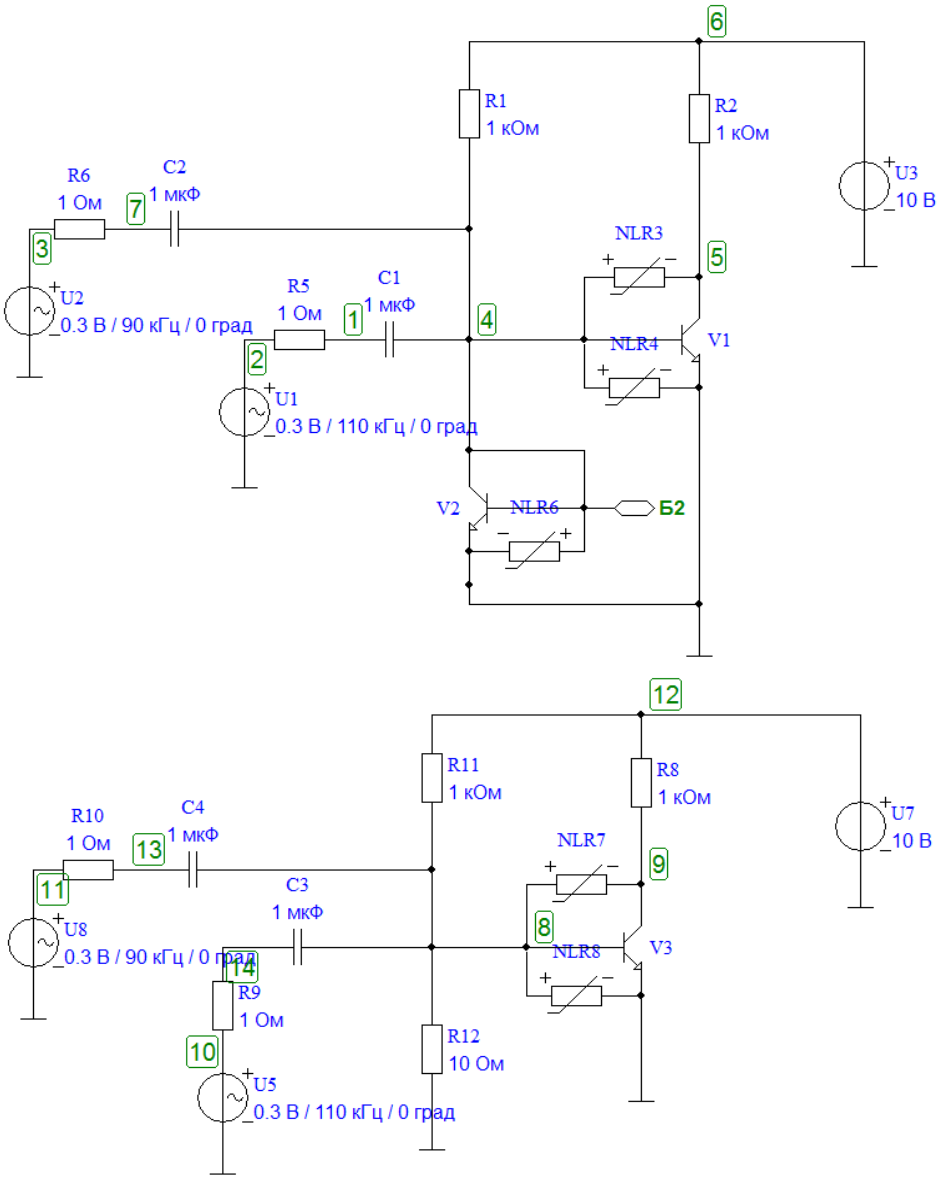

Figure 1. The diagrams of the electric circuits of cascades based on the current mirror (left) and the transistor cascade (right).

OBJECT OF RESEARCH

As the objects of research were chosen electric circuit mixers based on a transistor cascade and cascade current mirror (Figure 1). These electric circuits are widely used as an individual cascades, and are the basis for designing more complex circuits of frequency mixers, which are widely used in electronics and measuring technology of the manufacturing and the laboratory investigations of nanoelectronic devices and materials of the nanotechnology [1 – 4].

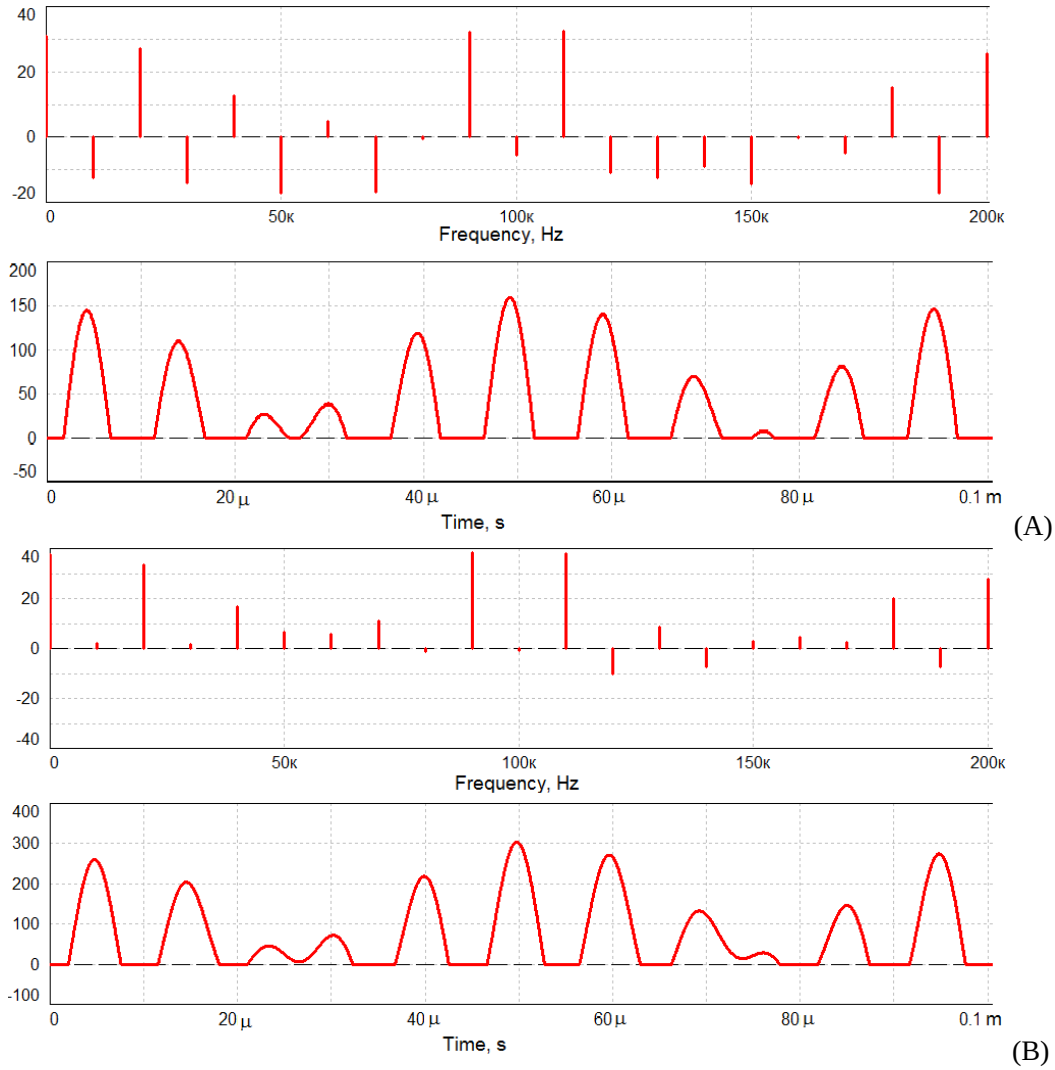

Figure 2. Spectrum and timing diagrams of the electric circuit of cascade based on the current mirror (a) and of the electric circuit of the transistor cascade (b).

METHOD OF RESEARCH

To obtain the spectral and temporal characteristics of the output signal and to make the comparative analysis of the linearity's parameters of the cascades electric circuits was used the computer program for simulation of electrical circuits FASTMEAN 6.0 [5]. Its make possible to carry out spectral research of the different structures of the mixers over a wide dynamic range, applying a built-in database of the elements, or to use nonlinear models based on exponential or polynomial approximation with required accuracy.

Generally, the most schemes electrical circuits are based on semiconductor elements, comprising one or more *p–n* junctions. Current–voltage characteristic (CVC) of the *p–n* junction has a pronounced non-linear dependence form. To make the qualitative analysis of

the schemes important is the selection of the best approximation of the CVC *p*–*n*–junctions of the amplifying elements with a display of its nonlinearity. At this research was used the nonlinear model of transistors based on experimental data.

RESULTS AND DISCUSSION

In the research we calculated parameters of the cascade electric circuits, which allow getting the specified amplitude of output signal and the transfer coefficient. Computer simulations of the frequency mixers schemes were made of common criteria, using the common computer simulation environment. To describe correctly the nonlinearity of current-voltage characteristics of bipolar transistors were used the equivalent models based on the experimental data. The Figure 2 shows the obtained spectral and temporal characteristics of the output signals of the mixers based on a transistor cascade and cascade current mirror.

CONCLUSION

Thus were obtained the main spectral and temporal characteristics of the output signal for electric circuits of the frequency mixers based on the transistor cascade and the current mirror cascade. These electric circuits are widely used as the frequency mixers in different devices, such as spectrum analyzers, and as the basis to design more complex electrical circuits of frequency changers, such as balanced and circular mixers. The analysis of results is shown that the base cell mixer based on the current mirror provides a lower level of combinational components. It's important in develop a high-quality equipment for measuring different parameters of materials and nanoscale structures and manufacturing of modern electronic devices. The computer program for simulation of electrical circuits FASTMEAN 6.0 allows to analyze the transient response and spectral characteristics with high precision and speed of calculations compared to the known standard algorithms. It can be a perspective environment of the computer simulation of quasi-linear electric circuits of devices of different complexity for further investigations and analysis of the linearity of its work.

REFERENCES

[1] Polyakov A. E., Strygin L. V. 2-Tone IP2 and IP 3 Measurement Technique. Trudy MIPT, 2012, №2. – P. 54 – 63.

[2] Gilbert B. The Micromixer: a highly linear variant of the Gilbert mixer using a bisymmetric Class-AB input stage e. *IEEE Journal of Solid-State Circuits*, 1997. Vol. 32, N. 9. − P. 1412-1423.

[3] Fomin N. N., Buga, N., Golovin O. V. Radio receivers: textbook for universities. - M: Techbook, 2007. – 520 p.

[4] Jones M. H. A practical introduction to electronic circuits. Third edition. Cambridge University Press, 1996. – 548 p.

[5] http://www.fastmean.ru.

ELECTROCHEMISTRY AND CORROSION

Smart Nanocomposites
Volume 7, Number 2
ISSN: 1949-4823

STRENGTHENING AND METALLIZATION OF LAYERED GRAPHITE MATERIALS SURFACE BY LITHIUM IONS DURING ELECTROMECHANICAL INTERACTION

V. Yu. Bazhin [*] ***and A. V. Saitov*** [†]
Saint Petersburg Mining University
Saint Petersburg, Russia

ABSTRACT

There is a need to protect the surface of the carbon-graphite material from mechanical erosion and the impact melts during the technological process. Carbon and graphite materials are used for the cathodes of reduction cells and furnace linings. Effect of ionization on the surface of carbon and graphite cathode during electrolysis of molten lithium carbonate based was achieved. There is a filling of layered graphite structures with the subsequent formation of intercalation compounds during the ionization effect under the influence of saturated vapor. The structure and composition of the surface layers by X-ray powder diffraction method was studied.

Keywords: carbon graphite materials, cathode, electrolysis, lithium ions, intercalation compounds

INTRODUCTION

Currently in the development of resource and energy saving technologies are actual tasks that are aimed at improving the performance of carbon and graphite cathode lining to protect against sodium diffusion by using different coatings. In spite of all the advantages offered by recent decisions, they are not widely used in the industry due to their high cost, susceptibility to abrasive erosion and the complexity of their implementation in current production. Studies with lithium electrolytes of the reduction cell with reversed polarity show a significant improvement of the physical properties and performance characteristics of the cathode blocks by intercalation of lithium in the surface layers. The effect of the introduction of lithium can

[*] bazhin-alfoil@mail.ru
[†] saitov.anton@inbox.ru

be considered as the most preferred solutions improve performance and physical characteristics of the cathode blocks. The effect on the basis of establishment of anti-diffusion barrier layer to form intercalation compounds by introducing of lithium atoms.

The lithium ion has the smallest radius of all the alkali metals and it can penetrate between the graphite structural layers by bending, twisting and deforming them as well as defective in cavities inside the layers, without swelling and degradation. The lithium ions have the smallest radius of all the alkali metals and it can penetrate between the graphite structural layers as bending, twisting and deforming them as in defective of cavities inside the layers, without swelling and degradation. Therefore, lithium is able to be adsorbed in amorphous and graphitic carbon materials (various relative inter-planar spacing from 3,34 Å to 3,44 Å) without the stress of the amount of deformation, which can destroy carbon material. LiC_6 compound is the ground state for lithium-graphite compounds, but some other amorphous forms of carbon able to packaging into the crystal lattice of Li to a compound Li_2C_2.

During the experiments found that heating in the shaft furnace of Li_2CO_3 to a temperature 750°C is formed lithium oxide by the reaction $Li_2CO_3 = Li_2O + CO_2$. During electrolysis Li_2O melt, namely, when the current power supply is switched on, a pink illumination in the melt is observed. This phenomenon is due to ionization effect (anodic effect of electrolysis) when the pair of metallic lithium go to ionic form under the influence of a constant current value of 10A and are introduced into the surface layers of graphite under vapour pressure.

Border of interaction melt with the sample can be traced in a structural study of the surface. However, the material swells in the interaction of carbon and graphite material with lithium, and the gaps are formed across the active area due to oversaturation. The effect of the introduction of lithium can be explained by partial penetration of lithium oxide in the micropores of carbon and graphite materials, and lithium ions are implanted create the effect of local grooves on surface. Thus, the surface on that part of the test sample that is above the melt during electrolysis at a temperature of 960°C was not subject to oxidation, unlike standard sample. Probably, lithium reacts with oxygen in the melt sublimation preventing destruction of the surface of the carbon and graphite sample.

Polished micro-section with different sample sites were made to determine the front reaction of carbon and graphite material with lithium. Method X-ray powder diffraction using JCPDS card file radiographs for lithium intercalation compounds with carbon was used to determine Li_xC_y phase in the sample. For this specimen from the part of the carbon-graphite sample, where the direct interaction with the melt and the part that is above it were selected.

X-ray diffraction (XRD) was conducted using a diffract meter Shimadzu XRD-7000. From obtained results, the phases of the initial materials such as Li_2CO_3 and graphite is contained in the reacted part. Presence Li_2CO_3 are explained its incomplete reaction on decomposition of lithium oxide followed by release of free metal in the form of lithium and ions.

Model formation of lithium ions, lithium recovery and its interaction with the graphite sample up to intercalation process during of electrolysis melt can be represented as follows:

- after heating to a temperature of 750°C of electrolyte Li_2CO_3 is formed of lithium oxide by the reaction $Li_2CO_3 = Li_2O + CO_2$;
- at a temperature of 960°C and passing a current through the electrolyte Li_2CO_3 – Li_2O lithium ions is formed;

- during the rising influence and the vapour pressure increase during the ionization effect of lithium atoms there is its introduction into the graphite layers of graphite materials;
- lithium is the introduction in space of layered structures with subsequent formation of various compositions intercalates with increasing time of exposure sample at the electrolyte and ionization enhancement effect.

CONCLUSION

Such as revealed that the phases of the initial materials such as Li_2CO_3 and graphite is contained in the reacted part. Presence Li_2CO_3 are explained its incomplete reaction on decomposition of lithium oxide followed by release of free metal in the form of lithium and ions. Thus, the conditions are created for introduction in the layered structure of graphite during lithium ionization effect, the passage of current and under the influence of excess vapour. This effect is an alternative for high-temperature processes in the chemically active environments melts in contrast to the known methods of introduction of lithium during obtaining lithium-ion batteries.

REFERENCES

[1] Janko E. A. Production of aluminum. Allowance for supervisors and workers shops electrolysis aluminum smelters: Publishing house of St.Petersburg University, 2007.

[2] Morten Sorlie, Harald A.Oye, Cathodes in aluminium electrolysis, 3rd edition, 2010.

[3] Diez M. A.. Modeling the degradation of carbon cathodes by sodium/M. A. Diez, H.Marsh. *Light Metals* (2001). P. 739-745.

[4] Mintsis M. J. Electrometallurgy of aluminum/M. J. Mintsis, P. V. Polyakov, G. A. Sirazutdinov//*Nauka*, Novosibirsk, 2001, 368.

[5] Rapoport M.B. Carbon graphite interlayer compounds and their value in aluminum metallurgy. M.: *Tsvetmetinformatsiya*. 1967. 66.

[6] Takashi Kyotani, Ken-Ya Suzuki, Naohiro Sonobe, Akira Tomita. Potassium-Graphite Intercalation Compounds From Thin Carbon Films Prepared Between Montmorillonite Lamellae. Carbon, Vol. 31. No. I. pp. 149-153. 1993.

[7] Qian Xu, Carsten Schwandt, George Z. Chen, Derek J. Fray. Electrochemical investigation of lithium intercalation into graphite from molten lithium chloride. *Journal of Electroanalytical Chemistr*y, 530 (2002), pp. 16-22.

[8] Qian Xu, Carsten Schwandt, Derek J. Fray. Electrochemical investigation of lithium and tin reduction at a graphite cathode in molten chlorides. *Journal of Electroanalytical* Chemistry, 562 (2004), 15–21.

[9] W. Rudorff. Graphite Intercalation Compounds. University of Tiibingen. Tuebingsn. Germany.

Smart Nanocomposites
Volume 7, Number 2
ISSN: 1949-4823

THE INFLUENCE OF LOW-CARBONACEOUS STEEL STRUCTURE IN ELECTROCHEMICAL AND CORROSION BEHAVOUR

Sergey N. Saltykov*, Natalia V. Tarasova, and Alexander M. Khoviv
Lipetsk State Technical University, Russia

ABSTRACT

The influence of steel with ferrite-cementite structure on kinetics of anodic dissolution process is studied. The anodic dissolution unit rate of free-structure ferrite and ferrite included to plate and to granular perlite is determined. The analysis of causes leaded to dependence between dissolution rate and ferrite structure is given. The role of interphase (ferrite/ferrite) and intergrain (ferrite/cementite) boundaries in anodic dissolution initiation is established. The general scheme for active dissolution of ferrite/cementite structure is offered.

Keywords: electrochemical dissolution, steel, ferrite cementite, interphase boundaries, intergrain boundaries

INTRODUCTION

The metal corrosion destruction is one of the most important problem in modern industry so the study of the electrochemical corrosion process mechanism as the basis for the development of corrosion protection new methods is a serious scientific and practical task. According to the electrochemical kinetics the mechanism of anodic oxidation is a multi-stage process containing fast and slow steps [1], so study of it is a complex task even for pure metal [2, 3]. During transition from a pure metal to heterophase alloys the anodic process mechanism occuring on surface becomes substantially more complicated. It is due to the phase composition and structure of the material comprising the grain boundaries, inclusions, defects that affect the surface energy and a mechanism for anodic dissolution consequently [4]. The development of new modern methods for material surface researching such as atomic force microscopy which provides the ability to monitor surface changes stimulated a new

* saltsn@mail.ru, +7(4742)-32-81-55.

round of scientific interest in the study of electrochemical kinetics of heterophase materials dissolution. The study of influence of the iron-carbon material structure (grain size, grain boundaries and interphase, cementite phase) on anodic dissolution of the example of low-carbon steel is the goal of this paper.

OBJECTIVES OF THE RESEARCH

The low-alloy steels with a carbon concentration from 0.017 at% (armco-iron) up to 1.20 at% (steel U12) covering the structure types from pure ferrite matrix to proeutectoid perlite were used as the object of study. To create the structure with a different geometry of the cementite phase the additional thermo-mechanical treatment to forming the plate, spherical and mixed perlite was realized. The kinetics of the electrochemical dissolution was researched using potentiodynamic voltammetry and chronopotentiometry methods. The surface state was studied using optical and atomic force microscopy.

RESULTS

The unit rates of anodic dissolution of ferrite which is a part of such structural components as: (a) structurally-free ferrite, (b) ferrite in a plate, (c) granular perlite were determined by experimentally. Under small anodic overvoltage (up to 100 mV) these values are: (a) 192.61, (b) 160.56, (c) 154.65 mA/cm^2 respectively. In our view the cause of dissolution rates differences between ferrite plate and granular perlite is the reducing of the defects in the ferrite during pearlite spheroidization process. The predominance of rate of structurally-free ferrite dissolution over the pearlite's ferritic matrix established by experimentally due to the presence of subgrain structure inside the ferrite grain which is a low-angle boundaries simulated by dislocations system. The subgrain structure is absent in the ferritic matrix of lamellar pearlite when the ferrite layers size is comparable with the free path length of dislocations in the ferrite. In this case the dislocations located separately will present in a ferrite matrix of the perlite. The getting of the dissolution rate of intergrain boundaries "ferrite/ferrite" over interfacial boundaries "ferrite/cementite" is caused by misorientation angle. The increasing of angle up to about 30° leads to an increase of boundary energy and, as a consequence, to increase of dissolution rate.

The formation of the active sites on the surface controlled the dissolution mechanism of heterophasic material is studied [5]. It is found that dissolution of pure ferrite matrix is initiated at the grain boundaries next it is passed at the ferrite grain body. On steels with ferrite-pearlite structure the dissolution process starts at the interfaces "ferrite/cementite" next at the grain boundaries "ferrite/ferrite" and after at the body of the structurally free ferrite grain. On hypereutectoid steels the dissolution process begins at the interfaces "ferrite/cementite" moving to the ferritic matrix. The causes of such difference are both fragmentary of intergrain and interphase boundiries and the defects of ferrite grain body. Qualitatively it is expressed as a ratio of the average diameter of ferrite and pearlite grains to each other.

On the basis of experimental data the generalized scheme of anodic dissolution of the steels with a ferrite and ferrite-pearlite structure is proposed. The scheme includes the processes: the formation of active centers and the development of anodic dissolution.

CONCLUSION

1. The anodic dissolution unit rate of structurally-free ferrite and ferrite included to plate and granular pearlite was determined.
2. The effect of the steel structure on the formation and distribution of dissolution active sites on elements of structure is studied as well as dissolution order of interphases boundaries, interfaces boundaries and grains body is established.
3. The generalized scheme of anodic dissolution of steels with ferrite and ferrite-pearlite structure is proposed.

REFERENCES

[1] Aleksanyan A. Yu., Podobaev A. N., Reformatskaya I. I. *Protection of Metals and Physical Chemistry of Surfaces.* 2007. V.43. №1. P. 66-69.

[2] Aleksanyan A. Yu., Reformatskaya I.I., Podobaev A.N. *Protection of Metals and Physical Chemistry of Surfaces.* 2007. V.43. №2. P.125-128.

[3] Fushimi K., Seo M. *Electrochimica Acta*. 2001. V. 47. P.121-127.

[4] Plaskeev A. V. *Protection of Metals and Physical Chemistry of Surfaces*. 2005. V. 41, № 2. P.131-137.

[5] Tarasova N. V., Saltykov S.N. *Protection of Metals and Physical Chemistry of Surfaces.* 2007. V. 43. №3. P. 231-234.

The researching was supported by RFBR (project 16-48-480162-p_a.)

ENERGY STORAGE MATERIALS AND DEVICES

Smart Nanocomposites
Volume 7, Number 2
ISSN: 1949-4823

STABILIZATION OF A NEW FORM OF Li_2MnSiO_4: AB-INITIO STUDY

Maxim Arsentev*, Marina Kalinina, Petr Tikhonov, Anastasia Shmigel, Nadezda Kovalko, and Tatiana Egorova
Institute of Silicate Chemistry, Russian Academy of Sciences,
St. Petersburg, Russia

ABSTRACT

A new crystalline form of Li_2MnSiO_4 was predicted by ab-initio computations. Surprisingly it was found to have a stable analogue occurring in nature – Na_2CaSiO_4 with the same structure. Using this information the possible routes of obtaining such material are presented.

Keywords: silicates, lithium batteries, electrode materials, DFT, Li_2MnSiO_4

INTRODUCTION

Li_2MnSiO_4 is one of the most promising materials for use in electric vehicles applications, but it suffers from instability [1]. It offers some advantages like high theoretical capacities, environmental friendliness, thermal stability, and inexpensiveness, but easily undergoes amorphization and shows poor cyclability due to layer exfoliation and/or need for octahedral coordination for Mn. Here we report the computational identification of a new form of Li_2MnSiO_4 as a stable candidate with acceptable characteristics. Surprisingly it was found to have a stable analogue – Na_2CaSiO_4 with the same structure. Using this information the possible routes of obtaining such material are presented.

EXPERIMENTAL SECTION

The 132 predicted structures of silicate lithium manganese compounds provided by Materials Project were used for the analysis with TOPOS software package [2]. The dimensionality of the inorganic framework of these potential intercalation compounds was performed using the ADS module. ADS (Automatic Description of Structure) module

* ars21031960@gmail.com

analyses the crystal structure topology and tests structures on isotypism. The availability of channels for Li ion migration was studied using the Dirichlet module. The algorithm relies on the representing atoms and molecules in the form of the Voronoi-Dirichlet polyhedra.

RESULTS

The main selection criteria were stability (the presence of three-dimensional framework), specific gravimetric and volumetric capacity, and the availability of channels for Li ion migration. Only 14 structures structures could be considered as satisfying these criteria. These structures range considerably in the value of volumetric capacitance. Among the 14 screened structures materials mp-761394 and mp-762566 have more than 30% higher volumetric capacitance than the others, but we was not able to find naturally occurring isostructural analogue for these materials. Another thing we have with sp6531_crystal297417 (Li_2MnSiO_4 (P213, space group number 198). It was found to have a stable analogue – Na_2CaSiO_4 with the same structure. Hence, one possible strategy can be a synthesis of Na_2CaSiO_4 with Ca partially substituted with Mn, though this may lead to loss of some capacity. We can even not to perform ion exchange of Na with Li. It can provide a sodium battery material, a new emerging field of investigations too.

In summary, we identified a new form of Li_2MnSiO_4 in the $P2_13$ structure as a stable and capacitive substitution of the Li_2MnSiO_4 in the $Pmn2_1$ structure. Surprisingly it was found to have a stable analogue – Na_2CaSiO_4 with the same structure. Using this information the possible synthesis strategies of the stabilization of this material are presented.

This work was supported by a grant from the President of the Russian Federation for state support of young Russian scientists (PhD MK-6004.2015.3).

REFERENCES

[1] D. Andre, S.-J. Kim, P. Lamp, S. F. Lux, F. Maglia, O. Paschos, B. Stiaszny: *J. Mater. Chem.* A Vol. 3 (2015), p. 6709.

[2] V. A. Blatov: *IUCr CompComm Newsletter* Vol. 7 (2006), p. 4.

Smart Nanocomposites
Volume 7, Number 2
ISSN: 1949-4823

THE USE OF POROUS GALLIUM PHOSPHIDE AS SUBSTRATES FOR SUPERCAPACITORS

Anton O. Belorus[1,*], B. D. Klimenkov[2], Veniamin L. Koshevoi[2], Nikolai S. Pshchelko[2], and V. A. Moshnikov[1]

[1]St. Petersburg Electrotechnical University "LETI" St. Petersburg, Russian Federation
[2]St. Petersburg Mining University, St. Petersburg, Russia

ABSTRACT

Use of porous GaP is proposed as substrates for supercapacitors. Porous substrates are prepared by electrochemical etching. A method of producing of porous GaP is presented. Analysis of the morphology of resulting structures based on porous GaP is investigated.

Keywords: semiconductors, porous semiconductors, supercapasitors, por-GaP, electro-chemical etching

INTRODUCTION

Supercapacitors are interesting for energy storage in hybrid electrical devices powered by batteries due to their high power density, excellent reversibility and a large number of rewrite cycles. Research in this area is aimed at the development of electrode materials, porous surface morphology and optimizing of specific parameters. Supercapacitor is a dielectric plate with the electrodes, where role of the plates carries a porous body, in which is a huge surface of the dielectric - gel (ionic liquid) that fills the cavities on the surface, the charge - ions, which are in the gel. Due to the fact that the surface is large, the capacity of the supercapacitor may be much more than the capacitance of capacitors.

Porous coal are conventionally used as the porous body. Nowadays, the manganese oxide is attracting the attention of scientists due to its low cost and environmental friendliness. However, these materials have several drawbacks, among which a low conductivity and low specific capacity. Alternatively active semiconductor chips, namely porous structures grown on them are actively consideres. It is known that the ability to exhibit vapor formation have such semiconductors as Si, Ge, A_3B_5 structures. A special place in this listing takes gallium phosphide due to the ease of producing porous layers on the basis and ease of management of its morphological properties.

* Corresponding author: mop_92@mail.ru

Electrodes of supercapasitances are usually made of porous material, the inner specific surface area of which reaches 500—3000 m^2/g. What is important is the pore size of the electrode material (from 20 nm to 500 nm): at large active surface area decreases, at small — relatively large carriers (electrolyte ions) don't get in the pores pores, which are also often surrounded by solvent molecules.

MATERIALS AND METHODS

To create a porous gallium phosphide (por-GaP) was used monocrystalline GaP, grown by Czochralski method. The thickness of the plates was 450 mm, the orientation (100). At the samples thin layer was formed by liquid phase epitaxy with thickness 20-50 μm, doped with Te.

Por-GaP was prepared in a single-chamber electrochemical cell by anodic etching using electrolyte solution based on hydrofluoric acid.

Preparation of the samples was conducted at the room temperature. During the experiment galvanostatic and potentiostatic regimes were used when selecting various process parameters: 1) the time of etching from 1.5 to 10 minutes 2) current density from 10 to 100 mA/cm^2.

Samples are thoroughly cleaned before the experiment. The purification process was consisted of the following steps: degreasing in acetone, with subsequent washing in distilled water and isopropanol. The morphology of the porous structure investigated by the scanning electron microscope TESCAN MIRA II.

EXPERIMENTAL RESULTS

From scanning electron microscopy (SEM) analysis for por-GaP:Te, it is seen that depending on various polishing surface, pore growth can be carried as in the surface regions with defects in the form of deepenings which are caused by chemical polishing, as well as with a developed pore system. Obtained porous semiconductor GaP:Te structures refers to macro- and mesoporous (pore size of 10 nm to 200 nm). For the samples obtained in galvanostatic regime, pores are represent system of spongy columns system with crystallographic direction (100) with a square cross section. The thickness of the porous layer of these samples is about 28 microns. In consequence of that we can speak of a high specific surface area. From earlier published works [1-6] it is known that with such pore size and thickness of the porous layer specific area reaches 800 m^2/g.

CONCLUSION

The paper presents a method of producing porous gallium phosphide. The morphology of the surface of the resulting structures And the possibility of the use of porous indium phosphide as a material for supercapacitor electrodes are analyzed.

The work was performed by the project contract code 0021109, competition UMNIK 15-12.

REFERENCES

[1] Porous silicon nanoparticles for target drug delivery: structure and morphology/Spivak Yu. M., Belorus A. O., Somov P. A., Tulenin S. S., Bespalova K. A., Moshnikov V.A. *Journal of Physics*: *Conference Series.* 2015. vol. 643. p. 012022

[2] The study of porous silicon powders by capillary condensation/Belorus A. O., Maraeva E. V., Spivak Y. M., Moshnikov V. A.//*Journal of Physics: Conference Series*. 2015. vol. 586. №1. p. 012017.

[3] Photoluminiscence studies of porous silicon obtained by photoelectrochemical etching/Belorus A. O., Koshevoi V. L., Spivak Yu. M., Levickij V.S., Moshnikov V. A.//*International Journal of Hydrogen Energy*. 2015. vol 23. (187). p. 126-132.

[4] Surface functionality features of porous silicon prepares and treated in different conditions/Spivak Yu. M., Myakin S. V., Moshnikov V. A., Panov M. F., Belorus A. O., Bobkov A. A //*Journal of Nanomaterials*. 2016. vol. 2016. p. 2629582.

[5] Investigation of the influence of etch process upon the morphologe of the porous silicon particles/Bespalova K. A., Belorus A. O., Shaidarov L. V., Tret'akov A. V.//Izvestiya SPbGETU "LETI". 2015. vol. 7. p. 10-13.

[6] Preparation and investigation of porous silicon nanoparticles for targeted drug delivery. Spivak Y. M., Maraeva E. V., Belorus A .O., Molchanova A.V., Nigmadzyanova N. R. Book: *Nanoscale-Arranged Systems for Nanotechnology* 2015. p. 162-165.

Smart Nanocomposites
Volume 7, Number 2
ISSN: 1949-4823

CALCULATION OF AN EXPERIMENTAL PSEUDOCAPACITOR SELF-DISCHARGE RATE WITH THE USE OF CYCLIC VOLTAMMOGRAMS

Alexandra G. Ivanova*, Oleg A. Zagrebelnyy, Maria S. Masalovich, Irina Yu. Kruchinina, and Olga A. Shilova
Institute of Silicate Chemistry of Russian Academy of Sciences,
Saint Petersburg, Russia

ABSTRACT

In this report we declare about a new computational method of self-discharge evaluation for such an energy storage device as a pseudocapacitor (PC). The cyclic voltammograms (CVAs) of testing PCs with different types of electrodes in organic and inorganic electrolytes were analyzed. The elaborated calculation procedure is the express method which facilitates the estimation of PC self-discharge rate.

Keywords: a pseudocapacitor, self-discharge, cyclic voltammograms, transition metal oxides, electrically conducting organic polymers

1. INTRODUCTION

The self-discharge phenomenon is known to play a crucial role in the deterioration of PCs performance. Despite numerous publications on the development of materials for energy storage devices in which much attention is paid to the specific capacity, cyclic stability and charge/discharge rate, there is little known about the self-discharge. Self-discharge is literally a spontaneous voltage drop in open circuit after charging the device. The self-discharge rate (SDR) of a battery is known to be lower than of a supercapacitor. Besides, supercapacitors solely based on electric double layer with specially treated coal electrodes possess lower SDR than the PCs operating mainly due to reversible surface redox reactions. Unlike batteries the thermodynamic instability of a supercapacitor system, and of a PC system in particular, is caused by electrochemical reactions taking place on the surface of PC electrodes rather than in the bulk. On the whole, the thermodynamic instability of such electrochemical systems as a supercapacitor or a PC is caused by possible side Faraday reactions at the electrode/electrolyte interface as well as by time-limited ion diffusion leading to potential redistribution in the electrode bulk and to the overcharge of the devices. The charge

redistribution is also possible in the pores of the PC electrode. Besides, when the electrochemical device constructed with defects, ohmic leakage significantly increases the SDR [1-4]. Thus, to clarify the means of eliminating these phenomena, especially for PCs, it is further necessary to study the electrode/electrolyte interface processes with the use of diverse electrode, electrolyte and support materials. Meanwhile, up to now the open circuit voltage drop measurement has been the only approach to determine the magnitude of the SDR. We suggest an alternative express method to calculate the SDR of a PC using CVAs. This method is based on the compare of the energy irreversibly absorbed by an electrode as a result of conversion into heat or chemical energy and the total energy transferred to the electrode [3].

2. RESEARCH GOAL

The goal of the research is to test the experimental PCs with different types of electrodes in organic and inorganic electrolytes and estimate the SDR of the electrochemical systems with the help of the elaborated method.

3. EXPERIMENTAL PART

Electrochemical experiments have been carried out in a three – electrode cell (a half - cell). Two groups of working electrodes were tested. The first one is pieces of steel mesh covered with an oxide layer (WO_{3-x} or MnO_2). The second one is platinum plates with a layer of electrically conducting polymer (e.g., polythiophene).

The recorded CVAs have been processed with the software package Mathcad 15.0. The SDR values were calculated automatically according to the consequent set of previously derived formulas [3].

4. EXPECTED RESULTS

The results obtained by the express calculation method comply with the ones registered by the classic long-term open circuit method. The high correlation index (0.71) has been achieved.

The research has been supported by the funding programs of Chemistry and Material Sciences Department of Russian Academy of Sciences (№2, №7).

REFERENCES

[1] Conway, B. E., Electrochemical supercapacitors: scientific fundamentals and technological applications (1999). Kluwer Academic, New York: 685.

[2] Andreas, H. A., Self-discharge in electrochemical capacitors: a perspective article (2015) *J. Electrochem. Soc*. (162) 5: A5047-A5053.

[3] Zagrebelnyy, O. A., Ivanova, A. G., Masalovich, M. S., Kruchinina, I. Yu., Shilova, O. A., Metodika otsenki samorazryada elektrohimicheskogo psevdokondensatora po tsiklicheskoy voltamperogramme electroda (2017) Physika i chimia stekla (in press). [Electrochemical pseudocapacitor self-discharge estimation procedure based on the electrode cyclic voltammograms (2017) Glass Physics and Chemistry].

[4] Masalovich, M. S., Shevtsova, Yu. A., Ivanova, A. G., Zagrebelnyy, O. A., Kruchinina, I. Yu., Shilova, O. A., Electrochemical synthesis of polythiophene-polyacrylamide composite coatings used for pseudocapacitors (2016), *Glass Physics and Chemistry* (42) 6: 635-636.

FULLERENES, CARBON STRUCTURES, QUANTUM DOTS

Smart Nanocomposites
Volume 7, Number 2
ISSN: 1949-4823

THERMODYNAMIC MODELING OF THE BEHAVIOR OF HIGHER FULLERENES C84 WHEN HEATED IN AN INERT ATMOSPHERE

Nick M. Barbin[1,2,*], Vasiliy P. Dan[1], Dmitriy I. Terentiev[1], and Sergey G. Alekseev[1]

[1]Ural Institute of State Fire Service of Emercom of Russia, Ekaterinburg, Russia
[2]Ural Agrarian State University, Ekaterinburg, Russia

ABSTRACT

Thermodynamic modeling of the behavior of the higher fullerene C_{84} by heating in Ar. Modeling consists of the thermodynamic analysis of the system using the software complex "Terra". The result was calculated compositions of gas and condensed phases temperature in the system-Ar C84. Calculated equilibrium constants for the reactions with the selection of temperature intervals.KEY WORDS: fullerene, thermodynamic modeling, carbon nanoparticles, carbon nanotubes, heating.

INTRODUCTION

The study of carbon fullerene structures is of interest for nanophysics and nanomaterial technology [1]. The study of carbon fullerene structures is a subject of interest of science. However, to achieve practical applications of these molecular systems it is necessary to study their thermal properties. This paper studied the behavior of the higher fullerenes C_{84} when heated in argon at atmospheric pressure. The research was conducted by using thermodynamic modeling.

THE METHOD OF CALCULATION

Thermodynamic modeling consists of the thermodynamic analysis of the equilibrium state of the system in general. One of the most developed and effective programs that implement such thermodynamic calculations, is the software package TERRA.

* Corresponding author: Prof. N.M. Barbin, Prof. of Ural Institute of SFSE Russia, Ekaterinburg, Russia, E-mail: nmbarbin@mail.ru

Calculations of the composition of the phases and characteristics of equilibrium are carried out using the reference database on properties of individual substances [2-5].

RESULTS AND DISCUSSION

Computer experiment allows determining the phase distribution of carbon in the system C_{84}-Ar on the whole considered temperature interval.

THE GAS PHASE DEPENDENCE OF THE TEMPERATURE IN THE SYSTEM C_{84}-AR

When the temperature in the system C_{84}-Ar to 2473 K, the concentration of the vapor group C, C_2, C_3, C_4, C_5 increase. Vapor concentration C and C_2 increase over the entire temperature range, and upon reaching 4273 K to reach values $9{,}459\cdot10^{-4}$ mole fraction and $6{,}043\cdot10^{-4}$ mole fraction. Vapor concentration C_3 and C_4 increases until the system temperature 4073 K and reach values $1{,}827\cdot10^{-3}$ mole fraction and $2{,}990\cdot10^{-5}$ mole fraction. In the temperature interval from 4073 K to 4273 K the vapor concentration C_3 and C_4 are reduced to values of $1{,}584\cdot10^{-3}$ mole fraction and $2{,}349\cdot10^{-5}$ mole fraction. A pair of C_5 concentration increases until the system temperature 3973 K and achieve value $9{,}788\cdot10^{-5}$ mole fraction. In the temperature interval from 3973 K to 4273 K focus a pair of C_5 decreases to a value $4{,}569\cdot10^{-5}$ mole fraction. When the system temperature 3773 K the composition of the gas phase is replenished with ions C^+, C^{2-}, C^{2+}. At a temperature 4273 K their concentrations are $6{,}482\cdot10^{-9}$ mole fraction, $6{,}263\cdot10^{-9}$ mole fraction, and $2{,}088\cdot10^{-9}$ mole fraction respectively.

THE DEPENDENCE OF THE COMPOSITION OF THE CONDENSED PHASE THE TEMPERATURE IN THE SYSTEM C_{84}-AR

In the interval of temperatures from 473 K to 3973 K condensed the concentration of C decreases to 0,012 mole fraction to $7{,}024\cdot10^{-3}$ mole fraction. In the temperature range from 473 K to 3473 K parabolically increase the concentration of the condensed C_2 and C_3; they reach values $2{,}286\cdot10^{-3}$ mole fraction and $5{,}232\cdot10^{-4}$ mole fraction. In the temperature interval from 3973 K to 3473 K the concentration of condensed C_2 decreases to a value of $1{,}750\cdot10^{-3}$ mole fraction. The concentration of the condensed C_3 in the temperature range from 3473 K to 3773 K reduced to $4{,}590\cdot10^{-4}$ mole fraction. In the temperature interval from 3973 K to 3773 K To the concentration of the condensed C_3 is increased to $5{,}599\cdot10^{-4}$ mole fraction. In the temperature range from 973 K to 3573 K the concentration of condensed C_4 parabolically increases to the value $1{,}206\cdot10^{-4}$ mole fraction. In the temperature interval from 3973 K to 3573 K the concentration of the condensed C_4 decreases linearly to $8{,}298\cdot10^{-5}$ mole fraction. In the interval of temperatures from 1373 K to 3273 K parabolically increases the concentration of condensed C_5 to $2{,}165\cdot10^{-5}$ mole fraction. In the temperature interval from 3273 K to 3973 K condensed C_5 concentration increases linearly and reaches a value of

$5{,}025 \cdot 10^{-4}$ mole fraction. In the temperature interval from 3373 K to 3573 K linearly increase the concentration of condensed C_{94}, C_{84}, C_{90}, C_{70} and C_{76}, reaching values of $2{,}007 \cdot 10^{-4}$ mole fraction, $3{,}148 \cdot 10^{-5}$ mole fraction, $2{,}755 \cdot 10^{-5}$ mole fraction, $7{,}817 \cdot 10^{-6}$ mole fraction, $3{,}705 \cdot 10^{-6}$ mole fraction. In the interval of temperatures from 3973 K to 3573 K concentration above condensed components of the system parabolically increase and reach values $1{,}417 \cdot 10^{-3}$ mole fraction, $2{,}571 \cdot 10^{-4}$ mole fraction, $1{,}792 \cdot 10^{-4}$ mole fraction, $7{,}258 \cdot 10^{-5}$ mole fraction, $3{,}457 \cdot 10^{-5}$ mole fraction. In the temperature interval from 3973 K to 3473 K the concentration of the condensed C_{60}, C_{56}, C_{50}, C_{44}, C_{28} and C_{32} parabolically increase and reach values $9{,}213 \cdot 10^{-6}$ mole fraction, $6{,}038 \cdot 10^{-6}$ mole fraction, $3{,}185 \cdot 10^{-6}$ mole fraction, $2{,}036 \cdot 10^{-6}$ mole fraction, $1{,}354 \cdot 10^{-6}$ mole fraction, $1{,}256 \cdot 10^{-6}$ mole fraction.

CONCLUSION

The higher fullerene C_{84} is the third representative of fullerene stability, which significantly expands the range of its practical application in various fields of industry. The analysis of the obtained data indicates that the temperature increase leads to the increase of the components of the gas and condensed phases.

REFERENCES

[1] Barbin Nick M., Dan Vasiliy P., Dmitriy Terentiev I., Alekseev Sergey G. Modeling the Behavior of Carbon Nanoparticles C44 When Heated in an Argon Atmosphere. Computer Experiment. - *Smart Nanocomposites* 2016. Volume 7 Issue 1.

[2] Gurevich L. V., Weitz I. V., Medvedev, V. A., Thermodynamic properties of individual substances: reference. ed-e in 4 volumes. – M.: *Nauka*, 1982. -8540 S.

[3] Moiseev G. K., Vatolin N.. Thermodynamic properties of some gaseous fullerenes. *Journal of physical chemistry* a, 2002, volume 76, No. 2, pp. 217-220

[4] Moiseev G. K., Vatolin N., Computer simulation of the formation of various condensed forms of carbon. *Journal of physical chemistry* a, 2002, volume 76, No. 8, pp. 1366-1370

[5] Moiseev G. K., Vatolin N.. Evaluation of the thermodynamic properties of a number of condensed carbon compounds. *Journal of physical chemistry* a, 2002, volume 76, No. 3, pp. 424-428.

Smart Nanocomposites
Volume 7, Number 2
ISSN: 1949-4823

DETERMINATION OF DIMENSIONAL PARAMETERS OF MATERIALS BY DISPERSING METAL PARTICLES AND MINERALS

Ilia I. Beloglazov [*] ***and Alina A. Byzova***
Automation of Technological Processes and Production Department,
Faculty of Mineral Processing, Saint Petersburg Mining University, Russia

ABSTRACT

Dispersing agents to nanometer size particles leads to emergence of qualitatively new physical properties. The most striking example of a fundamental change of matter properties are the optical properties of metal nanoparticles (MNP) of the limited size of the object, which can be very different from the same characteristics of the "bulk" material. Such particles are capable to absorb electromagnetic radiation in the spectral ranges, where the bulk material did not absorb. These features are the cause of manifestation of unique colors, for example, nanoparticles of copper, gold, silver, and various minerals.

Keywords: nanomaterials, metal nanoparticles, dimensional characteristics

INTRODUCTION

Similar effects involving the MNP and minerals are the object of research and find numerous applications in both the scientific and practical purposes. Among the wide range of devices, which are based on the optical properties of the MNP can be mentioned optical filters, nonlinear-optical switches and guides light, spectral and polarization-selective film materials for optical data storage, reversible photosensitive glass, label biomolecules; these properties also can be used to increase the sensitivity of Raman spectroscopy, etc.

The optical characteristics of the MNP and minerals are studied by using classical spectroscopy, therefore the majority of works [1–5] devoted to different methods of producing nanoparticles and investigation of their physical properties are analyzed primarily the absorption spectra. Optical spectra contain information about the most important physical

[*] Corresponding author: Assist. Prof. Dr. Beloglazov I.I. Automation of Technological Processes and Production Department, Faculty of Mineral Processing, Saint-Petersburg Mining University, Russia, Tel.: + 79217785984, E-mail: beloglazov@spmi.ru

characteristics of the media with the MNP such as the particle and distribution size, degree of aggregation, the thickness of adsorbed layers, etc.

These spectra allow observing changes in the electronic structure of the minerals in the transition from the "volume" of a substance to small particles. Such small particles are widely distributed among the natural and technogenic objects. These include minerals, metals, alloys, microorganisms, ash, dust, fumes etc. An extensive literature study on the properties of nanoparticles has been accumulated, the special properties of nanomaterials that cannot always be explained in terms of classical physics [6–9] identified. Many issues of the physics of nanoparticles remain unresolved. These include the issue of the upper size limit of the nanoparticles, the role of structural defects, and the methods of producing nanomaterials with stable properties.

The following abnormal properties are set to nanomaterials: changing the melting point of metals, the eutectic temperature for alloys, specific heat, thermal conductivity, a significant increase in hardness and reduced ductility and variation of the crystal structure type and other characteristics. It is essential that the dependence of "size – property" is nonmonotonic.

The lack of data about the upper limit of nanoparticles leads to non-reproducibility properties of nanomaterials, which complicates their practical use. The maximum size of nanoparticles are calculated on the basis of geometrical considerations [9,10], and do not include any type of crystal structure or the size of the unit cells of various substances.

Abnormal properties of nanoparticles explain a significant share of interfaces that is the increase in the number of surface chemical bonds with decreasing particle size.

REFERENCES

[1] Kiefer J., Grabow J., Kurland H. D, Müller F. A. Characterization of Nanoparticles by Solvent Infrared Spectroscopy. Anal Chem 2015;87:12313–7. doi:10.1021/acs.analchem.5b03625.

[2] López-Lorente Á. I., Valcárcel M. The third way in analytical nanoscience and nanotechnology: Involvement of nanotools and nanoanalytes in the same analytical process. *TrAC Trends Anal Chem* 2016;75:1–9. doi:10.1016/j.trac.2015.06.011.

[3] Majedi S. M., Lee H. K. Recent advances in the separation and quantification of metallic nanoparticles and ions in the environment. *TrAC Trends Anal Chem* 2016;75: 183–96. doi:10.1016/j.trac.2015.08.009.

[4] López-Lorente Á. I., Mizaikoff B. Recent advances on the characterization of nanoparticles using infrared spectroscopy. *TrAC Trends Anal Chem* 2016. doi:10.1016/j.trac.2016.01.012.

[5] Bovand M., Rashidi S., Ahmadi G, Esfahani J. A. Effects of trap and reflect particle boundary conditions on particle transport and convective heat transfer for duct flow - A two-way coupling of Eulerian-Lagrangian model. *Appl Therm Eng* 2016;108:368–77. doi:10.1016/j.applthermaleng.2016.07.124.

[6] Smirnov B. M. *Clusters and Small Particles*. New York, NY: Springer New York; 2000. doi:10.1007/978-1-4612-1294-2.

[7] Gusev A. I. Nanomaterialy, nanostruktury, nanotechnologii. Fizmatlit; 2007.

[8] Roco M. C, Mirkin C. A., Hersam M. C., Hersam M. C. Nanotechnology research directions for societal needs in 2020 : retrospective and outlook. Springer; 2011.

[9] Yoda M., Garden J. L., Bourgeois O., Haque A., Kumar A., Deyhle H., et al. *Nanostructured Materials*. Encycl. Nanotechnol., Dordrecht: Springer Netherlands; 2012, p. 1766–1766. doi:10.1007/978-90-481-9751-4_100564.

[10] Palumbo G., Erb U., Aust K. T. Triple line disclination effects on the mechanical behaviour of materials. *Scr Metall Mater* 1990;24:2347–50. doi:10.1016/0956-716X (90)90091-T.

Smart Nanocomposites
Volume 7, Number 2
ISSN: 1949-4823

PROCESSING OF CARBON NANOPARTICLES BY SUBLIMATION

Anna A. Kovalchuk[1,2,*], Alexander V. Prikhodko[2], and Natalia N. Rozhkova[1]

[1]Institute of Geology Karelian Research Centre Russian Academy of Science, Petrozavodsk, Russia

[2]Peter the Great Saint Petersburg Polytechnic University, Saint Petersburg, Russia

ABSTRACT

The carbon film was obtained by the method of sublimation. The film was formed of carbon nanoparticles. Carbon nanoparticles were revealed by optical methods

Keywords: nanocarbon; nanoparticles; sublimation; scanning electron microscopy; Raman spectroscopy

INTRODUCTION

Carbon nanoparticles have unique conductive, thermal conductivity and mechanical properties. They are widely used in composite materials for electronics.

Sublimation method is known as one of the methods of carbon nanoparticles production. Method involves sublimation of the starting material and subsequent condensation of the vapors on substrate element. The method was used successfully to produce films of fullerenes. It was challenging to apply the same method for sublimation of natural nanocarbon material.

EXPERIMENTAL

In this paper, the sublimation method was implemented in a vacuum heat chamber.

As a starting material was chosen nanopowder shungite type I from Shunga. Shungite powder (shungite type I, Shunga deposit) with particle size 0.01 - 1 μm was used as a starting material for sublimation.

* eniaam@list.ru

The powder was placed on the bottom of the heat chamber and heated to 335°C. Sublimation of shungite carbon started when the temperature reached 335°C.

Carbon deposition occurred on a glass substrate coated with a film of In_2O_3. The substrate was placed on the top of the heat chamber.

The cooler was used to stabilize the film growth conditions. It is placed over the substrate.The temperature of the coller did not exceed 100 °C.

Sublimation process continued until a temperature of 750°C.

On completion of the sublimation process a carbon film 8 mm in diameter and 3 mm thick was formed on the substrate.

Structural pecularities of the films were studied by Raman spectroscopy (RS) and scanning electron microscopy (SEM) methods.

RESULTS

Comparative analysis of the RS spectra of the films, shungite powder and shungite carbon nanopartcles in aqueous dispersion was carried out. The main peaks of the RS of the film coinside with the RS spectra of shungite carbon nanoprticles in aqueous dispersion [1].

Raman spectra of the film showed an affinity with the spectra of graphene [2]. That indicates presence of graphene in the film.

The morphology of the films was studied by means of 3D laser scanning microscope. The film surface has a uniform relief [3].

SEM data showed that carbon nanoparticles are located between In_2O_3 grains and formed a deformed mesh [3]. An average particle size ranges from 50 to 100 nm, which is consistent with the results of dynamic light scattering for the aqueous dispersions of carbon nanoparticles [4].

Nanoparticles in the carbon film and carbon nanoparticles in the dispersion are very similar, but the film was able to remove the hydration component, namely the basic elements of shungite carbon could be picked out without water.

REFERENCES

[1] Rozhkova, N. N. 2012. Aggregation and stabilization of carbon nanoparticles shungites. *Environmental Chemistry*. 4, 240-251.

[2] Golubev, E. A. 2013. Physical properties and structural characteristics of shungite (natural nanostructured carbon). *Solid State Physics*. Vol. 55, 5, 995-1002.

[3] Konkov, O. I., Mikhaylina, A. A., Prikhodko, A. V., Rozhkova N. N. 2016. Nanostructured membranes based on a natural carbon material. *Journal of Optical Technology*. 83, 286-289.

[4] Rozhkova, N. N., Gribanov, A V 2007.K on the basic structural element of shungite carbon. *Mineralogy, petrology and metallogeny Precambrian Complexes in Karelia*. 86-89.

Smart Nanocomposites
Volume 7, Number 2
ISSN: 1949-4823

TRIBOLOGICAL PROPERTIES OF FULLERENE C60

Victor A. Krasnyy*
Saint Petersburg Mining University
Saint Petersburg, Vasil'evsky Island, Russia

ABSTRACT

This review studies the application of C60 fullerene as an anti-friction coating, as well as an additive to lubricating oils. C60 fullerene id used for example to increase wear resistance of a number of critical parts, and as well as an anti-corrosion coating. Using C60 fullerene addresses a number of tribological problems. Fretting is a sort of friction between the surfaces due to the nominally fixed external vibrations. Shown promising tribological applications of C60 as additives for lubricating oils, as well as coatings in fretting conditions for samples of steel and brass. It was concluded that the effectiveness of C60 coatings as a solid lubricant, particularly in those cases where a liquid lubricant supply to the friction node is constructively complicated. The results of studies on the wear of brass coated and uncoated samples, allow concludion that the ability of C60 prevents surface grasping at high loads.

Keywords: wear, fretting corrosion, fullerene, additives, anti-friction coatings

GOALS

The aim of the work was to study the effect of the application of the C60 fullerene to increase the wear resistance of machine parts in an anti-friction coatings, solid lubricants, protective films, additives in lubricating oils, particularly in fretting when under low amplitude sliding wear products are not removed from the contact zone.

INTRODUCTION

Information on the tribological properties of fullerenes are few and concern mainly the C60 fullerene as a thin film, and additives to lubricants in sliding friction with some of the normal load. The grounds for this conclusion may also serve as general information about the properties of the C60 molecules - their high elasticity and strength, low surface energy, high chemical stability, weak intermolecular interactions, as well as quasi-uniform.

* vikras1955@yandex.ru

A number of studies indicated the prospect of C60 for various tribological problems:

- the use of solid films (cutting tools, titanium parts, medical supplies, and ceramic glass, no-wear sliding electrical contacts, etc.);
- the use of fullerenes to form tribological and tribochemical protective films on details of the mechanism, the internal surface of the pipeline and process tanks, anti-corrosion protection;
- the use of fullerenes with lubricants as multipurpose additives for greases, oils, coolants; use as a solid lubricant.

Fretting corrosion is a frequent cause of breakdown of a number of critical parts of internal combustion engines, in particular, those of oversize mining trucks, drilling equipment parts and other ones operating under vibration and high subgrade stresses. Fretting is peculiar to nominally fixed structural connections (e.g., part attachment points, etc.). As a rule, it arises under vibrations that cause oscillatory relative movements and deformations of various kinds. Fretting is often accompanied by chemical processes occurring on friction surfaces (fretting corrosion). Wear caused by fretting manifests itself in “wasting” of material at part fastening points. Unlike other types of sliding friction, a characteristic feature of fretting is small amplitude of counter bodies' relative movements comparable with the distance between tops of microroughnesses on the friction surface; therefore, removal of wear products from the contact zone is protracted. Whereupon wear products begin to act as an abrasive, causing additional wear.

In the present study we investigated the effect of C60 in the form of anti-friction coatings and additives for reducing wear in the lubricating oil of steel and brass samples under fretting.

MATERIALS AND METHODS

Test samples were carried out in a special unit working on the drive standard friction machines. The coatings were applied to samples of fixed, mobile counter samples had coatings. The influence C60 fretting wear on steel and brass specimens from steel counter samples adding C60 introduced into the liquid and grease in the form of powder containing 2.5% under vigorous mechanical agitation, and as a coating of the brass sample. The test conditions were as follows: 150 microns amplitude oscillation frequency 500 cycles / min, the normal load in the tests with a lubricant, 4.2 MPa and 3.2 MPa without lubrication.

RESULTS AND DISCUSSION

The results of tests of C60 fullerene additive to lubricating oil and grease steel samples and counter-samples and brass samples and steel counter-samples demonstrate that introduction of 2.5% powder into lubricating oil reduces fretting wear significantly.

Whereupon introduction of analogous powder to lubricating grease proved to be effective only in respect of a combination of brass and steel samples; this is probably caused by high viscosity of grease and its insufficient mechanical stability under shear deformations. In a number of cases wear particles were transferred to the counter-body under study; negative

wear values bear witness to that. However, even for such type of lubrication introduction of C60 reduced wear as compared to oil without additives

Tests of brass samples coated with C60 demonstrated that under normal pressure amounting to 4.2 MPa uncoated and unlubricated samples seized and the counter-sample rotation visibly slowed down. Therefore, it was required to reduce load to 3.2 MPa. Rotation slowdown was not observed when a coated brass sample was used. The wear of a coated brass sample was 3 times less than that of an uncoated and unlubricated one, there was no transfer of copper onto the counter-sample. Therefore, it is possible to make a preliminary conclusion that it is effective to use such kind of coatings as a solid lubricant, especially when supplying the friction unit with a liquid lubricant is structurally complex.

CONCLUSION

As a result of the research shows the possibility of using C60 as lubricant additives and coatings in terms of fretting corrosion of steel and brass surfaces. These data extend the application of fullerenes to solve complex tribological problems.

REFERENCES

[1] Ginzburg B. M., Krasnyy V. A., Kozyrev Y. P. , Bulatov V. P. Effect of fullerene C60 on the wear of metals under fretting. *Russian journal of theoretical physics*. Vol. 23 (1997), No. 15, pp. 1-6.

[2] Ginzburg B. M., Krasnyy V. A., Kozyrev Y. P., Bulatov V.P. The decrease in the fretting-wear of metals under the action of fullerene C60. Journal of friction and wear.Vol. 18(1997), No. 4, pp. 523-526.

[3] Krasnyy V., Maksarov V., Olt J. Improving fretting resistance of heavily loaded friction machine parts using a modified polymer composition. *Agronomy Research* 2016, 14(S1), pp. 1023-1033.

[4] Maksarov V. V., Krasnyy V. A. The mechanisms of friction of thin-layer nano-coatings under conditions of fretting. *Scientific and technical Gazette of St. Petersburg GPU*. 226, (2015), №3, pp. 111-120.

Smart Nanocomposites
Volume 7, Number 2
ISSN: 1949-4823

FROM GRAPHENE FRAGMENTS OF SHUNGITE NANOCARBON TO GRAPHITE

Natalia N. Rozhkova*

[1]Institute of Geology Karelian Research Centre Russian Academy of Science, Petrozavodsk, Russia

ABSTRACT

The paper presents results of the study of shungite carbon (ShC) nanoparticles structural evolution under heat treatment in the temperature range 1500–2000-2950°C. Graphenes and stacks of ShC nanoparticles can be released through stable aqueous dispersion and revealed themselves in different solvents. This provides opportunities for local translation of graphene fragments and their stacks and opens new prospects for the graphitization of ShC. Heat-treated ShC nanoparticles are characterized by high structural ordering, confirmed by X-ray diffraction and Raman spectroscopy data.

Keywords: shungite carbon nanoparticles, graphene, Raman spectroscopy, X-ray diffraction

INTRODUCTION

Shungite carbon (ShC) structure formed by globular particles when "splicing" stacks of graphene fragments is characterized as highly uniform in size and structure of the primary fragments and a certain ordering of their packing in the secondary levels. Water plays a key role in ShC structure formation and its spatial stabilization in 3D-nets [1].

High scientific interest in the preparation and study of synthetic molecular graphenes allows us to compare ShC graphene fragments with synthetic ones [2].

The metastable ShC is known as non-graphitizable carbon [3]. Since ShC is regarded as a multifunctional material for nanotechnology, its behaviour at high temperatures is of the most importance. Is the resistance to graphitization of ShC preserved when the nanoparticles are released?

The aim of the research is to study the structural changes in ShC nanoparticles during heat treatment (HT).

* rozhkova@krc.karelia.ru

NON-GRAPHITIZABLE SHUNGITE CARBON

Difference between graphitic and non-graphitic carbons becomes obvious from comparison of apparent carbon layer size (La) and the average number of carbon layers per stack (Lc). Thus, the early progressive structural ordering of non-crystalline carbon may sometimes be put into effect as interlayer or intralayer ordering [4]. It has been shown that ShC from different deposites is remarkable for distinguishable interlayer and intralayer ordering. For example, ShC from Nigozero has Lc of 1.3 nm, but La of 4.7 nm [3].

Heat treatment of ShC in inert atmosphere up to 2900 °C did not result in graphitization. The same conclusion was made based on structural investigation of ShC in natural conditions at the contact with the intrusive dolerite sills. The maximum degree of structural order in ShC was recorded. La, Lc determined by Raman spectrometry (RS) and X-ray diffraction (XRD) were 5.3 nm and 5.9 nm, respectively. Merging of globular structural elemets and their polyedrization was observed at the contact of ShC with dollerites. Increasing of structural ordering was observed repeatedly on the mineral grains of quartz and mica selicates. It was concluded that nanoscale variation in structure ordering of ShC caused by mineral template induced graphitization [4].

SHC NANOPRATICLES UNDER HIGH TEMPERATURE TREATMENT

ShC nanoparticles for the study were concentrated in the stable aquesous dispersion and dried in air. Their structure and microtexture and the evolution of the main parameters during HT in the temperature range 1500-2000-2950 ºC were studied by RS and XRD methods.

The significant changes in Raman spectra were observed after HT at 2950°C. In addition to the narrow strong G peak there appeared the peak of the second order 2D with the amplituide comparable to G peak. The main parameters determined from the spectra are shown in the Table 1. The structural ordering of ShC is supported by XRD data. For example, d_{002} changes from 0.347(3) to 0.339(3) nm with increasing of the average crystalline size from 2.0 nm to 18.7 nm for the pristine and heat treated samples, respectively.

Table 1. Positions of the main peaks of the Raman spectra and ratio of the intensities ID/IG, I2D/IG

Samples studied	D, sm^{-1}	G, sm^{-1}	2D, sm^{-1}	ID/IG	I2D/IG
ShC pristine	1346	1596	2675	1.57	0.14
ShC- nano 1500°C	1351	1592	2684	1.26	0.23
ShC- nano 2000°C	1354	1593	2692	1.34	0.24
ShC- nano 2950°C	1354	1584	2697	0.23	0.88

REFERENCES

[1] Rozhkova, N. N., Rozhkov, S. P., Goryunov, A.S. In Carbon Nanomaterials Sourcebook. Ed. K. D. Sattler. CRC Press 2016. Vol.1, P.151-174.

[2] Sheka, E. F., Natkaniec, I., Rozhkova, N. N., Buslaeva, E. Y., Tkachev, S. V., Gubin, S. P, Mel'nikov, V. P. 2016. Parent and reduced graphene oxide of different origin in light of neutron scattering'. *Nanosystems: Physics, Chemistry, Mathematics* Vol. 7(1), 71-80.

[3] Kovalevski, V. V. 1994. Structure of shungite carbon. *Russ. J. Inorg. Chem*., V 39, 28–32.

[4] Chazhengina, S. Y., Kovalevski, V. V. 2013. Structural characteristics of shungite carbon subjected to contact metamorphism overprinted by greenschist-facies regional metamorphism *Eur. J. Mineral.,*V. 25, 835–843.

OIL AND GAS EXPLORATION: ECOLOGICAL SAFETY

Smart Nanocomposites
Volume 7, Number 2
ISSN: 1949-4823

EFFECT OF GRAIN SIZE ON WEAR RESISTANCE OF EXCAVATOR BUCKET MATERIAL

V. S. Bochkov[1], V. I. Bolobov[1], I. I. Mishin[1], and L. S. Chigincev[2]*

[1]Electromechanical Faculty, St. Petersburg Mining University,
St. Petersburg, Vasil'evsky Island, Russia
[2]Research Laboratory "Metallurgical Expertise,"
St. Petersburg Polytechnic University, Russia, St. Petersburg

ABSTRACT

There is examined one of the options for increase in term operation of excavator bucket teeth by their thermomechanical processing. It is found that the application of thermomechanical processing at production of an excavator bucket tooth will allow to increase their wear resistance to 70%.

Keywords: hadfield steel, abrasion, hardness, thermomechanical treatment

INTRODUCTION

The main material used for production of the working bodies of mining equipment, in particular teeth of excavator buckets, is a Hadfield steel (steel 110G13L). In order to increase its wear resistance there is widely used mechanical strengthening (work hardening), which is most effective in case of shock-abrasive wear. However, during the operation of the equipment on strong breeds abrasive wear meets very often. In some literature [1, 2] there are data that for increase in wear resistance of Hadfield steel thermal and thermomechanical processings are used.

For the purpose clarification of efficiency this or that processing there was carried a number of experiments on the thermal and thermomechanical processing of samples from steel 110G13L . Experiments were made according to the scheme provided in the Figure 1.

* Corresponding Author email: bochkof@list.ru

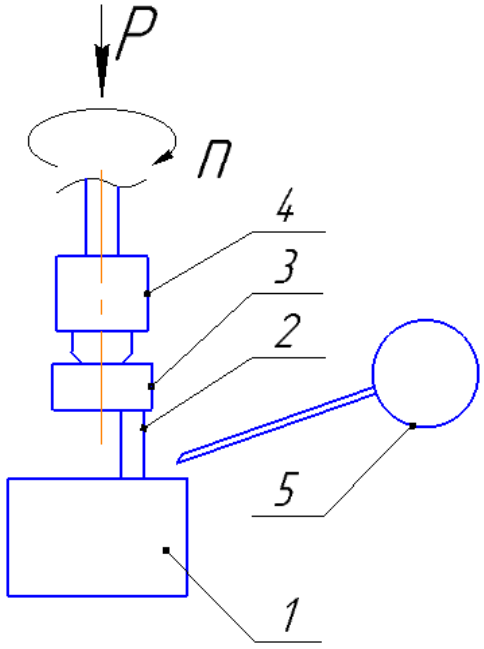

Figure 1. The experimental setup for testing samples for abrasion: 1 - abrasive disc; 2 - the test sample; 3 - the holder; 4 - spindle vertical drilling machine; 5 - water supply unit.

For the experiments there were taken 5 cylindrical samples (Figure 1), which have been subjected to the processings shown in the table. Further, the samples have been subjected to abrasive wear (losses of weight in time are presented in the table) about electrocorundum.

As mathematical processing of experimental data showed, the sample №. 6 has the lowest speed of wear Ki (2,1 mg /(mm^2·min)), and the sample №. 1 showed the highest (3,5 mg/(mm^2·min)). These data indicate a high efficiency degree of thermomechanical processing for increase in abrasive wear resistance.

Table. Characteristics of wear and hardness of samples of Hadfield steel after different processing modes

№ of sample	Sample processing method	α	Hardness, HB	K_i, mg/(mm^2·min)
1	Heat and exposure at 1150ºC followed by quenching	-	180	3,5
2	Heat and exposure at 1150ºC followed by quenching	-	180	3,3
3	Quenching immediately after forging	1,56	228	3,0
4	Quenching immediately after forging	2,25	228	2,7
5	Quenching immediately after forging	1,56	254	2,9
6	Quenching immediately after forging	2,25	264	2,1

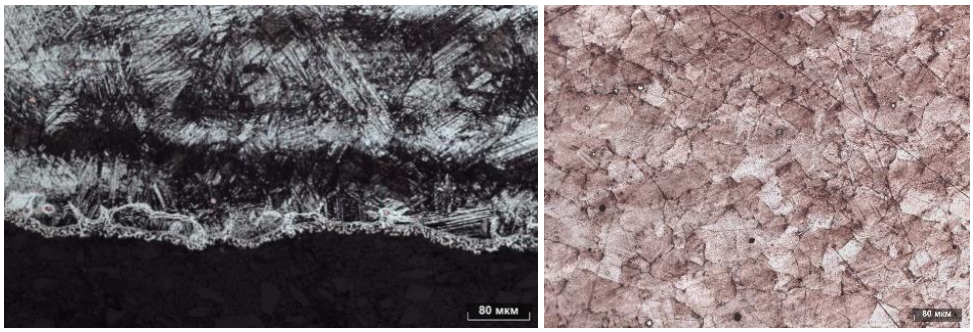

a) b)

Figure 2. Hadfield steel structure after thermomechanical (a) and thermal processings (b).

After carrying out experimental researches on abrasive wear the samples were transformed into microsections, that have been studied on a metallographic microscope. As a result, it was found that on the surface of the sample №6 a finely dispersed martensite is formed (Figure 2,a), which thickness of the plates was 5-30 nm, and the martensitic structure of the steel, as is known, has a high abrasion resistance. At the same time on microsection of the sample №1 there is observed homogeneous coarse-grained (grain size 30-50 mm) austenitic structure (Figure 2,b).

REFERENCES

[1] Barroqueiro, B., Dias-De-Oliveira, J., Pinho-Da-Cruz, J., Andrade-Campos, A. Multiscale analysis of heat treatments in steels: Theory and practice. *Finite Elements in Analysis and Design.* 2016. Volume 114. P. 39-56.

[2] Properties of plastically deformed high-manganese steel/Blucher V. V. Parfenov L. I., Volchok I. P.//*Metallovedenie i termicheskaya obrabotka metallov*. 1970. №12.- pp 32-33.

Smart Nanocomposites
Volume 7, Number 2
ISSN: 1949-4823

THE RESEARCH OF ACID-BASE CENTERS OF THE SURFACE OIL SHALE

Maxim Yu. Nazarenko*, Natalia K. Kondrasheva, Svetlana N. Saltykova, and Emil V. Salaev
Saint Petersburg Mining University,
Department of Processing Mineral Raw Materials,
Saint Petersburg, Vasil'evsky Island, Russia

ABSTRACT

The distribution and content of acid–base centers at the surface of oil shales and shale ash are determined. The results indicate that they may be used as fillers in polymer composites, filter materials, and sorbents. The surface of oil shales is characterized by the presence of centers with p*K*a = +1.5, p*K*a = +3.5, p*K*a = +6.4, p*K*a = +9.5, and p*K*a = +14.2. At the surface of shale ash, we find centers with p*K*a = +1.5, p*K*a = +4.1, p*K*a = +6.4, p*K*a = +9.5, and p*K*a = +14.2. The presence of acidic and basic Bronsted centers indicates sorptional activity with respect to organic pollutants (petroleum and its products, for example) and ionic heavy metals.

Keywords: oil shale, shale ash, acid-base center, surface area, micropores

INTRODUCTION

Oil shales are promising for use in the power, chemical, and coke industries. In contrast to other solid fossil fuels, oil shales contain considerable quantities of hydrogen in their organic matter and a large proportion of mineral components [1]. To determine suitable applications for oil shales, we need information regarding their chemical and mineralogical composition, the structure of the organic matter, and the changes at different stages of thermal and chemical treatment. Oil shales from the Baltic Basin contain up to 50% mineral impurities (including SiO_2, $Al2O_3$, CaO, and Fe_2O_3), as established in [2-3]. The mineral and functional compositions of oil shales and shale ash have also been determined. In mineral composition, oil sales are similar to natural minerals such as quartz sand, zeolite, or shungite, which are used for filtration or sorption. In the present work, we determine the surface reactivity of oil shales and shale ash.

* max.nazarenko@mail.ru

The donor–acceptor reactivity of the surface may be characterized by the acid–base properties, which are related to practically all the fundamental parameters of a solid. Therefore, if we determine the composition and content of the active centers, we may predict the reactive and sorption properties of solids used as catalysts and as fillers in polymer composites, filter materials, and sorbents [4-5]. To this end, we determine the distribution and content of acid–base centers at the surface of oil shales and shale ash; and we study the surface area of the material and the distribution of micro- and macropores.

EXPERIMENTAL METHOD

We study oil shales from the Baltic Basin in the Leningradsk field (<=0,125 mm fraction) and also shale ash (<0,125 mm fraction).

To determine the distribution and concentration of acid–base centers at the surface of oil shales and shale ash, we use the indicator method. By that means, we may investigate the distribution of surface centers and the correlation between the adsorption by specific surface centers and the activity of the surface as a whole. The indicator method is based on the adsorption of monobasic indicators from an aqueous medium by a solid surface. In analytical conditions, the indicator is adsorbed both at Bronsted centers and at Lewis centers, where water molecules are adsorbed by a coordination mechanism in accordance with the corresponding p*K*a value. As a result, quantitative determination gives the total content of Lewis and Bronsted centers of the corresponding strength at the surface of the oil shales and shale ash.

RESULTS AND CONCLUSION

Knowing the composition and content of the active centers in oil shales, we may predict their suitability as catalysts and as fillers in polymer composites, filter materials, and sorbents.

The following conclusions follow from the distribution of acid–base centers at the surface oil shales and shale ash.

1. The surface of oil shales is characterized by the presence of centers with p*K*a = +1.5, p*K*a = +3.5, p*K*a = +6.4, p*K*a = +9.5, and p*K*a = +14.2.
2. At the surface of shale ash, we find centers with p*K*a = +1.5, p*K*a = +4.1, p*K*a = +6.4, p*K*a = +9.5, and p*K*a = +14.2.
3. The distribution of acid–base centers depends on the mineral component of the oil shales and shale ash, the specific surface area, and the micropores. Carbon in the organic component of the oil shales affects the intensity of the peaks corresponding to the acid–base centers.
4. The presence of acidic and basic Bronsted centers (p*K*a = +1.5, p*K*a = +3.5, p*K*a = +6.4) and the shale ash (p*K*a = +1.5, p*K*a = +4.1, p*K*a = +6.4) indicates sorptional activity of the oil shales and shale ash with respect to organic pollutants (petroleum and its products, for example).

5. The peaks with p*K*a = +9.5 and p*K*a = +14.2 (in the region of basic Bronsted centers) indicate sorptional activity of the oil shales and shale ash with respect to ionic heavy metals.

REFERENCES

[1] Leimbi Merike R., Tiina H., Eneli L., Rein K. Composition and properties of oil shale ash concrete/*Oil Shale.* 2014. Vol. 31, №. 2. 147–160.

[2] Bityukova L., Motler R. Composition of oil shale ashes from pulverized firing and circulating fluidized-bed boiler in Narva thermal power plants/*Oil shale*. 2010. vol. 27. № 4. 339–353.

[3] Swift T., Mayer S. Study of thermal conversion of oil shale under N_2 and CO_2 atmospheres/*Oil shale*. 2010. vol. 27. № 4. 309–320.

[4] Nazarenko M. Yu., Bazhin V.Yu., Saltykova S.N., Konovalov G.V. Physicochemical properties of fuel shale/*Coke and Chemistry*. 2014. №3. 44-49;

[5] Nazarenko M. Yu., Kondrasheva N. K., Saltykova S.N. Surface reactivity of fuel shales from the Baltic basin/*Coke and Chemistry*. 2016. №5. 33-37.

Smart Nanocomposites
Volume 7, Number 2
ISSN: 1949-4823

DEVELOPMENT AND RESEARCH OF ECOLOGICALLY SAFE DISPLACING OIL-DRILLING AGENT

Olga A. Shilova[1,2], Ekaterina E. Zakharova[1,3]*,
Larisa N. Krasilnikova[1], V. Yu. Dolmatov[4], and Elena Yu. Shits[5]
[1]Institute of Silicate Chemistry of the Russian Academy of Sciences,
St. Petersburg, Russia
[2]St. Petersburg State Technological Institute (Technical University), Russia
[3]Russian State Hydrometeorological University,
St. Petersburg, Russia
[4]Special Design and Technology Bureau "Technology,"
St. Petersburg, Russia
[5]Institute of Oil and Gas Problems of Siberian Branch of
the Russian Academy of Sciences, Yakutsk, Russia

ABSTRACT

This research is devoted to development of the ecologically safe displacing oil-drilling agents for carbonate rocks. It is found a positive effect of carbon nanoparticles on properties thin clay drilling agent. Involving of the carbon nanoparticles into the drilling mud fluids allowed reducing a drilling agent superficial tension of by 30%.

Keywords: drilling agent, calcareous soil, thin clay drilling muds, carbon nanoparticles

1. INTRODUCTION

The oil-drilling agent is an important element of technology of drilling of oil-bearing layer. It is known that about 60% of oil are lost in steam channels and capillaries of breed [1-2]. The studies on the increasing in the oil recovery efficiency are actively developing. One of the direction of exploratory researches is to develop new compositions and drilling fluids technology. The effectiveness of the oil-drilling agent depends, primarily, on the oil-containing rocks composition, oil properties and characteristics of the drilling fluid.

It is typical to several areas of Yakutia the calcareous soil - derived rock of medium and heavy loamy structure [3]. In these cases additives of clay particles to drilling agents promote

* Corresponding Author: kat.rumiantseva@yandex.ru

impossibility to extract the oil residues. Efficiency of effect of drilling agents depends on the properties of oil and oil-containing breed and characteristics of the drilling agent. Thus, the uses of drilling agents with high concentrations of clay have not always useful. To resolve this problem, thin clay drilling muds or ones without clay are used [1-5].

The thin clay drilling muds have a number of advantages over conventional muds with high clay concentration:

1. Increasing the drill penetration rate;
2. Reduce of the bit balling;
3. Increase of wear resistance of a chisel;
4. Reduce the hydraulic resistance of oil stratums.

Existing the water-based drilling agents contain components, which regulate the rheological properties, density, viscosity, etc.

Analysis of published data and our own experience suggests a positive effect of carbon nanoparticles as an alternative to the excess clay. This assumption is due to the fact that carbon nanoparticles have highly active surface enriched by various functional groups (hydroxyl, organic radicals), which provide the possibility of controllable selective interaction with the oil and the oil-bearing rock. An important fact is that the carbon nanoparticles are environmentally harmless. A number of carbon nanoparticles (fullerenes, detonation nanidiamond etc.) are soft biocides [6]. This is an important factor that carbon nanoparticles are significantly more environmentally safe in comparison to most often used additives to drilling fluids.

OBJECTIVES OF THE RESEARCH

The purpose of this research is development of ecologically safe displacing oil-drilling agents for carbonate rocks.

To achieve this research goal it is necessary to solve the following scientific and technological tasks:

1. Development of the composition of environmentally safe drilling agents, the pH of which is close to neutral.
2. Creating drilling mud fluids with a low content of the solid phase.
3. Creating the mud with a low content of the solid phase.
4. Investigation of the interfacial tension at the interface between the oil and drilling fluid depending on the composition of drilling agents.
5. Study of the effect of the carbon deposit additives to modify the interfacial tension at the interface between oil and drilling fluid.
6. Study of the effect of carbon deposits on the properties of drilling fluids (surface tension, rheological properties).
7. Research of the biocidal properties of drilling fluids with carbon deposites.

EXPERIMENTAL

For modeling the drilling fluid suitable for a more complete extraction of oil from carbonate rocks, the following ingredients are selected: water; surfactant, finely divided sodium bentonite, stabilizer of drilling fluids, carbon nanopowders. We are going to use the crude graphitized detonation nanodiamond, including one enriched by different chemical elements as carbon powders.

EXPECTED RESULTS

Involving of the carbon nanoparticles into drilling mud fluids allowed to reduce a drilling agent superficial tension of by 30%. It can increase essentially productivity of boring process and improve ecology.

REFERENCES

[1] Podkrepin, B. V., *Razrabotka neftyanykh i Gazovykh mestirozhdenij* (2015). Publishing Feniks: 320 [Podkrepin, B. V., *Development of oil and gas fields* (2015) Publishing Feniks: 320].

[2] Kudajkulova, G. A., *Byrovye glinistye rastvory* (2003), Teaching aids, Almaty: 103-107 [*Drilling clay muds* (2003), Teaching aids, Almaty:103-107].

[3] Kondrat'eva, K., Fotiev, S., Danilova, N., et al., *Geokriologiya USSR. Srednya Sibir'* (1989), Publishing Nedra Moskva): 413 [Kondrat'eva, K., Fotiev, S., Danilova, N., et al., *Geocryology of the USSR. Middle Siberia* (1989) Publishing Nedra, Moscow): 413].

[4] *Karbonatnye Porody. Genezis, Rasprostranenie, Classifikatsyya* (1), Ed. Chilingar, J., Bissell, G., Feyrbridzh, R. (1970). Trans. English, Ed. Kholodov, V. N., Publishing Mir.: 396 (*Nauki o Zemle. Fundamental'nye Trudy zarubezhnykh uchenykh* (28) [*Carbonate Rocks. Genesis, distribution, classification* (1), Ed. Chilingar, J., Bissell, G., Feyrbridzh, R. (1970), Trans. English, Ed. Kholodov, V. N, Publishing Mir.: 396 (*Earth Science. Fundamental works of foreign scientists* (28)].

[5] Kirkinskaya, V. N., Smekhov, E. M., *Karbonatnye Porody – Kollektory Nefti i Gaza*. (1981) Publishing Nedra: 255 [Kirkinskaya, V. N., Smekhov, E. M., *Carbonate Rocks – Reservoirs of Oil and Gas* (1981) Publishing Nedra: 255].

[6] Khamova, T. V., Shilova, O. A., Vlasov, D. Yu., Ryabusheva, Yu. V., Mikhal'chukc, V. M., Ivanov, V.K., Frank-Kamenetskaya, O. V., Marugin, A. M., Dolmatov,V.Yu., Bioactive coatings based on nanodiamond modified epoxy siloxane sols for stone materials (2012) Inorg. Mater (48) 7: 702–708.

PLASMA TECHNOLOGIES AND ELECTROMAGNETIC WAVES ABSORPTION

Smart Nanocomposites
Volume 7, Number 2
ISSN: 1949-4823

NONLOCAL KINETIC THEORY OF PLASMA DISCHARGES

Igor D. Kaganovich[1], Dmytro Sydorenko[2], Yevgeny Raitses[1], Vladimir I. Demidov[3], Huihui Wang[4], Alexander S. Mustafaev[5,*], and Vladimir S. Sukhomlinov[6]

[1]Princeton Plasma Physics Laboratory, Princeton, New Jersey, USA
[2]University of Alberta, Edmonton, Alberta, Canada
[3]West Virginia University, Morgantown, West Virginia, USA
[4]School of Physical Electronics,
University of Electronic Science and Technology of China, Chengdu, China;
[5]Saint Petersburg Mining University, Saint Petersburg, Russia
[6]Saint Petersburg State University, Saint Petersburg, Russia

ABSTRACT

The purpose of the talk is to describe recent advances in nonlocal electron kinetics in low-pressure plasmas and plasma nanotechnology. Low-pressure discharges are widely used in industry as the main plasma sources for many applications including plasma processing, discharge lighting, plasma propulsion, particle beam sources and nanotechnology. Being partially-ionized, bounded, and weakly-collisional, the plasmas in these discharges demonstrate nonlocal electron kinetic effects, nonlinear processes in the sheaths, beam-plasma interaction, collisionless electron heating, etc. Such plasmas often have a non-Maxwellian electron velocity distribution function. The plethora of kinetic processes supporting the non-equilibrium plasma state is an invaluable tool, which can be used to adjust plasma parameters to the specific needs of a particular plasma application. We report on recent advances in nonlocal electron kinetics in low-pressure plasmas where a non-Maxwellian electron velocity distribution function was "designed" for a specific purpose: in dc discharges with auxiliary biased electrodes for plasma control, hybrid DC/RF magnetized and unmagnetized plasma sources, and Hall thruster discharges. We show using specific examples that this progress was made possible by synergy between full-scale particle-in-cell simulations, analytical models, and experiments.

Keywords: nonlocal electron kinetic effects, nonlinear processes in the sheaths, beam-plasma interaction, collisionless electron heating

* alexmustafaev@yandex.ru

INTRODUCTION

Low temperature plasmas (LTPs) are widely used in applications and are strongly affected by the presence of neutral species—chemistry adds enormous complexity to the plasma environment. Electron energies in such plasmas are of order a few electron volts with sufficient population of electrons with energies above the threshold energies of the excited states of neutral atoms and molecules. The power transfer from electrons to these atoms and molecules produces activated species (e.g., radicals, excited states, and photons). Due to the low degree of ionization, the mean energy of electrons and ions in such plasma considerably exceeds the temperature of the neutral species. This provides a unique set of conditions wherein plasma species can efficiently react with adjacent surfaces resulting in their beneficial modification. With such properties, low temperature plasmas are widely used in technological processes, ranging from manufacturing of semiconductor chips, solar and plasma-display panels, to the treatment of organic and bio-objects [1]. Examples of recent progress are described in Special Section of Physics of Plasmas "Electron kinetic effects in low temperature plasmas" [2].

The next logical step in the development of electron kinetics was not only explaining the observed kinetic phenomena but using this accumulated knowledge to explore ways of actively crafting electron energy distribution functions (EEDFs) to achieve required effects. This research is the focus of DOE funded Center for Predictive Control of Plasma Kinetics: Multi-phase and Bounded Systems [3]. The complex dependence of different chemical reactions on electron energy places an extraordinary premium on optimally shaping EEDFs to influence the rate of interaction of a particular process. The ability to control the efficiency of the interaction of charged particles with their environment (gas atoms and molecules, or surfaces) depends on the ability to craft and control charged particles and photons distribution functions. Advancing LTP science requires the ability to control and to shape charged particles and photons distribution functions for beneficial treatment of surfaces, which is a challenging task considering the diversity and complexity of the variety of discharge conditions. However, improving the performance of these new plasma tools is still a significant challenge for plasma engineering. Exploitation of nonlocal plasma properties allows additional dimensions and flexibility in adjusting plasma parameters. A remarkable property of such plasmas is that changing conditions in one place may lead to unexpected changes far away in another part of the plasma. Additionally, plasmas with nonlocal EEDF allow independent and effective managing of electrons belonging to different energy ranges [4]. This, in turn, allows modification of the plasma properties in desirable ways, because different energetic groups of electrons are responsible for different processes, and their density modifications yield control over corresponding plasma processes. We report on recent advances in nonlocal electron kinetics in low-pressure plasmas where a non-Maxwellian EEDF was "designed" for a specific purpose.

REFERENCES

[1] At http://science.energy.gov/fes/news-and-resources/workshop-reports for 2008 Report on Scientific Directions for Low Temperature Plasma sponsored by Department of Energy.

[2] I. D. Kaganovich, V. Godyak, and V. I. Kolobov, *Physics of Plasmas*, Vol. 20, Article ID 101501 (3 pp.), 2013.

[3] See http://doeplasma.eecs.umich.edu/index.htm for the new Center for Predictive Control of Plasma Kinetics: Multi-phase and Bounded Systems, which is funded by a five-year grant from the U.S. Department of Energy.

[4] L. D. Tsendin, "Analytical approaches to glow discharge problems," *Plasma Sources Sci. Technol.*, Vol. 20, Article ID 055011 (18 pp.), 2011.

POLYMERS AND POLYMER-RELATED TECHNOLOGIES

Smart Nanocomposites
Volume 7, Number 2
ISSN: 1949-4823

HYDROPHOBIC COATINGS BASED ON SILOXANE BLOCK COPOLYMERS

Yulia V. Khoroshavina[1,*], Yulia V. Frantsuzova[1], Irina N. Tsvetkova[2], Olga A. Shilova[2], and Gennady A. Nikolaev[1]

[1]FSUE Institute of Synthetic Rubber,
St. Petersburg, Russia
[2]Institute of Silicate Chemistry of the. I. V. Grebenshchikov,
St. Petersburg, Russia

ABSTRACT

The aim of this work was to obtain hydrophobic coatings based on siloxane-polyphenylsilsesquioxane block copolymer. A range of polyphenylsilsesquioxane - polydimethylsiloxane block copolymers general formula $M_nD_{300}T_{70}$ with a ratio of D/T-units 300/70 and various contents of hydroxyl- groups have been synthesized. These block copolymers were investigated as a component of hydrophobic coatings. This coatings were obtained on the basis of alkoxide silicon with additional introduction hydrophobic filler Aerosil by the sol-gel synthesis.

Keywords: hydrophobic and superhydrophobic coatings, polyphenylsilsesquioxane-polydimethylsiloxane block copolymer, films, anti-icing coatings

INTRODUCTION

In present time hydrophobic and superhydrophobic coatings represent a great practical interest. It's actively carried out a development of materials having high water resistance and resistance to icing, as well as biological stability.

Previously, we obtained polyphenylsilsesquioxane-silicate resins, which were introduced as filler in vulcanizates grafted copolymer of polydimethylsiloxane and styrene, demonstrating chemically neutral and hydrophobic.

* e-mail: julhor@yandex.ru

Table 1. The basic physical properties and appearance of coatings based on block copolymers

Polymer formula	Wetting angle	Wetting angle, after heat treatment (250°C, 40 min.)	The picture of the composite	The picture of the composite after heat treatment	Notes
			with magnification × 10		
$M_2D_{300}T_{70}$	96,8	100		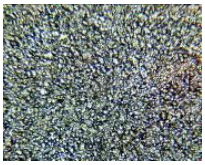	Transparent coating, the drop flow down, leaving no trace
$M_7D_{300}T_{70}$	95	98,4	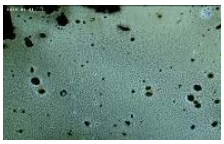	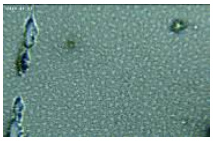	
$M_{14}D_{300}T_{70}$	122	120	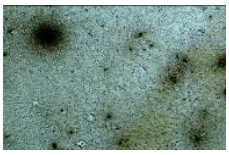	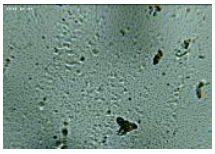	
$D_{300}T_{70}$	98	95	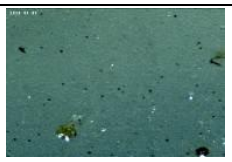	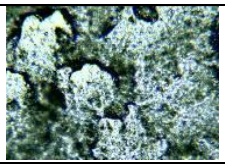	Clear coat, sticky, easy to wash

Later these resins have been used as a “hard” block in the synthesis of polyphenyl-silsesquioxane - siloxane block copolymers - materials, combining the properties of both linear siloxanes: flexibility, elasticity, processability and silsesquioxane - hardness, wear resistance [1].

We have synthesized a range of polyphenylsilsesquioxane - polydimethylsiloxane block copolymers general formula $M_nD_{300}T_{70}$ with a ratio of D/T-units 300/70 and various contents of hydroxyl- groups. The content of hydroxyl- groups was regulated by the introduction of monofunctional units M to the synthesis, ratio M/T = 0,03÷0,2(mol.).

The block copolymers ($M_2D_{300}T_{70}$, $M_7D_{300}T_{70}$, $M_{14}D_{300}T_{70}$, $D_{300}T_{70}$) were investigated as a component of hydrophobic coatings. This coatings were obtained on the basis of alkoxide silicon with additional introduction hydrophobic filler Aerosil by the sol-gel synthesis. To improve the adhesion of the coating to the substrate and increasing roughness were carried out pre-drying and heat treatment at a temperature of 250°C for 40 minutes.

As it can be seen from the above data, the reduction of the content of hydroxyl groups (the increase in the proportion of M-units) leads to an increase in the values of the wetting angle, until the hydrophobic coating (120^0). A small part of M-units ($M_2D_{300}T_{70}$) increases the

strength of the coating compared to films made from the original block copolymer, without affecting its hydrophobicity.

As it can be seen from table 2, after formation of the coating the formation of multimodal surface due to the combined effect of a macromolecular siloxane component, among other things, enhance adhesion to the substrate and hydrogenated Aerosil 972, embedded in the silicate structure and is responsible for the formation of spongy superhydrophobic surface.

This project was supported by Federal Target Program (grant 14.576.21.0028), code - RFMEFI57614X0028.

Table 2. The basic physical properties and appearance of coatings based on copolymers with filler – Aerosil

Polymer formula	Wetting angle	Wetting angle, after heat treatment (250°C, 40 min.)	The picture of the composite	The picture of the composite after heat treatment	Notes
			with magnification × 10		
$M_{14}D_{300}T_{70}$ - sole MTƏOS -Aèrosil 972	102,8	120	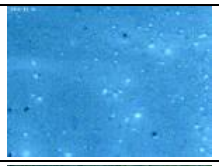		The angle increases on average by 20% transparent, washable .
$M_7D_{300}T_{70}$ - sole MTƏOS -Aèrosil 972	115,7	150	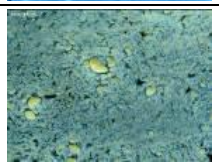	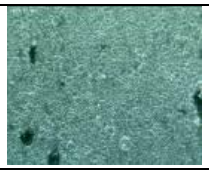	
$M_2D_{300}T_{70}$ - sole MTƏOS -Aèrosil 972	138	146	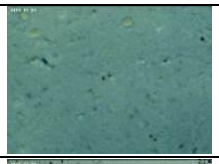	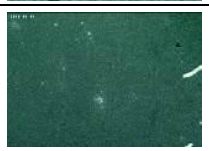	
$D_{300}T_{70}$ – vinyloxime	106,5	105,5		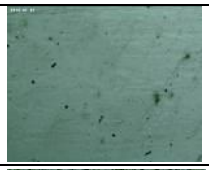	Transparent, smooth, drop leaves no trace
$D_{300}T_{70}$- vinyloxime- - sole TƏOS -Aèrosil 812	108,6	140	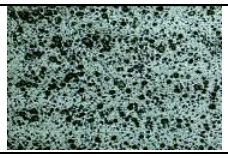	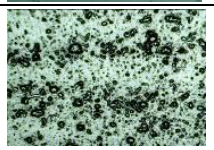	Transparent, smooth, drop leaves no trace

REFERENCES

[1] Khoroshavina Yu. V.; Frantsuzova Yu. V.; Nikolaev G. A.//*International Polymer Science and Technology*. 2016. V. 42. № 9. P.T/13-T/15.

Smart Nanocomposites
Volume 7, Number 2
ISSN: 1949-4823

MECHANICAL PROPERTIES OF POLYACRYLIC ACID - POLYVINYL ALCOHOL HYDROGELS AT COMPRESSION AND EXTENSION

I. S. Kuryndin, I. Yu. Dmitriev, N. V. Bobrova, Z. F. Zoolshoev, and G. K. Elyashevich*
Institute of Macromolecular Compounds, Russian Academy of Sciences
St. Petersburg, Russia

ABSTRACT

Cylinder and ring shaped samples of hydrogels were prepared by polymerization of acrylic acid in the solution of polyvinyl alcohol. The swelling degree and mechanical properties of the hydrogels were determined. The two-components hydrogels are characterized by a higher breaking strength and elasticity than the polyacrylic acid gels. It was found that the hydrogels demostrate the electromechanical response.

Keywords: hydrogels, polyacrylic acid, polyvinyl alcohol, swelling degree, mechanical properties

INTRODUCTION

Hydrogels are of great interest to researchers as elements of artificial muscles. At present the hydrogels prepared of polyelectrolyte polymers are promising materials for the soft robotic applications due to easy manufacturing and low voltages for their actuation. The problem is to provide the polyelectrolyte gels sufficient level of breaking strength and elasticity. It may be solved by the preparation of two-components interpenetrating networks containing strong polyelectrolyte and also the component to optimize the mechanical properties of hydrogels. The goal of this work was to synthesize the electroactive hydrogels based on polyacrylic acid and polyvinyl alcohol and to investigate the dependence of their swelling degree and mechanical properties on the preparation conditions.

* Corresponding Author address: Email: elya@hq.macro.ru

MATERIALS AND METHODS

The preparation technique of polyacrylic acid (**PAA**) - polyvinyl alcohol (**PVA**) hydrogels of required shape has been elaborated. The hydrogels were synthesized by free-radical copolymerization of acrylic acid in water solution of PVA ($M_w = 7 \cdot 10^4$) at 30^0C. Methylenebisacrylamide was used as crosslinker. Concentrations of PVA in solution were chosen as 5, 10 and 15%. Three-component initiator (ammonium peroxydisulfate/ Mohr's salt/sodium sulfite) was used to synthesize PAA - PVA hydrogels. As a result the semi-interpenetrating network of PAA and PVA was formed. Cylinder and ring shaped samples were prepared. Swelling degree of the hydrogels and their mechanical properties under compression and extension have been measured.

RESULTS AND DISCUSSION

It was observed that equilibrium swelling degree of hydrogel PAA-PVA in distilled water decreases (from 4.0 to 3.2 g/g) as the concentration of PVA in solution increases. All of the PAA-PVA samples demonstrated a swelling degree lower than one of PAA hydrogel (13.8 g/g).

The swelling degree of the samples PAA-PVA in 5% water solution of Na_2SO_4 is about 20% lower than in distilled water because of the substitution of H^+ ions in PAA by Na^+ ions in the salt solution, and, as a result, partial transformation of PAA to sodium polyacrylate.

The cylinder shaped hydrogels swollen in distilled water were tested under compression. It was found that all the PAA-PVA hydrogels exhibit a higher breaking strength than PAA gels (160 kPa). Maximal value (250 kPa) was observed for the PAA-PVA gels synthesized in 5% solution of PVA, and it decreases as the concentration of PVA increases. When PVA content grows from 5 to 15% the elastic modulus diminishes (from 75 to 50 kPa) and breaking deformation rises (from 60 to 80 %). All of the PAA-PVA gels are characterized by a higher breaking deformation and lower elastic modulus than PAA ones (40 % and 207 kPa, respectively).

The ring shaped PAA-PVA gels swollen in distilled water were used for mechanical tests at extension. It was shown that the increasing of PVA concentration from 10 to 15% results in the increase of breaking strength from 60 to 65 kPa and elongation at break from 125 to 168%; at the same time elastic modulus decreases from 63 to 46 kPa.

The ring-shaped PAA-PVA gels synthesized at PVA concentration equal to 10 % and swollen in 5% water solution of Na_2SO_4 are characterized by a higher deformation at break (375%), a higher breaking strength (70 kPa) and a lower elastic modulus (23 kPa) than these samples swollen in distilled water.

It was found that the elastic rings of the PAA-PVA hydrogels demonstrate the electromechanical response (compression) under electric voltage. The effect is more pronounced when the rings swell in Na_2SO_4 solution as compared with their swelling in water. These results evidence that the PAA-PVA gels may be used as linear electric actuators (artificial muscles).

ACKNOWLEDGMENTS

This work was supported by the Russian Foundation for Basic Research (Project № 16-03-00265a) and Project of Collaborative Research of the Russian Academy of Sciences and the University of Ljubljana (Slovenia) (ARRS-BI-RU/16-18-017).

SEMICONDUCTOR TECHNOLOGIES

Smart Nanocomposites
Volume 7, Number 2
ISSN: 1949-4823

STUDY OF PRODUCING SENSORS BASED ON POROUS GAP SEMICONDUCTORS WITH THE USE OF ELECTROADHESION CONTACTS

Veniamin L. Koshevoi[1] and Anton O. Belorus[2]
[1]Saint Petersburg Mining University, Saint Petersburg
[2]Saint Petersburg Electrotechnical University "LETI"
Saint Petersburg, Russian Federation

ABSTRACT

This paper describes the study of porous layers of semiconductors A_3B_5 group. Using SEM were determined pore size and thickness of the porous layer of obtained films. These films are used as the working fluid in sensors using electrodiffusion contacts.

Keywords: semiconductors, sensors, transducers, etching, porous semiconductors, transport, electrodiffusion contact

INTRODUCTION

The last few years attracted the attention of researchers, along with the porous silicon and other porous semiconductors, particularly compounds A_3B_5 (GaP, GaAs, GaN, InP, etc.). The porous substrate based on semiconductor compounds A_3B_5, are promising materials for producing homo- and heteroepitaxial layers of high structural perfection. Also A_3B_5 porous semiconductors have great prospects to create the different types of sensors [1, 6-8].

The objective of the work was to study the creation of electrodiffusion contacts for sensors based on porous semiconductors A_3B_5 group and also study themselves porous films obtained in the course of the experiment (pore size, thickness, etc.).

Working part of the sensor is a porous semiconductor A_3B_5 group obtained by electrochemical etching in an aqueous solution of hydrofluoric acid [2]. On a porous surface with a mask deposited dielectric film. To connect the semiconductor wafer and the dielectric substrate is used adhesive uncontrollable contact based on Johnson - Rabek effect. Then a metallic layer is applied and attached probe.

THE EXPERIMENTAL PART

We have been developed technology for producing porous gallium phosphide - (GaP por).

Layers of porous GaP: Te (100) were obtained by electrochemical etching in a hydro-alcoholic (isopropanol) solution of hydrofluoric acid. In the experiment, 3 samples were prepared under different etching conditions. Sample 1 was obtained at a current density of 5 mA/cm^2, t = 30 min. Sample 2 was obtained at a current density of 25 mA/cm^2, t = 10 min. Sample 3 was obtained at a current density of 50 mA/cm^2, t = 10 min.

EXPERIMENTAL RESULTS

SEM data showed porous semiconductor structure (GaP: Te) refers to macroporous. Also SEM data shows that the thickness of the porous layer is 28 microns.

Next we plan to lay siege to the working part of the dielectric film for the implementation of electrodiffusion contacts and the subsequent creation of the contacts on the sensor. For the deposition of dielectric films on wafer we plan to use chemical vapor deposition method from the gas phase using a plasma activation [3].

The contact between the semiconductor and the insulator will be carried out at the expense of electrodiffusion contacts which is based on Johnson – Rabek effect: between two solid state having different electrical potentials occur electrostatic (ponderomotive) forces [4].

Under certain conditions we can create electrodiffusion contacts, persistent (due to mutual diffusion) and after a power failure. This connection is called the unmanageable electrodiffusion contacts. For large pulling forces at the points of actual contact, we can use the migration polarization observed in ionic dielectrics [5].

CONCLUSION

Considered technology has a number of advantages: fastening materials can be connected in a solid state at a temperature substantially below the melting point without any intermediate layers (glues, solders, etc.), pulling the electric field acts on the details of the “inside” of the connecting seam (which allows you to connect fragile parts), a special expensive equipment is not required for implementing the method [5, 9-10].

Sensors, obtained by this method can be used in various enterprises, vehicles for environmental control and etc. These sensors (gas, chemical) will help catch dangerous gases, which can damage the equipment, and chemicals dangerous for peoples and the environment. This production technology of sensors is simple and does not require special expensive equipment.

The work was performed by the project contract code 0021109, competition UMNIK 15-12.

REFERENCES

[1] Surface functionality features of porous silicon prepared and treated in different conditions/Spivak Yu. M., Myakin S. V., Moshnikov V. A., Panov M. F., Belorus A. O., Bobkov A. A. *Journal of Nanomaterials*. - 2016. - T. 2016.

[2] Morphology and internal structure of porous silicon powders in dependence on the conditions of post-processing/A. O. Belorus K. Bespalova Yu. M. Spivak *Conference Paper – February 2016 – DOI: 10.1109/EIConRusNW.2016.7448108 – Conference: 2016 IEEE NW Russia Young Researchers in Electrical and Electronic Engineering Conference (EIConRusNW).*

[3] The study of the phase composition of polymorphous silicon film by Raman spectroscopy. V. L. Koshevoi N. S. Pshchelko A. O. Belorus V. S. Levitskiy. *Conference Paper February 2016 – DOI: 10.1109/EIConRusNW.2016.7448119 – Conference: 2016 IEEE NW Russia Young Researchers in Electrical and Electronic Engineering Conference (EIConRusNW).*

[4] The study of porous silicon powders by capillary condensation/Belorus A. O., Maraeva E. V., Spivak Y. M., Moshnikov V. A. *Journal of Physics: Conference Series*. – 2015. – T. 586. – № 1. – P. 12-17.

[5] Porous silicon nanoparticles for target drag delivery: structure and morphology/Spivak Yu. M., Belorus A. O., Somov P.A., Tulenin S. S., Bespalova K. A., Moshnikov V. A. *Journal of Physics: Conference Series*. – 2015. – T. 643. – P. 012022.

[6] Structure and morfology of Si films grown on Porous Silicon by reduction of Dichlorosilane A.A. Kovalevskii/Kovalevskii A. *Inorganic materials* – 1999. - Vol. 35 - №2.

[7] Gold Nanorods, DNA Origami and Porous Silicon nanoparticles functionalized biocompatible double emulsion for Versatile targeted therapeutics and antibody combination therapy/Kong F., Zhang H., Qu X., Hai M. *Advanced Materials. – 2016. - DOI: 10.1002/adma.201602763.*

[8] Mesoporous biomaterials – multifunctional materials for future medical therapies and bioanalysis/Canham L., Santos H., Palestino G. *De gruyter open* – 2015.

[9] The investigation of p- and as diffusion in liquid gallium./Gorokhov V.A., Dedegkaev T. T., Ilyin Y. L., Moshnikov V.A., Petrov A.S., Sosov Y.M., et al. *Crystal Res Technol. 1984;19(11):1465–8. doi:10.1002/crat.2170191112.*

[10] Dynamics of mass transport during nanohole drilling by local droplet etching/Christian H., Thorben B., Stefano S., David J., Wolfgang H. *Heyn* et al. *Nanoscale Research Letters (2015) 10:67 DOI 10.1186/s11671-015-0779-5.*

Smart Nanocomposites
Volume 7, Number 2
ISSN: 1949-4823

GROWTH AND PROPERTIES OF AL_2O_3 NANOLAYERS ON III–V SEMICONDUCTORS

Yu. K. Ezhovskii*
St. Petersburg Technological Institute (Technical University),
St. Petersburg, Russia

ABSTRACT

It describes the process of forming a nanolayers of aluminum oxide, obtained by atomic layer deposition (ALD-technology) on the surface of GaAs, InAs and InSb. The conditions for layer-by-layer growth of surface nanostructures are established, and some of their dielectric parameters are evaluated.

Keywords: atomic layer deposition, nanolayers of aluminum oxide, to obtain, the properties

INTRODUCTION

In recent years, atomic layer deposition (ALD) has been the subject of intense attention as a process for growing high-quality ultrathin layers [1–3]. The advantages of this technology and its potential for fabricating submicron-sized components of integrated devices have been demonstrated in several studies [4-6]. ALD takes advantage of surface chemical processes previously referred to as molecular layering, whose physicochemical foundations were developed as early as the 1970 [7].

EXPERIMENTAL

The use of surface chemical reactions, basic to the ALD process, allows one to grow low_dimensional structures with their composition and thickness controlled on a monolayer scale. In this approach, the growth of oxide layers involves, as a key step, self-limiting chemisorption of a metal halide (MCl_n) and water vapor under limiting surface coverage conditions. For example, the process on hydroxylated surfaces (symbol |) can be run according to the schemes

* E-mail: ezhovski@pochta.ru

$$\left|\text{-OH}\right)_m + MCl_n \rightarrow \left|\text{-O-}\right)_m MCl_{n-m} + mHCl. \quad (1)$$

$$\left|\text{-O-}\right)_m MCl_{n-m} + (n\text{-}m)H_2O \rightarrow \left|\text{-O-}\right)_m M(OH)_{n-m} + (n\text{-}m)HCl, \quad (2)$$

The value of m depends on the surface density of hydroxyls; e.g., $m \approx 2$ for silicon surfaces [8].

RESULTS AND DISCUSSION

Comparison of the present experimental data with previous results for other substrate materials and other oxides shows that the growth of Al_2O_3 nanolayers on III–V semiconductor substrates follows the same general mechanisms, inherent in this process. In particular, analysis of the effect of deposition temperature indicates that the growth of oxide nanostructures via sequential chemisorption of metal halide and water vapors may follow three mechanisms: reaction between components in a polymolecular adsorbed layer, leading to the formation of hydrous oxides; sequential growth of monomolecular layers (layer-by-layer growth mechanism); and formation and subsequent growth of two-dimensional islands. Aluminum chloride chemisorbs in the form of dimers without thermal activation. This leads to high d_0 values for Al_2O_3 at any temperature.

Structural characterization of the deposited films by electron diffraction showed that, over the entire temperature range studied, the Al_2O_3 layers less than 100nm in thickness were amorphous at T_s<450K and contained α-Al_2O_3 at higher temperatures. In all cases, increasing the Al_2O_3 layer thickness and deposition temperature led to the formation of crystalline domains as supramolecular structures.

The dielectric properties of Al_2O_3 films produced under layer-by-layer growth conditions meet the requirements for dielectric films. Therefore, the ALD process can be used to grow dielectric structures, including multilayers, for submicron_sized components of micro- and nanoelectronic systems (e.g., gate dielectrics in MIS structures), capacitors, and barrier layers.

REFERENCES

[1] Suntola, T., *Mater. Sci. Rep.*, vol. 4, no. 7, p. 261. (1989).
[2] Seidel, T., Londergan, A., Winkler, L., *Solid State Technol.*, no. 5, p. 67. (2003).
[3] Nishizava, J. and Kurabayash, T. *Chem. Sustainable Dev.*, no. 8, p. 5. (2000).
[4] Ming, X., *Solid State Technol.*, vol. 44, p. 70. (2001)
[5] Gelatos, J., Chen, L., Chung, H., Thakur, R, *Solid State Technol.* vol. 2, p. 44. (2003).
[6] Puurunen, R. L. *J. Appl. Phys.*, vol. 97, no. 12, p. 121301. (2005).
[7] Aleskovskii, V. B. *Vestn. Akad. Nauk SSSR*, no. 6, p. 48. (1975).
[8] Ezhovskii, Yu. K., *Usp. Khim.* vol. 73, no. 2, p. 209. (2004).

Smart Nanocomposites
Volume 7, Number 2
ISSN: 1949-4823

CORRELATION COLLAPSING OF ENERGY GAP IN VANADIUM DIOXIDE

Aleksandr V. Ilinskiy[1], Rene A. Kastro[2], Vladimir A. Klimov[1], Evgeniy I. Nikulin[1], and Evgeniy B. Shadrin[1,*]
[1]Ioffe Physical Technical Institute of the Russian Academy of Sciences, Russia
[2]Herzen State Pedagogical University, Russia

ABSTRACT

At low temperatures ($77 < T < 273$ K) due to investigation of temperature dependence of electro-conductivity physical parameters of VO_2-films are determined: the depth of energy position of the donor type impurity centers ($E_d = 0.04$ eV) and the width of forbidden zone $E_g = 0.8$ eV. It is shown, that with growth of temperature the width of forbidden zone (energy gap in electronic spectrum) E_g decreases up to 0 eV in a temperature range $273 < T < 300$K, that is caused by narrowing of energy gap owing to the correlation effects inherent vanadium dioxide.

Keywords: vanadium dioxide, energy gap, electronic spectrum, correlation effects

INTRODUCTION

Many decades VO_2-crystals draw attention of scientists [1]. It is connected with unique physical properties of vanadium dioxide. At low temperatures and at room temperature VO_2 is semiconductor, and at temperature $T_c = 68^oC$ (340 K) it undertakes the semiconductor metal phase transition. Offered paper is devoted to studying of temperature dependence of electro-conductivity of vanadium dioxide thin films in a wide temperature interval ($77 < T < 373$ K). It allows to show the important property of vanadium dioxide - the temperature collapse of the forbidden zone due to correlation effects [2-5]. Objectives of the research are an experimental check of this statement by measurement of temperature dependence of electroconductivity of a vanadium dioxide film and a check of its ability by use of Arrhenius coordinates.

Samples of VO_2-films with area $10 \cdot 10$ мм^2, thickness $9 \cdot 10^{-2}$ microns and specific resistance $7 \cdot 10^6$ Ohm·m (293 K) are received by laser ablation method. The following

* E-mail: shard.solid@mail.ioffe.ru

experimental results have been received. On figure the temperature dependences of electro-conductivity of vanadium dioxide film in a range of temperatures from temperature of liquid nitrogen up to room temperature are submitted.

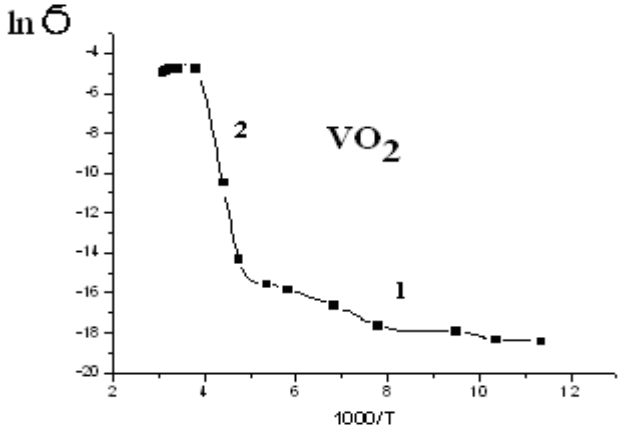

Figure shows the result of definition of thermal ionization energy by investigation of two temperature sites of conductivity change.

Low temperature part 1 corresponds to the case of strong thermal ionization of shallow donors. For this low temperature site from expression

$$n_1 (T) = n_1 (0) \exp (-E_d/kT),$$

one can receive: $\ln[n_1 (T)] = -E_d/kT + \text{const}$. The use of Arrhenius coordinates leads to linearization of low temperature part. By tangent of slope angle of linear part of function $\ln [n_1 (T)]$ the ionization energy of donors is determined as $E_d = 0.04$ eV. The high-temperature part 2 corresponds to a case of thermal electron transport from d||-zones to π^* - zone, i.e., to inter-zoned transitions through the forbidden zone with E_g width. The analysis of part 2 of function $\ln[n_2 (T)] = -E_g/kT + \text{const}$ allows in Arrhenius coordinates to determine the activation energy $E_g = 0.8$ eV.

Here we pay special attention to fact that with temperature rise the slope $\ln\sigma(1/T)$ decreases from value 0.8 eV up to zero and last value is achieved at temperature approximately 270 K, i.e., in area 0°C.

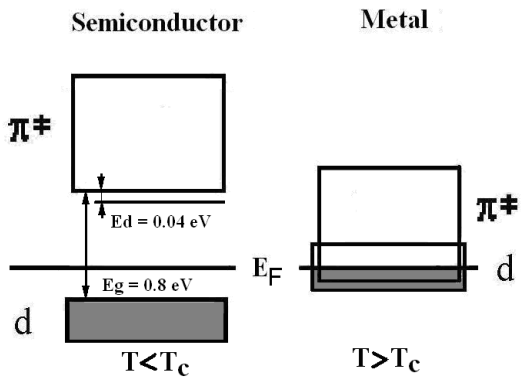

In complex model [5] of phase transition offered in this paper the electronic Mott-transition gradually increasing conductivity of VO_2 because of correlation effect and narrowing the energy gap, is primary. Structural phase transition is secondary. In our paper we show that in the back process of phase transition of the material from metal to semiconductor phase the electronic transition initiates structural phase transition too. At that the electronic phase transition in VO_2 is ahysteretic, but structural phase transition in VO_2-microcrystal has a thermal hysteresis with width which depends, first of all, on the size of a microcrystal.

CONCLUSION

In VO_2 correlation effects reduce a gap at heating a sample. The gap is an energy distance between bottom 3d-subzone and π^*-zone. The width of a gap changes from starting size 0.8 eV up to 0 eV because of movement of energy zones towards each other due electrons transition through a gap. The reason of movement of energy zones is that energy position of energy zones live in inverse dependence to their occupation of electrons.

REFERENCES

[1] W. Bruckner, H. Opperman, W. Reichelt, G. Wolf, F. A. Chudnovsky, E. I. Terukov. *Vanadium dioxide (*Berlin, Academy-Verlag, 1983).

[2] N. F. Mott, *Metal–Insulator Transitions* (Nauka, Moscow, 1979; Taylor Francis, London, 1974), 342 c.

[3] S. Shin, S. Suga, M. Taniguchi, M. Fujisawa, H. Kanzaki, A. Fujimori, H. Daimon, Y. Ueda, K. Kosuge, S. Kachi. *Phys.Rev*. B, 41, 4993 (1990).

[4] W. W. Li, Q. Yu, J. R. Liang, K. Jiang, Z. G. Hu et al. *Appl. Phys. Lett.* 99, 241903 (2011).

[5] A. V. Il'inskii, O. E. Kvashenkina, and E. B. Shadrin. *Semiconductors* 46, 422 (2012).

Smart Nanocomposites
Volume 7, Number 2
ISSN: 1949-4823

STEP-BY-STEP SOLUTION OF ONE-DIMENSIONAL QUANTUM-MECHANICAL PROBLEM IN PROCESS OF NANO-TECHNOLOGICAL EDUCATIONS

Aleksandr V. Ilinskiy[1], Marina E. Pashkevich[2], and Evgeniy B. Shadrin[1,*]

[1]Ioffe Physical Technical Institute of the Russian Academy of Sciences, Russia
[2]St. Petersburg State Polytechnical University, Russia

ABSTRACT

In education process exist a problem of create of ability of establishing of connections between properties of real physical object and mathematical model describing such properties. We propose the solution of this problem which is based on a studying of correlation between physical properties of nano-crystal vanadium dioxide thin films and details of quantum-mechanical model of a one-dimensional chain hydrogen-like atoms describing these properties. The main accent is made here on gradual complication of the description of the semiconductor - metal phase transition at T_c = 68°C which occurs in nano-crystal grains of VO_2-thin films. Consideration in educational process of the nature of phase transition begins on the solution of one-dimensional quantum-mechanical problem, and comes to end with concept of correlation energy and discussion of Mott-idea about dependence of position of energy zones on their electron occupation.

Keywords: education, vanadium dioxide, phase transition, correlation effects

INTRODUCTION

One of problems of any educational process (and nano-technological, including) is maintenance of development at pupils of skill to establish connections between properties of real physical object and the mathematical model reflecting these properties. The purpose of the message is an illustration of any variants of the decision of this problem in this article we speak about the message to pupils about the information on a correlation between physical properties of nano-crystal vanadium dioxide chain of atoms, describing these properties. The

* E-mail: shard.solid@mail.ioffe.ru

main thing in educational process is the accent on the semiconductor - metal phase transition (PT) at $T_c = 68^oC$ which occurs in nano-grains of VO_2 films [1, 2].

Studying of properties of VO_2-elementary cell begins with studying the theory of valence bounds which approves, that in an elementary cell each of vanadium atom forms (as a result of $3d^24s^14p^3$-hybridization [3]) six **σ**-bounds with six atoms of oxygen fixed in picks of an octahedron. The arrangement of oxygen octahedrons in VO_2-crystal lattice corresponds formation in tetragonal phase one-dimensional chains of vanadium ions fixed in the centers of oxygen octahedrons. These chains go parallel to tetragonal C_R axis. Thus, in VO_2 there is the unique case at which the one-dimensional hydrogen-like chain atoms containing only one electron on external orbital, is stabilized in space due to others orbitals of the same atom. Because of this fact metal-type bound arises in a one-dimensional chain along C_R axis. Thus, in this model at low temperatures everyone nano-crystal of VO_2 - film represents a metal grain. It cannot make any phase transition, but V can make phonon fluctuations. In such model the quantum mechanic description of properties (near to Fermi's level) of vanadium dioxide nano-crystals can be made on the base of idea of rigid quasy-one-dimentional chains of the atoms having one electron on external orbitals.

Schrödinger equation for such chain with Hamilton operator, taking into account only interaction with the nearest neighbors, have the exact solution and may be written as:

$$[d^2\Psi(x)/dx^2] + (2m/\hbar^2)[E-V(x)]\Psi(x)=0,$$

where V(x) - the potential energy equal the sum potential energy of electron in a field of separate ions.

In this model the metallic conductivity along one-dimensional chain should be kept at any temperatures. However, as experiment shows, at temperature $T < T_c = 68^oC$ vanadium dioxide is the semiconductor, instead of metal. It forces us to complicate the described simple model, having refused from idea of a rigid chain: theoretical consideration includes fluctuations of atoms of a one-dimensional chain. In each half-cycle of fluctuations atoms of vanadium in pairs come nearer to each other and create the formations named “dimmers”. The model of a one-dimensional chain is edited with idea of formation of the “dynamic” **σ**-bounds formed and disappeared during one half-cycle of phonon fluctuations. This idea has in itself a possibility of fulfillment of phase transition at T_c temperature by thermal destroying of dimmers. But phonons energy that is close to kT, at temperatures down to 500 K is not sufficient for electron transport through such energy gap. Therefore the described model requires the further complication. It is necessary to take into account multiparty interaction, i.e., interaction between electrons fixed in a periodic field of a lattice. The effects caused by such interaction are named correlation effects. According to calculations, the width of the gap because of correlation effects depends on a degree of electrons filling of the empty zones. Particularly calculations for VO_2 from first principles have shown, that correlation effects lead to lowering of a π*-zone at its filling by electrons in process of heating a sample, and the width of a gap becomes equal to zero at $T = 68\ ^oC$ (341 K). Reduction of a gap between a π*-zone and the bottom 3d-subzone sharply facilitates destruction of **σ**-bounds of dimmers. Thus, in the given model electronic Mott-transition initiates a structural phase transition [4, 5].

And the last stage of education process is connected to the account of martensitic character semiconductor - metal phase transition in VO_2.

CONCLUSION

In summary we will notice, that, having started our consideration of nature of semiconductor – metal phase transition from simple model, we finish this consideration by introduction of concept of correlation energy and idea of dependence of position of energy zones from their occupation.

REFERENCES

[1] W. Bruckner, H. Opperman, W. Reichelt, G. Wolf, F. A. Chudnovsky, E .I. Terukov. *Vanadium dioxide*, Berlin, Academy-Verlag (1983), 252.

[2] A. A. Bugaev, B. P. Zakharchenya, and F. A. Chudnovskii, *Metal–Semiconductor Phase Transition and Its Application* (Nauka, Leningrad, 1979) [in Russian]. 183 c.

[3] C. E. Hausecroft, E. C. Constable. *Chemistry: An Integrated Approach.* (London. 1997) **1**, 540.

[4] N. F. Mott, *Metal–Insulator Transitions* (Nauka, Moscow, 1979; Taylor Francis, London, 1974), 342 c.

[5] S. V. Vonsovskii and M. I. Katsnelson, *Quantum Solid State Physics* (Nauka, Moscow, 1.

Smart Nanocomposites
Volume 7, Number 2
ISSN: 1949-4823

DISCUSSION OF DATA INCONSISTENCIES ON TRANSPORT PHENOMENA IN CRYSTALS OF P-SB2TE3-XSEX

Sergey A. Nemov[1,2,*], Ali. A. Allahkhah[1], and Arseny A. Rulimov[1]
[1]Peter the Great St. Petersburg Polytechnic University, St. Petersburg, Russia
[2]Zabaikal'skii State University, Chita, Russia

ABSTRACT

It is shown that accounting of interband scattering allows eliminating contradictions in the literature between interpretations of the electrical properties of $A_2^V B_3^{VI}$ materials with the hole conductivity and describing observed temperature dependences of the kinetic coefficients as well as the parameters of the band spectrum.

Keywords: $A_2^V B_3^{VI}$ materials, Interband scattering, Scattering parameter, Kinetic coefficients, Acoustic mechanism of hole scattering

INTRODUCTION

Investigations of layered semiconductor $A_2^V B_3^{VI}$ materials have been being carried out since the middle of last century. Constant interest in these materials is caused by their wide usage in thermoelectric energy converters (in the form of ternary and quaternary solid solutions based on bismuth and antimony chalcogenides).

DISCUSSION

The experimental data obtained in the middle of the 20th century were summarized and systematized in Gol'tsman monograph [1]. However, the features of the energy spectrum of $A_2^V B_3^{VI}$ materials and the mechanisms of charge-carrier scattering are still discussed. Also the differences in the interpretation of experimental data of transport phenomena at low (T = 4.2 K) and medium (77 - 300 K) temperatures are stored. Results of the quantum

* Corresponding author; Prof. Sergey Aleksandrovich Nemov, Professor of the Department "Materials Science and Technology of Materials," Peter the Great St. Petersburg Polytechnic University, St. Petersburg, Russia, Tel.: +7 (921) 347-30-33. E-mail: nemov_s@mail.ru.

oscillations research at liquid-helium temperatures have confirmed the Drabble-Wolfe one-band six-ellipsoidal model for crystals with low hole concentration [2, 3].

Most of experimental investigations of transport phenomena in $A_2^{V}B_3^{VI}$ compounds are related to the temperature range 77 - 300 K.Unlike the low-temperature data, the kinetic coefficients (the conductivity σ, the thermopower α, the transverse Nernst-Ettingshausen effect Q) do not have any differences from the nature of the temperature dependences predicted by the theory within one-band model (at the temperature range 77 – 450 K). Therefore, the one-band model is widely used for analysis of the electrical properties of materials, estimates of energy spectrum parameters and for the calculations of the thermoelectric efficiency.

From our point of view, the above-mentioned contradictions in interpretation of the experimental data can be eliminated by correction of the mechanisms of hole scattering. According to available literature data all three components of the Nernst-Ettingshausen tensor are negative numbers at temperatures $T \geq 77$ K in all investigated $A_2^V B_3^{VI}$ materials. In the one-band model such behavior of the Nernst-Ettingshausen coefficient clearly indicates the dominance of the acoustic mechanism of hole scattering. In the two-band model in the samples with the Fermi level located closely to the top of the secondary extremum of the valence band the channel of additional scattering of kinetic moment of charge carriers appears. This mechanism is called interband scattering. The concepts of interband scattering were originally introduced by N.V. Kolomoets [4] to explain anomalies in the concentration dependences of the thermopower in iron group alloys.

CONCLUSION

Produced estimates show that accounting of interband scattering allow describing observed temperature dependences of the kinetic coefficients and determining the parameters of the band spectrum more correctly.

REFERENCES

[1] B. M. Gol'tsman, V. A. Kudinov, I. A. Smirnov. Semiconductor thermoelectric Bi2Te3 based materials. *Nauka*, Moscow (1972). 320 p.
[2] Von Middendorff, G. Landwehr. *Sol. State Com*., 11, 203, 1972.
[3] V. V. Sologub, R.V. Parfen'ev, A. D. Goletskaya. *JETP Letters*, 21, (12), 711 (1975).
[4] N. V. Kolomoets, SSP, 1966, t.8, N 4, 997 p.

Smart Nanocomposites
Volume 7, Number 2
ISSN: 1949-4823

SYNTHESIS OF SI- OXIDE NANOSTRUCTURES ON THE SURFACE OF H-BN THE METHOD OF MOLECULAR LAYERING

N. V. Zakharova [1], A. A. Malkov[1], and A. E. Verstakov [2]
[1] Saint Petersburg State Institute of Technology (Technical University);
[2] Federal Unitary Enterprise SCTB "Technologist"

Keywords: Composite materials, heat conductivity, surface modification, functional groups

INTRODUCTION

Creation of the high-diathermic composites having good dielectric properties is the actual task which arises because of developing the electronic package demanding in providing the heat sink in electronic devices. Use of the polymers differing in high insulation properties, simplicity of receiving, lightweight and low cost can be the solution of this task. However, low thermal conduction of polymers is their essential shortcoming. One of the main paths of increase in heat conductivity of polymeric materials is introduction to them structure of dispersible fillers with a high thermal conductivity.

However, in the result of mixture of components with various chemical nature, phase state and ratio the phase boundary reducing conduction of composites [1] is formed. For optimization of composite's properties in the desirable direction the modifying of filler surface for formation of stronger and homogeneous bond with polymer [2-3] is necessary. One of methods of regulation of chemical composition and a structure of the interface is the method of the molecular layering (ML). The essence of process is based on realization of cyclic chemical reactions between the functional groups on a surface of a solid-phase matrix and the reagents brought to them according to the given program from a gas or liquid phase [4-5].

MATERIALS AND METHODS

The objects of research are the hexagonal BN with a specific surface area is 8,4 sq.m/g, the low-molecular reagents $(CH_3)_2SiCl_2$ and C_2H_5OH, which have been chosen for modifying of a surface, and epoxy polymer SLK-45 (TU 16-504.052-86), which has been chosen for creation of composite material.

The synthesis of Si-oxide nanostructures has been carrying out on the facility with the reactor of flowing type by the way of the serial processing (1 – 4 times) of the disperse BN by vapors of $(CH_3)_2SiCl_2$ and C_2H_5OH at 180°C. The character of formation of the nanostructures has been studied by chemical analysis, IK-spectroscopy of diffusion reflection (DRIK), spectroscopy of diffusion reflection in UF and visible area. Registration and differentiation of the donor-acceptor centers of the boron nitride sample's and the products of its modifying surface have been carried out by use of the acid- base indicators with pKa values in the range of 0 ÷ 14.

RESULTS AND DISCUSSION

The surface of boron nitride is characterized by existence of the centers of both acid, and bases type with an index of acidity of H_0 = 4,7. In distribution of the centers of adsorption ranges there are acid centers in area with pKa (2,5 … +5,0) with the maximal maintenance of qpKa = 14 mmol/g, which are bound with such functional groups as =NH and – NH_2. Less intensive strips are observed at pKa=1,3 and in the field of the bases centers of Brensted, which are bound with presence on a surface of hydroxyl groups of B-OH, capable to take part in synthesis process (Figure 1 and 2).

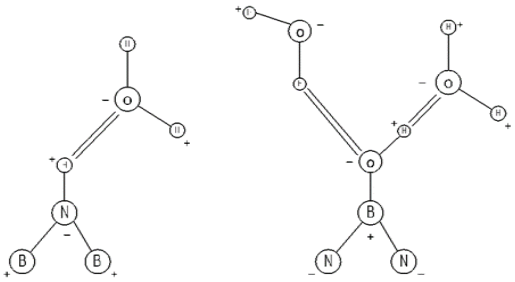

Figure 1. Functional Groups of BN.

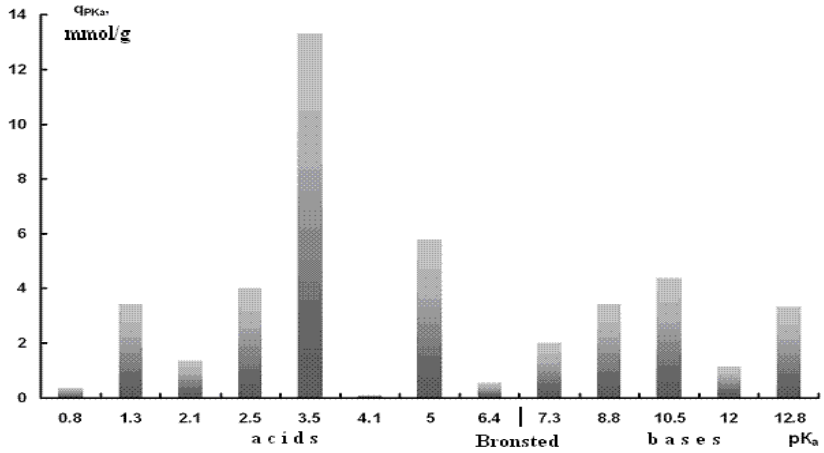

Figure 2. Acid-Base Properties of BN.

It is shown that the main active centers on a surface of initial BN on which takes place interaction of molecules $(CH_3)_2SiCl_2$ are the Brensted centers with a pKa = 3,5 and 5,0.

The received polymeric compositions on the basis of the modified BN have the increased heat conductivity (1,02 W/m·K) in comparison with the composition containing an initial filler (0,96 W/m·K).

Work has been done with partial support of a grant of RSF (demand No. 16-03-00214) and the Ministry of Education and Science (the state task for No. 601 SRW).

REFERENCES

[1] Karnthidaporn Wattanakul, Sittisak Satasit. The Versatile Method to Control the Orientation of BN Particles in Thermoset Matrix. *J. Chem. Chem. Eng*. – V.6. – 2012. – P. 769-773.

[2] Thermal Conductivity of Polymeric Composites: A Review. I.A. Tsekmes, R. Kochetov, P. H. F. Morshuis, J. J Smit. *IEEE International Conference on Solid Dielectrics*, Bologna, Italy, June 30 – July 4, 2013. – P. 678 - 681.

[3] Shyan-Lung Chung, Jeng-Shung Lin Thermal Conductivity of Epoxy Resin Composites Filled with Combustion Synthesized h-BN Particles. *Molecules* V. 21. – 2016. –P. 670–681.

[4] Malygin A. A. The Molecular Layering Method as a Basis of Chemical Nano-technology. *Natural Microporous Materials in Environmental Technology*, V.362 of the series NATO Science Series, 1999. – P. 487– 495.

[5] Malygin A. A. The Molecular Layering Nanotechnology: Basis and Application. *J. Ind. Eng. Chem*. 2006. – V. 12, No 1. – P.1–11.

SENSORS, MATERIALS WITH LUMINISCENT PROPERTIES, POROUS MATERIALS

Smart Nanocomposites
Volume 7, Number 2
ISSN: 1949-4823

HIERARCHICAL NANOMATERIALS FOR MULTISENSOR SYSTEMS

Irina E. Kononova [*] ***and Vyacheslav A. Moshnikov***
Saint Petersburg Electrotechnical University "LETI"
Saint Petersburg, Russia

ABSTRACT

Hierarchical gas sensing, magnetic and ferroelectric nanomaterials were obtained by sol-gel method. Morphological characteristics, electrical, optical, magnetic properties of materials were studied. It revealed that combination of various physical properties of hierarchical nanostructures in a single technological performance is promising in the practice of multisensor systems.

Keywords: hierarchical nanomaterials, porous semiconductors, gas sensitivity, magnetic, ferroelectrics nanostructures

INTRODUCTION

Hierarchical architecture of functional material [1-9] allows using a single technologic platform to create materials with greater diversity of useful characteristics, by controlling the composition of substructures on one or several levels of hierarchical architecture. The purpose of this publication is to study the properties of hierarchical systems based on gas sensitivity, magnetic and ferroelectric materials.

EXPERIMENTAL

Nanomaterials were obtained by sol-gel method. The reactions of hydrolysis and polycondensation of tetraethoxysilane are conducted in the presence of inorganic salts of tin, zinc, indium, iron, nickel. Tetraethoxysilane (TEOS) was chosen to improve the adhesion to the substrate in a sol-gel method annealing was carried out at a temperature 600–800 ºC. Lead acetate and titanium isopropoxide were chosen for obtaining ferroelectric material.

[*] iegrachova@mail.ru

The investigation of the surface condition of the nanostructured films was done on a nanolaboratory instrument Ntegra Terma. It was performed by means of a «semi-contact» vibrational AFM mode. Probe type sensors with cantilevers series NSG 01 in the form of a rectangular cross-section rafter were used in the investigation. This has a resonance frequency of 150 кHz and was purchased from the NT-MDT Company.

Optical transmittance was measured using UV-visible-NIR spectrophotometer at wave lengths from 300 to 1200 nm. The electrical properties of nanostructures were studied by means of impedance spectroscopy measurments. Measuring the frequency dependences of the complex resistivity modulus and determination of the phase shift angle between the current and voltage in the capacitance circuit were carried out in the frequency range between 1 Hz to 500 kHz.

The investigations of the phase composition of the obtained materials were done on a low angle registration electron-diffraction apparatus (SELMI, Ukraine) and on an X-ray analytical equipment using desktop «DRN Farad». The microstructure of materials were studied by thermal desorption of nitrogen using device SORBI.

RESULTS AND CONCLUSION

Hierarchical nanomaterials were obtained by sol-gel method from the liquid phase under conditions of spinodal decomposition. Hierarchical gas sensing, magnetic and ferroelectric materials were studied. In the range from 400 to 1000 nm the optical transmittance of hierarchical nanomaterials of tin, zinc, indium was more than 80-85 %.

The possibility of directed sol-gel synthesis of materials based on magnetic nanoscale grains dispersed within the hierarchical network silica structures was shown to prevent aggregation of magnetic particles and to provide good compatibility with standard silicon electronics for the next generation of micro- and nanotechnology.

The analysis of the experimental results allows us to conclude that under the conditions of changes in the gas environment, the impedance behavior can be controlled by imposing a disturbing action with variable frequency on the system of sensor structures; this opens new prospects for increasing the sensitivity and selectivity of multisensor systems of an electronic nose type. It revealed that combination of various physical properties of hierarchical nanostructures in a single technological performance is promising in the practice of multisensor systems.

ACKNOWLEDGMENTS

This work was supported by the agreement № 14.584.21.0005.30000000.

REFERENCES

[1] Wang Y., Wang X., Yi G., Xu Ya., Zhou L., Wei. Synthesis of layered hierarchical porous SnO_2 for enhancing gas sensing performance//*Journal of Porous Materials*. 2016. P. 1-8.

[2] Bowen Zh., Wuyou F., Huayang L., Xinglin F., Ying W., Hari B., Xiaodong W., Guang S., Jianliang C., Zhanying Zh. Synthesis and characterization of hierarchical porous SnO_2 for enhancing ethanol sensing properties//*Applied Surface Science*. 2016. Vol. 363. P. 560-565.

[3] Chen Z., Lin Z., Yu H., Li N., Xu M. Hydrothermal synthesis of hierarchically porous Rh-doped ZnO and its high gas sensing performance to acetone//Journal of Materials Science: *Materials in Electronics*. 2016. Vol. 27, № 3. P. 2633-2639.

[4] Abrashova E. V., Gracheva I. E., Moshnikov V. A. Functional nanomaterials based on metal oxides with hierarchical structure//*Journal of Physics: Conference Series*. 2013. Vol. 461. №1. P.012019.

[5] Gracheva I. E., Moshnikov V. A., Maraeva E. V, Karpova S. S., Alexsandrova O. A., Alekseyev N. I., Kuznetsov V. V., Olchowik G., Semenov K. N., Startseva A. V., Sitnikov A. V., Olchowik J.M. Nanostructured materials obtained under conditions of hierarchical self-assembly and modified by derivative forms of fullerenes//*Journal of Non-Crystalline Solids*. 2012. Vol. 358. P. 433-439.

[6] Moshnikov V. A., Gracheva I. E., Kuznezov V. V., Maximov A. I., Karpova S.S., Ponomareva A. A. Hierarchical nanostructured semiconductor porous materials for gas sensors//*Journal of Non-Crystalline Solids*. 2010. Vol. 356, № 37-40. P. 2020-2025.

[7] Kononova I. E., Moshnikov V. A., Olchowik G., Gareev K.G., Soboleva E.A., Kuznezov V. V., Olchowik J. M. The preparation and properties of "porous silicon-nickel ferrite" nanoheterocomposites for gas detector//*Journal of Sol-gel Science and Technology*. 2014. Vol.71., №2. P. 233-240.

[8] Tarasov S. A., Gracheva I.E., Gareev K.G., Gordyushenkov O.E., Lamkin I.A., Men'kovich E.A., Moshnikov V.A., Presnyakova A.V. Atomic force microscopy and photoluminescence analysis of porous metal oxide materials//*Semiconductors*. 2012. Vol.46, №13. P. 1584-1588.

[9] Gracheva I. E., Olchowik G., Gareev K. G., Moshnikov V. A., Kuznezov V. V., Olchowik Ja. M. Investigations of nanocomposite magnetic materials based on the oxides of iron, nickel, cobalt and silicon dioxide//*Journal of Physics and Chemistry of Solids*. 2013. Vol. 74., № 5. P. 656-663.

[10] Kononova I. E., Gareev K. G., Moshnikov V. A., Almyashev V. I., Kucherova O. V. Self-assembly of fractal magnetite silica aggregates in a static magnetic field//*Inorganic Materials.* 2014. Vol.50, №1. P. 68-74.

Smart Nanocomposites
Volume 7, Number 2
ISSN: 1949-4823

SYNTHESIS $NaBaPO_4:Eu^{2+}$ LUMINESCENT PHOSPHORS WITH ENHANCED DISPERSION

Vitalii V. Malygin, Vadim V. Bakhmetyev*, Mariia V. Keskinova, Maxim M. Sychov, and Sergey V. Mjakin
Department of Material Science, Saint Petersburg State Institute of Technology (Technical University), Saint Petersburg, Russia

ABSTRACT

$NaBaPO_4:Eu^{2+}$ luminescent phospors with enhanced dispesity are obtained by sol-gel precipitation followed by high temperature annealing in molten NaCl. The suggested approach involving annealing in molten NaCl provides $NaBaPO_4:Eu^{2+}$ phosphors with nanocrystalline structure, 3.8-fold reduced average particle size and 11-fold increased content of finely dispersed (less than 1 μm) fraction compared with a similar material synthesized without NaCl addition.

Keywords: luminescent phosphors, sol-gel, mixed phosphate, Eu^{2+}

INTRODUCTION

Finely dispersed phosphors are required for a number of applications, including medicine and bioimaging. One of the approaches to obtaining finely dispersed materials is based on sol-gel precipitation from solutions. However, thus prepared phosphors require a subsequent high temperature processing that results in sintering of small particles into large agglomerates.

This study is aimed at the development of a process for obtaining finely dispersed $NaBaPO_4:Eu^{2+}$ phosphors using a sol-gel precipitation followed by a high temperature annealing in a molten salt according to the approach earlier suggested in [1] for $Y_2O_3:Eu^{3+}$ based phosphors.

* Corresponding Author: vadim_bakhmetyev@mail.ru

MATERIALS AND METHODS

The synthesis involved $BaCl_2$ and $EuCl_3$ as initial reagents and $Na_3PO_4 \cdot 12H_2O$ as the precipitation agent. The precipitation from an aqueous solution followed by evaporation yields a solid mixture of $NaBaPO_4:Eu^{3+}$ and NaCl subsequently annealed in air at 600°C and milled. Then Eu^{3+} was reduced to Eu^{2+} by annealing in $5\%H_2 + 95\%N_2$ gas mixture at 1050°C followed by washing with hot bidistilled water to remove NaCl. Then the phosphor was separated from the solution by centrifugation and dried under vacuum.

For comparison, a similar phosphor sample was synthesized via a process developed in our previous studies [2] using $Ba(NO_3)_2$ and $Eu(NO_3)_3$ initial reagents and involving sol-gel precipitation and product separation by filtering followed by annealing in air and reducing atmosphere without NaCl addition.

RESULTS AND DISCUSSION

SEM characterization of the above $NaBaPO_4:Eu^{2+}$ phosphors revealed that the addition of NaCl as a fluxing agent at annealing significantly improves the phosphor dispersion providing a 3.8-fold decrease in the mean equivalent diameter to 2.56 μm and an 11-fold increase in the finely dispersed (less that 1 μm) phase content to 44.5% compared with 9.8 μm and 4.0% respectively for the samples annealed in the absence of NaCl.

XRD profiles of the synthesized phosphors correspond to $NaBaPO_4$ monoclinic phase (PDF card 81-2250) free of any admixture phases. However, narrow peaks relating to the phosphor annealed without NaCl indicates its coarsely crystalline structure while the sample prepared in the presence of NaCl features with broad peaks suggesting a nanocrystalline structure. The crystallite size calculated according to the Scherrer equation for the phosphors annealed in the absence and in the presence of NaCl melt is 72.4 nm and 30.2 nm respectively.

Upon UV, electron beam and X-ray excitation the prepared phosphors provide an efficient luminescence with the maximum intensity in the "blue" region (430…460 nm). No significant effect of NaCl addition at annealing upon the luminescence spectra was observed.

CONCLUSION

Thus the performed studies resulted in the development of a process affording the synthesis of $NaBaPO_4:Eu^{2+}$ phosphors with enhanced dispersion.

ACKNOWLEDGMENTS

The reported study was funded by RFBR according to the research project No. 16-33-00998 мол_а.

REFERENCES

[1] Mamonova D. V., Kolesnikov I. E., Golyeva E. V., Mikhailov M. D., Pulkin S. A., Smirnov V. M., (2015). Synthesis and study of $Y_2O_3:Eu^{3+}$ nanoparticles. *Nanotechnologies in Russia* 10 (9), 701-705.

[2] Malygin V. V., Lebedev L. A., Bakhmetyev V. V., Keskinova M. V., Sychov M. M., Mjakin S. V., Nakanishi Y., (2016). Synthesis and study of luminescent materials on the basis of mixed phosphates. *Advances in intelligent systems and computing* 519, 47-54.

Smart Nanocomposites
Volume 7, Number 2
ISSN: 1949-4823

RESEARCH ON POROUS STRUCTURE PARAMETERS OF METAL-OXIDE MATERIALS FOR VACUUM SENSORS

Evgeniya V. Maraeva[1], Maria S. Istomina[1], Anton A. Bobkov[1], Vyacheslav A. Moshnikov[1], Svetlana S. Nalimova[1], and Igor A. Averin[2]

[1]Saint Petersburg Electrotechnical University "LETI"
Saint Petersburg, Russian Federation
[2]Penza State University, Russian Federation

ABSTRACT

The specifics of applying the inert gas thermal desorption method for studying the porous structure parameters of nanomaterials based on SiO_2 – SnO_2 for vacuum sensors are studied. The possibilities for modifying the metal oxide layers to manage the parameters of their porous structure, and selection of modifying agents are discussed.

Keywords: porous nanoparticles, sol-gel synthesis, pore size distribution, atomic force microscopy, thermal desorption

INTRODUCTION

The manufacturers of modern instruments and devices currently show great interest in porous nanostructured materials. Thus, the grade of surface development and availability of a multi-layer system of pores play a defining role in technology of semiconducting metal oxide gas sensors, where different pore types can facilitate different functionality. The structure features (pore size, size distribution, pore volume, specific surface area) are combined under the term "porous body texture." As recommended by IUPAC, the porous systems are classified by predominant pore size into microporous (pore diameter up to 2 nm), mesoporous (2 to 50 nm), and macroporous (over 50 nm). In metal oxide sensors, the macropores can facilitate the feed of gas or liquid materials to nanoreactors, as well as carry away the reaction products. The micropores appear to be a key player in adsorption processes of semiconducting gas sensors. In mesh structures, there is a micropore system that blocks and unblocks the conductivity.

Currently, there are several groups of research methods for porous structure parameters of materials [1-4]. When studying the materials with multi-layer pore system, it is definitely interesting to look into the adsorption and desorption processes in wide range of relative partial pressures, including the cases with capillary condensation of inert gases. This allows to obtain data not only on specific surface area, but also on the pore size distribution, as the pore content nature for physical adsorption can be judged particularly by the initial section of adsorption isotherm and the section exposed to high pressures. However, despite the progress made in application of nanoporous materials over the recent decades, the task of evaluating their fractality remains unresolved.

EXPERIMENTAL

The main purpose of this work was to research the specifics of applying the inert gas thermal desorption method for studying the porous structure parameters of nanomaterials based on SiO_2 – SnO_2 for vacuum sensors. The stated purpose implies the following objectives:

1. To develop the process solutions for synthesizing the porous metal oxide nanomaterials in a system based on SiO_2 – SnO_2 with controlled morphology and 2 to 50 nm pore size distribution;
2. To identify the correlation between the synthesis process modes and the parameters of porous structure of metal oxide systems, which respond to the atmospheric composition and gas pressure.

The sol-gel technology was used to synthesize the porous nanomaterials based on silicon dioxide and stannic oxide. To control properties of the synthesized nanomaterial surface, the nitrogen thermal desorption (Sorbi MS) and atomic force microscopy (NTEGRA-Therma nanolaboratory) were used.

RESULTS

For research purposes, a set of specimens with different component ratio was prepared. The work scope included analysis of possibilities for modifying the metal oxide layers to manage the parameters of their porous structure, and selection of modifying agents. The modifying agent of choice was the carbon-bearing materials, including the amorphous carbon.

For all the patterns pore distribution measurements were made using Sorbi MS that realizes physical adsorption and desorption of noble gas by the sample to be studied [4]. In terms of studying the capillary condensation processes in nanomaterials based on SiO_2 – SnO_2, it was established that there is the so-called sorption hysteresis in the middle adsorption isotherm of all specimens. The assessment of porous structure parameters showed that in all cases the introduction of carbon-bearing modifying agent leads to formation of an additional system of pores with average radius of 15 to 20 nm. The obtained results correlate with the findings of research [5].

The surface diagnostics of $SiO_2 – SnO_2$ layers via scanning probe microscopy showed that the most developed porous structure belongs to nanocomposite specimens with 85 molecular percent content of stannic oxide. The pore size depends on the centrifuge rotation rate. Lower rate leads to formation of porous structure with larger mesopores.

CONCLUSION

The work defines the process modes for synthesizing the porous metal oxide materials in the system "silicon dioxide - stannic oxide" with various modifying agents with controlled morphology and 2 to 50 nm pore size distribution. The technology has been worked out for production of nanomaterials based on $SiO_2 – SnO_2$ with the required component ratio and the set pore size, using the carbon-bearing agents. The methods for studying the gas capillary condensation processes in metal oxide nanomaterials based on $SiO_2 – SnO_2$ with the set pore size have been developed for evaluation of parameters of porous structure. The results can be used for optimizing the technology of metal oxide structure synthesis for gas-sensing devices.

The reported study was funded by RFBR, according to the research project No 16-32-50173 mol_nr.

REFERENCES

[1] Low dielectric constant materials for microelectronics/Maex K., Baklanov M. R., Shamiryan D., Iacopi F., Brongersma S. H., Yanovitskaya Z. S. *Journal of Applied Physics*. 2003. vol. 93, № 11, p. 8793-8841.

[2] Determination of pore-size distribution in low-dielectric thin films/Gidley D. W., Frieze W. E., Dull T. L., Sun J., Yee A. F., Nguyen C. V., Yoon D. Y. *Applied Physics Letters*. 2000. vol, 76, № 10, p. 1282- 1284.

[3] Nondestructive determination of pore size distribution in thin films deposited on solid substrates/Dultsev F. N., Baklanov M. R. *Electrochemical and Solid-State Letters*. 1999. vol. 2, № 4, p. 192-194.

[4] Pore-volume and surface area in microporous–mesoporous solids/Schneider P., Hudec P., Solcova O. *Microporous and Mesoporous Materials*. 2008, vol. 115, № 3, p. 491-496.

[5] The study of porous silicon powders by capillary condensation / Belorus A. O., Maraeva E. V., Spivak Yu. M., Moshnikov V. A. *Journal of Physics: Conference Series*. 2015. vol. 586, p. 012017.

[6] Study of porous sol-gel nanocomposites based on silicon dioxide and tin dioxide modified by fullerenol $C_{60}(OH)_n$ (n = 22-24)/Maraeva E. V., Istomina M. S., Moshnikov V. A., Nalimova S. S., Maximov A. I., Alexeev N. I., Semenov K. N. *Journal of Physics*: *Conference Series*. 2016. vol. 690, p. 012031.

Smart Nanocomposites
Volume 7, Number 2
ISSN: 1949-4823

LOW DIMENSIONAL FORMS OF SUBSTANCES IN POROUS GLASS MATRIX: SYNTHESIS, STRUCTURE, PROPERTIES

Vyacheslav N. Pak*
Herzen State Pedagogical University of Russia
Saint Petersburg, Russia

ABSTRACT

The methods used to synthesize oxides, sulfides, and complex compounds at the surface of through channels of porous glass plates are considered. The concentration and dimensional dependences of the state and properties of host substances have been studied. The possibilities for the directional production of materials with controllable spectral, luminescent and photochromic properties, as well as electron and proton conductivity, are shown.

Keywords: porous glass, included substances, nanoparticles, monolayers, photochromism, luminescence, conductivity

INTRODUCTION

Porous glass (PG) presents wide ranging possibilities for the production and study of substances in a low dimensional state [1]. Indeed, the upper limit of the cross section of compounds synthesized in a porous space of PG is regulated by the nanometer diameter of pores. So, in most cases, we speak of partial, sometimes low, filling of pores with encapsulated substances. Hence, PG operates as a nanoreactor determining the nanodimensional peculiarity of chemical processes in it and the properties of the synthesized objects. Nevertheless, the dimensional dependences of the optical and electrical properties of substances included in PG remain weakly studied.

In the case of PG plates with a through porosity, a procedure of step-by-step accumulation can be successfully used, which provides a preset content of host substances in the carrier. So, the deposition of most oxides onto the walls of the channels of PG membranes can be successfully implemented. The content of oxides in the carrier for one step of

* E-mail: pakviacheslav@mail.ru

deposition (Q) is determined by the volume of PG pores (V_p) and is reliably controlled by the concentration of the impregnating solution as: $Q = cV_p\gamma$, where $\gamma \leq 1$ (the value typical for various types of glass) reflects the degree of filling of the space of pores with the solution. Thus, in order to obtain the necessary amount of oxides in PG, the procedure mentioned (impregnation–drying–baking) should be repeated several times with the use of the solutions of the required concentration. Similarly, a controllable step-by-step accumulation of metal sulfides is implemented by repeating the operations of saturation of PG with solutions of chlorides (nitrates) with the subsequent treatment in the vapors of hydrogen sulfide and cleaning of the formed acid. Other methods are also used, such as the method of molecular bedding, insertion in PG of two (and more) components with the subsequent reaction between them, reduction with hydrogen and formation of complex compounds [1].

The only three examples below demonstrate the use of PG as a carrier.

Charge transfer spectra [1, 2]. Dimensional changes in the spectra are distinctly revealed by the step-by-step accumulation of oxide nanoparticles in PG. So, the bands of charge transfer V_2O_5 reflect an excitation of electrons of the upper filled 2p-orbitals of oxygen to the vacant 3*d*-levels of vanadium (*V*). The merging of vanadium oxide polyhedrons into nanoparticles in the course of the accumulation of oxide in PG is accompanied by an increase in the number of states of the system and the gaining of the π-coupling of bonds V-O-V, which results in a rapid approach of the bands of the mentioned donor and acceptor states. Accordingly, a shift of the spectra in the series of samples of the system V_2O_5–PG is observed in a narrow interval of compositions with the approach to the spectrum of bulk oxide (modified PG gradually changes color from weakly to strongly yellow). Results close in their origin to the values of the registered shifts of the bands of charge transfer were obtained in the case of the systems MoO_3–PG, CdS–PG and others.

Photoluminescence [1-4]. Compounds of rare earth elements, which possess a strongly pronounced luminescence, can play the role of host substances in PG. So, in the series of samples of the system $EuCl_3$–PG obtained by a simple method of saturation of PG by aqueous salt solutions of varied concentrations small particles reveal the properties which distinguish them from those of a polycrystalline analog. The high symmetry of the Eu^{3+} coordination ambience in nanoparticles is indicated by the sharp increase in the intensity of the band of the supersensitive $^5D_0 \rightarrow {}^7F_2$ transfer with respect to the magnetodipole $^5D_0 \rightarrow {}^7F_1$. The weak concentration quenching of luminescence is also determined by the dimensional factor. Finally, the duration of red luminescence in the system $EuCl_3$–PG achieves 230 μs (80–90 μs for bulk $EuCl_3$), while the luminescence intensity for the content of the particles in PG of ~0.02 mass % is found to be several times higher than in bulk salt. Similar results were obtained for the system $TbCl_3$–PG, which provided a green luminescence.

Solid electrolytes based on PG [5, 6]. The development of the technology for fuel cells is substantially associated with the necessity to develop solid electrolytes with the high proton conductivity (σ) at temperatures above 100^0C. At the first stage, the conductivity in the system H_3PO_4–PG was studied. At room temperature, the values of σ are weakly sensitive to the PG's structural parameters and are close to the conductivity (0.078 Ohm^{-1} cm^{-1}) of a 85 mass % H_3PO_4 solution. By heating to 100^0C, σ grows monotonically, but then sharply drops to 10^{-4} Ohm^{-1} cm^{-1} because of the intense dehydration and decrease in the filling of the space of the PG's channels. Accordingly, the next version was a saturation of PG with acid, which was preliminarily dewatered at 200^0C. In the obtained composite σ stays stable at a level of 10^{-3} Ohm^{-1} cm^{-1}in an interval of 100–200^0C. A substantial improvement in the parameters is

achieved by the saturation of PG at 450^0C with a solution (melt) having a mol ratio of 1/1.5 of cesium dyhydroorthophosphate to phosphoric acid. The high values of the proton conductivity for the obtained composite ($CsH_2PO_4/1.5H_3PO_4$)–PG weakly depend on the porous structure of the PG and are reproducible in the course of a multiple increase (decrease) of the temperature in the interval of 100–230^0C.

REFERENCES

[1] Pak V. N., Gavronskaya Yu. Yu., Burkat T. M. Porous glass and nanostructured materials. N.Y.: Nova Science Publishers (2015).

[2] Pak V. N., Gavronskaya Yu. Yu., Shilov S. M. Optical and electrical properties of low dimensional forms of substances in porous glass. *Glass Phys. Chem*, 41(1), (2015), 68–72.

[3] Shilov S. M., Gavronskaya K. A., Levkin A. N., Pak V. N. Molecular layering method used to sensitize luminescence from terbium(III) oxide nanoparticles in porous glass//*Russian Journal of Applied Chemistry*. 81(10), (2008), 1754-1757.

[4] Petushkov A. A., Shilov S. M., Puzyk M. V., Pak V. N. Luminescence of europium(III) β -diketonate complexes in a nafion membrane. *Russian Journal of Physical Chemistry A* 81(4), (2007), 612-616.

[5] Lyubavin M. V., Burkat T. M., Pak, V. N. Temperature dependence of the electrical conductivity of orthophosphoric acid in porous glass. *Russian Journal of Applied Chemistry*. 82(7), (2009), 1238-1241.

[6] Pak V. N., Lyubavin M. V., Borisov A. N. Formation of the planar structure of ammonium dihydrogen orthophosfate in porous glass. *Russian Journal of General Chemistry*. 86(9), (2016), 2309-2312.

Smart Nanocomposites
Volume 7, Number 2
ISSN: 1949-4823

BAND-STOP OPTICAL FILTER BASED ON COMPOSITE POROUS SILICON – SILVER NANOSTRUCTURE

Rostislav S. Smerdov[1,*], Nikolay S. Pshchelko[1], Yulia M. Spivak[2], and Vyacheslav A. Moshnikov[2]

[1]Department of General and Thechnical Physics,
St. Petersburg Mining University,
St. Petersburg, Russia
[2]Department of Micro- and Nanoelectronics,
St. Petersburg State Electrotechnical University,
St. Petersburg, Russia

ABSTRACT

A method for constructing an optical band-rejection filter based on surface plasmon resonance of silver nanoparticle array is suggested. A synthesis technique for plasmonic array of silver nanoparticles is developed. Stability of attenuation characteristics is achieved by using porous silicon matrix. The possibilities of adjusting filter parameters such as the width of the absorption band, the value of suppression in the band and position of the absorption band are studied. The superiority of plasmon filter over modern interference filter in terms of adjustment of attenuation band position is revealed. The potential of reaching adequate level of attenuation in absorbtion band by synthesizing an array of silver nanoparticles with less size distribution is revealed.

Keywords: optical filters, band-reject filter, band-pass filter, plasmon resonance, drude model, fractals, unno-imai technique

INTRODUCTION

Optical band pass filters (BP) transmit light only within a particular range of wavelengths of less than one to tens of nanometers. Such filters are used in a wide range of scientific and industrial fields, including spectrophotometry, medical diagnostics, chemical analysis, colorimetry and astronomy. While optical spectrophotometry is considrerd BP filters have an

* Corresponding Author address: E-mail: rostofan@gmail.com

anvantage over monochromators due to better transmittance, and signal-to-noise ratio. Interference band pass filters are typically characterized by the central wavelength and bandwidth. Such filters consist of thin glass coated with a combination of dielectric materials (SiO_2, TiO_2, ZrO_2, TaO_2, ZnS, MgF_2) thereof, allowing to create constructive and destructive interference providing filtering effect.

The phenomenon of plasmon resonance can be used while creating bandpass and bandstop filters in the optical range (300-1200 nm). Surface plasmon resonance can be described as coherent delocalized electron gas oscillations existing on the boundary of the medium with positive permittivity (dielectric) and the metallic nanostructures (Ag, Au) [1].

Plasmon resonans wavelength does not depend on nanostructure size if free-space incident signal wavelength is lagrer than nanostructure dimensions. This electrostatic condition implies that for a system of practically identical in turms of shape and varying in size nanoparticles surface plasmone resonance wavelength is virtuall the same.

The wavelength of the plasmon resonance is determined by both the form and periodicity of the nanostructures in an array arrangement. In study [2] prototype reflective filter based on a hexagonal array of silver nanoparticles with a triangular base has been implemented exhibiting more stable attenuation characteristics and structural stability compared to silver nanoparticle nanoarrays with rhombic bases.

EXPERIMENTAL RESULTS

Plasmon band-rejection filters attenuation characteristics were obtained by using electron absorption spectroscopy technique.

$$A(\lambda) = \frac{P_{inc}}{P_{ref}}, \quad (1)$$

where $A(\lambda)$ – signal attenuation characteristic (dB), P_{inc}-incident signal level, P_{ref} – reflected signal level, λ – signal wavelength, nm.

Depending on the silicon substrate synthesis parameters (such as time and anodizing current density), porous silicon parameters (depth and branching of the pore structure) were modified, resulting in the formation of fractal aggregates of silver nanoparticles on the surface of the prototype. Figure 1 shows the attenuation characteristics of the filter prototypes, depending on the value of the anodizing current. The existence of a band attenuation at a wavelength λ_0 = 360 nm is consistent with the results of a study published in the paper [3] and is associated with the phenomenon of surface plasmon resonance of silver nanoparticles.

With an increase in the anodizing current density (from 2 to 30 mA/cm^2) rejection-band attenuation value increases, thus being indicative of an increase in the concentration of monodispersed pores, causing the formation of spherical silver nanoparticles on the porous Si surface.

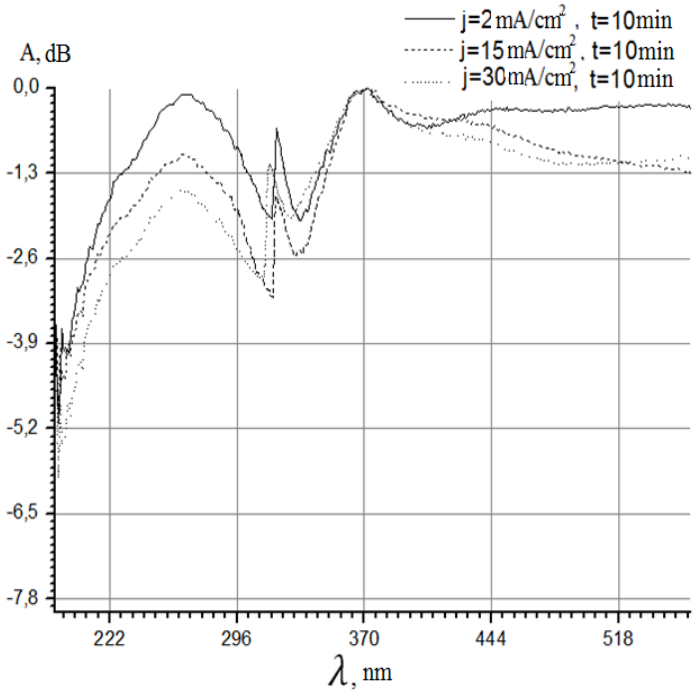

Figure 1. Plasmon filters optical absorption spectra depending on anodizing current density (j = 2, 15, 30 mA/cm^2, t = 10 min).

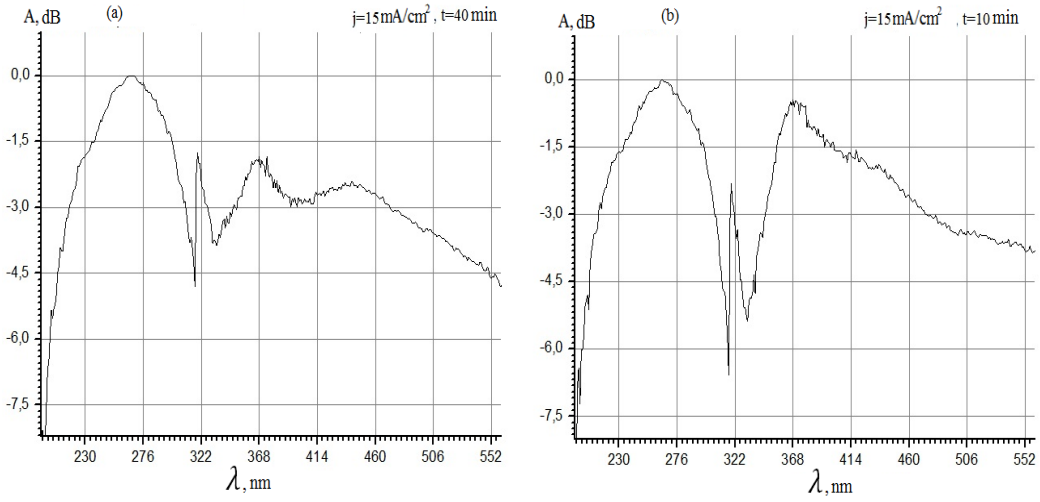

Figure 2. Plasmon filters optical absorbtion spectra depending on the anodizing time (j = 15, mA/cm^2 t = 40 min (a), t = 10 min (b)).

Figure 2 shows the attenuation characteristics of prototype plasmon filters depending on the anodizing time. In addition to the absorption band with λ_0 = 360 nm, the spectrum contains a broad band (60 nm) with an average wave length λ_0 = 265 nm. Its existence is due to the formation of fractal agglomerates of silver on the surface of the porous silicon substrate [4].

CONCLUSION

The magnitude of suppression of more than 3 dB within the attenuation band (up to 40 dB) can be obtained by synthesizing the composite structure having lesser size dispersion and fractal-shaped silver nanoparticles by increasing the anodisation current density at the stage of porous matrix synthesis [5], also leading to values of unevenness in the attenuation band of 0.1 dB. At the same time it would reduce the attenuation bandwidth to values comparable to the limit for contemporary thin-film interference filters (60 to 10 nm) [6].

REFERENCES

[1] Mayergoyz I. D. Plasmon Resonances in Nanoparticles, Singapore: World Scientific Publishing Co Pte. Ltd., 2013, 325.

[2] Fu Y. Q., Zhu S. L., Zhou X. L., Zhao W. Rhombic silver nanoparticles array-based plasmonic filter. International Journal of Modern Physics B, 2011, vol. 25, No. 19, pp. 2557-2566.

[3] Ghauharali, R. I. and Brakenhoff, G. J. Fluorescence photobleaching-based image standardization for fluorescence microscopy. Journal of Microscopy. 2001, vol. 198, No. 2. pp. 88-100.

[4] Moshnikov V. A., Gracheva I. E., Pshchelko N. S., Anchkov M. G., Levine K. L. Investigating Properties of Gas-Sensitive Nanocomposites Obtained via Hierarchical Self-Assembly in book: Smart Nanoobjects: Synthesis and Characterization, New York: Nova Science Publishers, 1999, 569.

[5] Moshnikov V. A., Gracheva I. E., Lenshin A. S., Spivak Y. M., Anchkova M. G., Kuznetsov V. V., Olchowik J. M. Porous silicon with embedded metal oxides for gas sensing applications. Journal of Non-Crystalline Solids. 2012, Vol. 358, no. 3, pp. 590–595.

[6] Liu Y. J., Si G. Y., Leong E. S. P., Optically tunable plasmonic color filters. Applied Physics A. 2012, vol.107, No. 1. pp. 49-54.